University of Bath

UNIVERSITY OF BATH

PHD

Mathematical models in eco-epidemiology

Bate, Andrew

Award date:
2014

Awarding institution:
University of Bath

Link to publication

Mathematical models in eco-epidemiology

submitted by

Andrew M. Bate

for the degree of Doctor of Philosophy

of the

University of Bath

Department of Mathematical Sciences

December 2013

Summary

Diseases have the capacity to not only influence the dynamics of their hosts, but also interacting species like predators, prey and competitors. Likewise, interacting species can influence disease dynamics by altering the host's dynamics. The combination of these two effects is often called eco-epidemiology, the interaction of ecology and epidemiology.

In this thesis, we explore this interplay of infectious diseases and predator–prey interactions, where the predator is a specialist. We start with an introductory chapter on modelling eco-epidemiology, with a particular focus on the myriad of different possible assumptions mathematical models in eco-epidemiology can have. In Chapter 2, we consider the effect predator–prey oscillations have on the endemic criteria for an infectious disease. In Chapter 3, we find a great variety of complex dynamics like tristability between endemic and disease-free states, quasi-periodic dynamics and chaos in a predator–prey model with an infectious disease in the predator. In Chapter 4, we consider the impact an infectious disease has on a group defending prey. Here, we find that the disease not only can coexist with a predator, it can actually help the predator survive where it could not in the absence of the disease, in stark contradiction to the principle of competitive exclusion which states that two exploiters should not coexist on a single resource. Lastly, in Chapter 5, we consider a spatial predator–prey model with a disease in the prey and focus on how preytaxis (the movement of predators along prey gradients) can alter various invasion scenarios. Through all these chapters, there is a common focus on the impact (endogenous) oscillations have in eco-epidemiology.

Acknowledgements

First and foremost, I thank my supervisor, Frank Hilker, for his time, wisdom and patience he has invested in me. He has been a real pleasure to work with and I wish him all the best in his future endeavours in Osnabrück.

I thank those whose company has kept me a relatively sane and pleasant fellow over the past three or so years. I thank the core staff and students within CMB; Nick, Jane, Ben, Frank, Ellie, James C., Finn, Hannah, Katy and Jenny; especially James C. and Finn for putting up with me during our conferences in Krakow and Knoxville. I thank my other office mates, whether they lasted the course or not; especially James C., Finn, Siân, Mason and Kris for our leagues of freehand circling, 'Achtung, die Kurve!' and pound shop mini pool. I thank my fellow pub quizzers, who helped answer the most fundamental pub quiz question, what is your team name? I thank my fellow maths footballers, a globetrotting bunch whose philosophy is that football is best played while still drunk from the night before. I thank the Drinks in the Paraders and Wednesday cakebakers, who have made PhD life a culinary experience with good conversion.

And finally, I thank my family for being my family. I would not be here without them.

Contents

List of Figures

List of Tables

Published parts of the thesis

The following parts of this thesis have been published in international peer-reviewed scientific journals.

- Chapter 2 is based on 'Bate, A.M., Hilker, F.M. (2013) Predator–prey oscillations can shift when diseases become endemic. Journal of Theoretical Biology 316:1–8' with kind permission from Elsevier. The published version is available on Science Direct.

- Chapter 3 is based on 'Bate, A.M., Hilker, F.M. (2013) Complex dynamics in an eco-epidemiological model. Bulletin of Mathematical Biology 75:2059–2078' with kind permission from Springer Science+Business Media.

- Chapter 4 is based on 'Bate, A.M., Hilker, F.M. (2014) Disease in group-defending prey can benefit predators. Theoretical Ecology 7:87-100' with kind permission from Springer Science+Business Media B.V.

During the course of this PhD, another paper was published but is not included in this thesis.

- Bate, A.M., Hilker, F.M. (2012) Rabbits protecting birds: Hypopredation and limitations of hyperpredation. Journal of Theoretical Biology 297:103–115

Chapter 1

Introduction: Predators, prey and prevalence

Each chapter has its own introduction and discussion, in which the context of each chapter is discussed. However, none of the chapters go into great detail about mathematical models in eco-epidemiology as a whole. We will give this overall picture for predator–prey interactions, where the predator is a specialist, as we only consider such predator–prey interactions within this thesis. This will be done by first highlighting and contextualising many of the key works of eco-epidemiology, a brief history if you will. After this, we will give a picture of the breadth of different models available in eco-epidemiology by going through various assumptions that can be made in the process of developing an eco-epidemiological model; to provide context to the choice of models in this thesis and the choice of models out there. Following this, we will briefly discuss the usefulness of the model rescaling used often in this thesis. Lastly, we will give an overview of the contents of this thesis.

1.1   A brief history of eco-epidemiology

For this thesis we will consider eco-epidemiology models that contain a predator–prey interaction, where the predator is a specialist. Consequently, this brief history will focus on such systems. For a more detailed review of the interaction between predator–prey interactions and parasite dynamics, see Hatcher and Dunn (2011, Chapter 3).

The first example of modelling the interaction between disease and ecological dynamics we know of is Anderson and May (1986). In this paper, a broad variety of simple eco-epidemiological models were considered (although quite briefly). A con-

ventional Lotka–Volterra model (linear growth of prey, linear death rates for predators, linear functional and numerical responses) was used for the disease-free predator–prey system (logistic growth for prey is also considered). The disease has density dependent transmission, infected hosts experience additional mortality and do not reproduce. For diseases in prey, they found that predators and disease could not coexist unless infected prey reproduce or predators select more infected prey over susceptible prey (Anderson and May, 1986, Table 6). This is akin to the principle of competitive exclusion (Hardin, 1960), where two consumers can not coexist on one prey resource (we will go over this in greater detail in Chapter 4). For diseases in predators, they found that the disease can persist as long as the prey population can sustain a large enough predator population, a result akin to those in food chains (Oksanen et al, 1981).

Following this, the next prominent eco-epidemiological paper was Hadeler and Freedman (1989). In this paper, the predator–prey system is of Rosenzweig–MacArthur type (logistic growth of prey, linear death rates for predators, Holling type II functional and numerical responses). Here, the disease infects both the predators and the prey and can only be transmitted trophically, i.e. predators are infected by consuming infected prey and prey are infected by proximity to infected predators (by assuming environmental transmission can be approximated by density dependent transmission). This model is a significant jump from Anderson and May (1986), and is investigated in much detail. There are many parasites that are transmitted trophically up the food chain, with the apex predator transmitting the parasite back to the environment, often via the predator's faeces (including many nematodes, trematodes, cesodes and acanthocephalans, Lafferty, 1999).

Anderson and May (1986) and Hadeler and Freedman (1989) are the two key eco-epidemiological papers. Most other papers follow on from at least one of these two papers.

During the 1990s, a handful of papers on eco-epidemiology started to filter through. An early pioneer is Ezio Venturino, who along with collaborators, has provided many papers in eco-epidemiology (Venturino, 1994, 2002, 2010, 2011a,b; Stiefs et al, 2009; Haque and Venturino, 2006, 2007; Haque et al, 2009; Sarwardi et al, 2011; Ferreri and Venturino, 2013). In particular, Venturino (1994) considers disease in the prey, whereas Venturino (2002)[1] considers a disease in the predators.

---

[1] Venturino (2002) was submitted in 1992, so definitely merits being discussed as an early paper considering a disease in the predator.

By the end of the 1990s the term *eco-epidemiology*[2] was first used for the combination of infectious disease and ecological dynamics (Chattopadhyay and Arino, 1999). A few years later, several papers in eco-epidemiology started to appear (Xiao and Chen, 2001b,a; Han et al, 2001; Chattopadhyay and Bairagi, 2001; Chattopadhyay and Pal, 2002; Chattopadhyay et al, 2003; Xiao and Van Den Bosch, 2003; Hethcote et al, 2004).

Many early works on eco-epidemiology focused on plankton systems (earlier Beltrami and Carroll, 1994; Chattopadhyay and Pal, 2002; Malchow et al, 2004). Following on from these plankton papers, two dynasties on eco-epidemiology were formed.

Horst Malchow, together with collaborators Frank Hilker, Ivo Siekmann and Michael Sieber, have made much work in eco-epidemiology (Malchow et al, 2004, 2005; Hilker and Malchow, 2006; Hilker et al, 2006; Hilker and Schmitz, 2008; Oliveira and Hilker, 2010; Siekmann et al, 2008, 2010; Siekmann, 2013; Sieber et al, 2007; Sieber and Hilker, 2011; Sieber et al, 2013).

The other 'dynasty' seems to have been established around Joydev Chattopadhyay, with collaborators Nandulal Bairagi, Mainul Haque and others (Chattopadhyay and Arino, 1999; Chattopadhyay and Bairagi, 2001; Chattopadhyay and Pal, 2002; Chattopadhyay et al, 2003; Singh et al, 2004; Haque and Venturino, 2006; Bairagi et al, 2007; Greenhalgh and Haque, 2007; Haque and Venturino, 2007; Upadhyay et al, 2008; Haque et al, 2009; Haque, 2010; Das et al, 2011; Haque et al, 2011; Sarwardi et al, 2011; Chatterjee et al, 2012; Das and Chattopadhyay, 2012)

Although outside of the remit of this thesis, there are also some important works that considers a generalist predator on host–disease systems, i.e. there are no predator dynamics (including Hudson et al, 1992; Packer et al, 2003; Hall et al, 2005; Holt and Roy, 2007). In particular, Packer et al (2003) suggested that predators can 'keep the herds healthy', which has helped shape the discussion on the possible benefits predators can have on limiting the prevalence of diseases in prey.

1.2   Forming an eco-epidemiological model

Throughout this thesis, we will focus on systems where diseases affect a predator–prey interaction, overlooking other forms of ecological interactions like competition or mutualism. Likewise, we will largely consider closed systems for simplicity, over-

---

[2]*Eco-epidemiology* was previously used in Susser and Susser (1996) where they describe the application of 'ecologism' (which seems to be synonymous with heterogeneity, as opposed to 'universalism' or homogeneity) to diseases in general (not limited to infectious diseases). This use of the word would not lead to confusion.

looking outside interference like additional food sources for predators or a constant spillover of disease from a reservoir species. On top of this, we largely consider only ODE models (Chapter 5 being an exception, where PDEs with one spatial dimension are considered). However, even with these simplifying starting assumptions, there are still many choices needed in making an eco-epidemiological model. This section will discuss these many different options.

Before we proceed, it is worthwhile noting that eco-epidemiological models are rather complicated, as they need to incorporate at least three variables (predator, prey and disease). This brings in many challenges. For example, with complicated models, they are often difficult to analyse and, more importantly, to evaluate to some interesting conclusion. One vital question, which is often overlooked, is whether these results only apply to a specific model or are these results applicable to many other models. Without attempts to generalise results, we will be forever working on a sequence of special cases.

1.2.1 The underlying ecology

There are several key questions for modelling the underlying disease–free predator–prey dynamics:

- What are the prey dynamics in the absence of predators? Do they experience density dependence? What type of density dependence (e.g. compensatory, depensatory/Allee effect)?

- Do predators attack susceptible prey? What is the predators' functional response?

- What are the predators' underlying dynamics?

Most models assume that the prey grow logistically in the absence of disease and predators, although models do exist where prey grow linearly, most notably the basic model in Anderson and May (1986) and the models in Venturino (1994). One matter up for discussion is whether logistic growth is caused by density dependent mortality or by density dependence in the birth rate. This distinction matters more when considering multiple interacting prey classes like with an infection in the prey, which we will discuss later.

Logistic growth is a form of compensatory density dependence, i.e. the prey's per capita growth rate decreases as prey density increases. However, there is the possibility

of including depensatory density dependence (also known as an Allee effect). This means that there are some prey densities (typically small densities, where difficulties finding mates limits the per capita growth) where increasing prey density increases the per capita growth rates. Allee effects are a fairly common assumption in ecological models, but they have rarely been considered in eco-epidemiological models.

Following the underlying prey dynamics, we then need to choose what effect a predator has on it. There are models where predators do not attack susceptible prey; in which case, predators can not survive in the absence of the disease in the prey. Assuming predators do attack susceptible prey, there are many choices of functional response. Most models consider a linear functional response or the hyperbolic Holling type II functional response. However, there are many other choices, most notably the sigmoidal Holling type III functional response and various ratio-dependent functional responses.

By far, the most common assumption for predators is that the predators' growth rate is proportional to the functional response together with a constant per capita death rate. However, there are other assumptions. For example, we can include density dependence, or we could include a carrying capacity dependent on prey density.

For a more thorough discussion on the variety of functional responses, numerical responses and predator–prey models, see Turchin (2003, Chapter 4).

1.2.2 The underlying epidemiology

There are several different questions when considering the host-disease dynamics that need to be addressed:

- Is the infectious agent a macroparasite or a microparasite?

- What stages of infection are there, i.e. is there latency, recovery, immunity?

- How is the disease transmitted? What is the force of infection?

- What are the consequences of infection (ignoring interaction effects)?

The standard assumption for modelling microparasitic infections is by following the method of splitting the host population into discrete, homogeneous classes (a method attributed to Kermack and McKendrick, 1927). This means that all individuals within an infected class are equally infected and infectious; there are no 'shades' of infection within each class. However, macroparasite modelling can be much more complicated. With macroparasites, the degree of infection within each host depends on

the number of parasites the host is carrying. For example, one flea may be a nuisance but an infestation of fleas is unhealthy. On top of this, macroparasites often have many life stages. Given this added level of complexity, many macroparasites problems are modelled as if they are microparasites.

With stages of infection, there is a great deal of choice. By far the most common assumption within eco-epidemiology is that there are only two host classes, susceptible and infected, and that once infected, the infection either remains until the host dies (the disease is an SI disease) or the host may recover from infected to susceptible (SIS). This contrasts with human epidemiology, where the most common assumption is for there to be three host classes, susceptible, infected and recovered, where infected individuals can recover from infection and establish immunity, which is either lifelong immunity (SIR), or temporary immunity (SIRS). There are many other types of classes, the two most noteworthy are the class for those with a latent infection (usually denoted as E), or the class of free infectious agents (e.g. viruses) in the environment (often denoted as V).

Infectious disease models normally require some kind of horizontal transmission (whether direct or via the environment). This transmission depends on the force of infection. There are two main choices for the force of infection, density dependent transmission (βSI) and frequency dependent transmission ($\propto \frac{SI}{N}$), where S, I and N are the susceptible host, infectious host and total host densities, respectively. The former transmission mode is based around the assumption of mass action, where the number of contacts for disease transmission is proportional to host density, whereas the latter transmission mode assumes that each infectious host has a constant number of contacts, independent of host density. Although rare, there are other choices for the force of infection. For example, Kooi et al (2011) assumed a 'Holling type II' force of infection (which is some generalisation of both the frequency and density dependent forces of infection); whereas Morozov (2012) suggested, for a disease in the prey only, a force of infection that also depended on predator density.

On top of horizontal transmission, vertical transmission (i.e. the inheritance of infection from parent to offspring) is a fairly common assumption.

Infections need consequences to be interesting. Typically, the simplest and most common assumption is that hosts experience increased mortality or morbidity. This is in stark contrast to many classic epidemiological models (particularly human models), where host dynamics are rarely considered; in such models, the downside of infection is infection itself. However, many models also have that infecteds are sterile or have reduced fecundity; reduced fecundity is particular common if there is vertical

transmission.

1.2.3 The underlying interaction of ecology and epidemiology

We have discussed the possible ecological and epidemiological questions. However, infected hosts may interact differently with other hosts and their predators/prey. This raises many more questions:

- Who is infected? If both, is the disease trophically transmitted?

- Does infection alter vulnerability to predators?

- Does infection limit a predators' ability to catch prey?

- Does infection alter ability to compete with conspecifics?

As we have already discussed when comparing Anderson and May (1986) and Hadeler and Freedman (1989), we can consider a disease that infects prey only, infects predators only, or a disease that infects both. Broadly speaking, almost every eco-epidemiological model fits into one of these three cases. However, there are several papers that don't quite fit this; for example, several models involve a disease in the prey where predators get sick when consuming infected prey (i.e. they have a negative numerical response with respect to predation on infected prey) but sick predators are not infectious (for example Chattopadhyay et al, 2003). Likewise, the model in Das et al (2011) has that there are separate diseases for predator and prey. Only a few models involve a disease that infects both predator and prey (Hadeler and Freedman, 1989; Han et al, 2001; Fenton and Rands, 2006). But since trophically transmitted diseases are common (Lafferty, 1999), we feel that trophic transmission should be explored more in an eco-epidemiological sense.

Infection may weaken prey, making them more susceptible to predation. This is a common assumption used in many models. For example, red grouse killed by predators have a larger burden of a parasitic nematode (Hudson et al, 1992). In fact, there are several models where predators only catch infected prey. On the other hand, predators may wish to avoid infected prey, either because they may get infected or sick too, or the disease makes the infected prey repulsive or unpalatable to predators. Note that for non-trophically transmitted diseases, the disease usually benefits from the host surviving for as long as possible, in which case reducing vulnerability to predators would increase the lifespan of the infection and thus benefit the disease. Infection may

also weaken predators, making them less capable at catching prey. This too is a fairly common assumption in eco-epidemiological models that have infected predators.

The concept of competition between infected and susceptible hosts is largely overlooked. However, Sieber et al (2013) (as well as the work in this thesis) include density dependent terms, giving an explicit formulation for phenomena like logistic growth. This is at the core of a comment in the ecology section; for logistic growth, we should either assume that births or deaths are density dependent. If births are density dependent, then if there is no vertical transmission, all density dependent terms will be included in the susceptible population (whereas for vertical transmission, both susceptible and infected classes will have density dependent terms). If it is deaths that are density dependent, then there should be density dependent terms within both susceptible and infected populations, independent of vertical transmission.

1.3   Rescaling: Predators, prey and prevalence

Throughout this thesis, we seek to simplify eco-epidemiological models. This is often done by various simplifying assumptions like infection does not change fertility, intraspecific competitive strength and so on. On top of this, we will rescale the models in the hope that terms will cancel. This is a technique that has been used before (Hilker and Malchow, 2006; Sieber et al, 2007; Hilker and Schmitz, 2008; Haque, 2010; Oliveira and Hilker, 2010; Siekmann et al, 2010; Sieber and Hilker, 2011; Sieber et al, 2013) and can be powerful if possible. Sieber and Hilker (2011) state that with indiscriminate predation, eco-epidemiological models can be reduced from intraguild predation to simpler forms. Throughout this thesis, we will transform the susceptible-host (S)–infected-host (I) formulation to a total-host ($S+I$)–prevalence $\left(\frac{I}{S+I}\right)$ formulation. There are benefits to this rescaling; one such benefit is that disease prevalence and total host density are usually easier to measure in wild populations. But, more importantly, with the models considered in this thesis, they do reduce the original intraguild predation structure to something considerably simpler (Figure 1-1).

For the diseased-prey models considered in Chapters 2, 4 and 5, we can reduce an intraguild predation structure to an exploitative competition structure (Figure 1-1(a)); whereas for the diseased-predators models considered in Chapters 2 and 3, we have reduced an intraguild predation structure to a food chain structure (Figure 1-1(b)). This means that in the diseased-prey model, one would expect that the infection and predator could not coexist (in other words, 'winner takes all', Siekmann, 2013), whereas for the diseased-predator model, we expect infection to be sustained only if
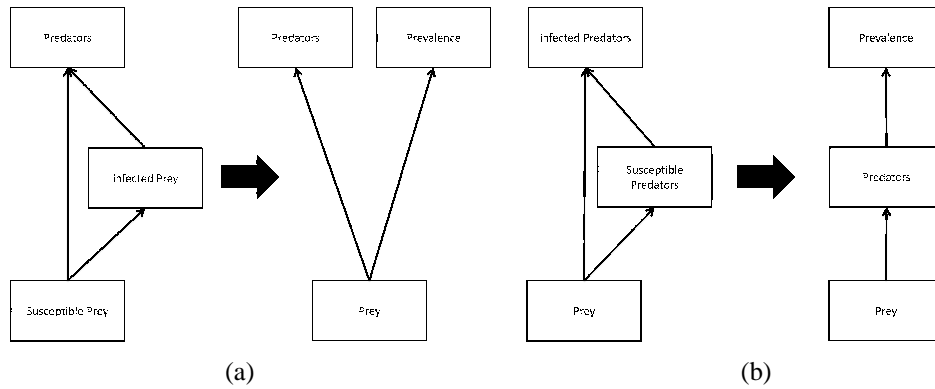
Figure 1-1: *Using disease prevalence instead of infected host density can simplify many eco-epidemiological models from an intraguild predation to something simpler. For example, (a) rescaling infected prey can give us an exploitative competition model, whereas (b) rescaling infected predators can give us a food chain model.*

there is enough prey to sustain enough predator population.

1.4 Predators, prey and prevalence: Oscillations

Oscillations in eco-epidemiology have been often overlooked. A typical eco-epidemiological paper consists of equilibrium-based analysis, i.e. find the steady states and then find their stability. This is important work, necessary for analysing an eco-epidemiological model. However, many eco-epidemiological models contain oscillations. These oscillations are usually not analysed; they are normally only demonstrated by the use of time profiles and phase portraits. Notable exceptions are Hilker and Schmitz (2008) and Kooi et al (2011), where they use bifurcation diagrams to demonstrate various bifurcations in the limit cycles as well as the equilibria.

1.5 Overview of Thesis

This thesis consists of four main chapters, each chapter tackles a different, but complementary, aspect of eco-epidemiology.

In Chapter 2, we will focus on the impact predator–prey oscillations can have on the endemic criteria for diseases to establish within a predator or prey host. Here we establish that the endemic criteria for a disease with density dependent transmission is dependent on the time-averaged host density of the predator–prey oscillations, which is generally not the same as the host density at the (unstable) predator–prey equilib-

rium, leading to the concept of $\overline{R_0}$, the time-averaged basic reproductive number. For frequency dependent transmission, there is no difference in endemic criteria.

In Chapter 3, we will investigate the diseased-predator model from Chapter 2 further, as well as a related, established model (Hilker and Schmitz, 2008), finding a variety of complex dynamics, some of which have not been found in eco-epidemiological models before. In fact, many of the phenomena have rarely been found in ecological and epidemiological models. These results are summarised in Table 3.1.

In Chapter 4, we consider a diseased-prey model similar to one of the models in Chapter 2, but this model considers group-defending prey. This chapter focuses on the coexistence of predators and disease in the prey (a point overlooked in Chapter 2). In particular, we look at cases where predators actually benefit from the presence of the disease. These cases involve the disease restricting prey densities to levels where group defence is weaker.

Lastly, Chapter 5 considers a spatiotemporal diseased-prey model with preytaxis, the movement of predators along prey gradients. Here we will investigate the consequence preytaxis has on disease and predator invasions, with a keen eye on the effect preytaxis has on the travelling wave and its wavespeed. We find that positive preytaxis can speed up predator invasions, whereas negative preytaxis may induce spatiotemporal oscillations/chaos not expected from the non-spatial dynamics. For disease invasions, there are scenarios where preytaxis can increase the infection wave's wavespeed, but the wave can never be slowed down by preytaxis.

Overall, this thesis expands the field of eco-epidemiology, especially with respect to the various effects and bifurcations that (endogenous) oscillatory dynamics may have, whether it be the different endemic criteria in Chapter 2, the various bifurcations and resulting dynamics in Chapter 3, the homoclinic destruction of the coexistent limit cycle in Chapter 4, or the spatiotemporal oscillations found in Chapter 5. Although there have been many papers concerning eco-epidemiology, very few consider the impact predator–prey oscillations can have on the wider eco-epidemiological system.

It is well worth noting that this thesis is completely theoretical. No data is used and no explicit biological system considered for making these models. This was done in attempts to provide general arguments, which help find important and interesting qualitative results and identifying the key parameters.

Chapter 2

Predator–prey oscillations can shift when diseases become endemic[1]

Abstract

In epidemiology, knowing when a disease is endemic is important. This is usually done by finding the basic reproductive number, R_0, using equilibrium-based calculations. However, oscillatory dynamics are common in nature. Here, we model a disease with density dependent transmission in an oscillating predator–prey system. The condition for disease persistence in predator–prey cycles is based on the time-average density of the host and not the equilibrium density. Consequently, the time-averaged basic reproductive number $\overline{R_0}$ is what determines whether a disease is endemic, and not the equilibrium-based basic reproductive number R_0^*. These findings undermine any R_0 analysis based solely on steady states when predator–prey oscillations exist for density dependent diseases.

2.1 Introduction

In epidemiology, the classical method of determining whether a disease will be endemic or die out is by finding the basic reproductive number R_0. The basic reproductive number is understood as the number of secondary infections from an infected individual, during its infectious period, in an otherwise purely susceptible host population (although more general definitions are available, see Bacaër and Ait Dads, 2012;

---

[1]This chapter has previously been published in Journal of Theoretical Biology (Bate and Hilker, 2013b) with kind permission from Elsevier. The published version is available on Science Direct.

Inaba, 2012). If the basic reproductive number is less than one, the disease will not survive, whereas if the basic reproductive number is greater than one, the disease will spread. Typically, this is calculated based on a constant population. However, not all populations are at equilibrium.

Oscillatory dynamics have recently become the focus of many epidemiologists studying both human and wildlife diseases. Although endogenous oscillations like predator–prey oscillations are mentioned occasionally (for example Greenman and Norman, 2007), the investigations that follow are invariably on exogenous oscillations caused by external forcing. These exogenous oscillations include periodic or stochastic forcing caused by seasonality, multi-annual periodic events like El Niño and anthropogenic interventions (Altizer et al, 2006; Greenman and Norman, 2007). Of these, seasonality is probably the most prominent. For example, Grassly and Fraser (2006) state that there are four types of causes of seasonality in human infectious diseases: (a) survival of pathogen outside host; (b) host behaviour; (c) host immune function; (d) abundance of vectors and non-human hosts.

Within this body of work, it has been shown that some exogenous oscillations can shift the endemic threshold (Greenman and Norman, 2007; Bacaër and Abdurahman, 2008; Nakata and Kuniya, 2010, for example). However, populations frequently cycle as the result of endogenous mechanisms. Density-dependence, delay effects and ecological interactions are probably the most prominent of numerous examples (Turchin, 2003). Predator–prey oscillations are particularly iconic, and the field of eco-epidemiology has begun studying the impact diseases have on ecological relationships like predator–prey interactions (and vice versa). So far, it has largely been assumed that the criteria for the disease becoming endemic is the same for predator–prey equilibria and oscillations. For example, papers based on Rosenzweig–MacArthur dynamics have ignored the possibility that they are different (for example Chattopadhyay and Arino, 1999; Chattopadhyay et al, 2003; Haque and Chattopadhyay, 2007; Bairagi et al, 2007). However, Hadeler and Freedman (1989) noted that the endemic thresholds are different for equilibria and oscillations, but they did not explain why. This phenomenon has only recently been rediscovered by Kooi et al (2011), where they briefly noted that the endemic thresholds are not the same, but they did not explain why either. In short, the consequences of oscillatory dynamics caused by predator–prey oscillations on disease establishment have not been thoroughly investigated and have often been overlooked.

In this chapter, we find that the basic reproductive number for a disease is different from the value derived from the (unstable) equilibrium when the host is involved

in predator–prey oscillations. This is the result of the basic reproductive number being based on the time average of the predator–prey oscillations and not on the corresponding predator–prey equilibrium. Two eco-epidemiological models are developed to demonstrate these results. One considers an SI disease in the predators, whereas the other considers an SI disease in the prey. In both models, transmission is density dependent, although we later consider the frequency dependent case as well.

Throughout this chapter, we will refer to the equilibrium-based basic reproductive number as R_0^* and the time-averaged basic reproductive number as $\overline{R_0}$. These 'decorations' allow us to distinguish these numbers from the actual basic reproductive number, R_0, which will be the barometer in which R_0^* and $\overline{R_0}$ are compared to. More precisely, it is the threshold property of R_0 that R_0^* and $\overline{R_0}$ are compared to, i.e the disease-free state is stable for $R_0 < 1$ and is unstable for $R_0 > 1$.

2.2   The models

The models used are based on the Rosenzweig–MacArthur model, i.e. logistic growth of prey, Holling type II functional response and exponential decay of the predator without prey. Hence, the underlying scaled predator–prey model is:

$$\frac{dN}{dt} = rN(1-N) - \frac{NP}{h+N},$$ (2.1)

$$\frac{dP}{dt} = \frac{NP}{h+N} - mP,$$ (2.2)

where N is the prey density and P is the predator density, r is the per-capita growth rate for the prey (when rare), m is the per-capita natural death rate for the predator, and h is the half-saturation density for the Holling type II functional response.

We will assume that there is an SI disease with density dependent transmission. This means the disease will split the host population into a susceptible population (S) and an infected population (I). There is one model where the disease infects predators and an analogous model with the disease infecting the prey. Here we will assume in both models that the disease causes more deaths, but that infected individuals are otherwise identical to susceptible individuals (unless otherwise stated, like in the Extensions (Section 4)). On top of this, all newborns are assumed to be susceptible, i.e. there is no vertical transmission.

We will formulate the models in terms of the total predator and prey populations and the prevalence of the disease in the host population, i.e. the fraction of hosts that

are infected. In other words, $i_P = \frac{I_P}{P} = \frac{I_P}{S_P + I_P}$ and $i_N = \frac{I_N}{N} = \frac{I_N}{S_N + I_N}$, where I_P (I_N) and S_P (S_N) are the infected and susceptible predator (prey) densities, respectively (the original SI models can be found in Appendix 2.A). This scaling is used to demonstrate the effect the disease has on the host in the predator–prey system, something that is not immediately clear when the host population is in two classes. Notice that i_P and i_N can take any value between 0 and 1, where a value of zero means there is no disease and a value of one means that every host is infected.

The scaling and parameters are equivalent to those in Hilker and Schmitz (2008); their model being the same as the diseased predators model except they used frequency dependent infection.

Diseased predators model

$$\frac{dN}{dt} = rN(1-N) - \frac{NP}{h+N}, \tag{2.3}$$

$$\frac{dP}{dt} = \frac{NP}{h+N} - mP - \mu P i_P, \tag{2.4}$$

$$\frac{di_P}{dt} = i_P \left((\beta P - \mu)(1 - i_P) - \frac{N}{h+N} \right). \tag{2.5}$$

Diseased prey model

$$\frac{dN}{dt} = rN(1-N) - \frac{NP}{h+N} - \mu N i_N, \tag{2.6}$$

$$\frac{di_N}{dt} = i_N((\beta N - \mu)(1 - i_N) - r), \tag{2.7}$$

$$\frac{dP}{dt} = \frac{NP}{h+N} - mP. \tag{2.8}$$

In both models, μ is the disease-induced death rate and β is the disease transmissibility. In the diseased prey model, r is defined as a per capita birth rate instead of a growth rate, i.e. there is no density independent mortality (see Appendix 2.A for details). This means that susceptible prey only experience mortality via predation and competition.

Parameter values are chosen such that the predator–prey system has a stable limit cycle in the absence of the disease $\left(\text{i.e. } m < \frac{1-h}{1+h}\right)$. Throughout this chapter, any variable that is 'starred', e.g. P^*, refers to the (unstable) steady state of that variable.

Likewise, any variable that has a 'bar', e.g. $\overline{P}$, is the time-average of that variable over the period. In this chapter, the time-average (of P, say) is defined as $\overline{P} = \frac{1}{T}\int_0^T P\,dt$, where T is the period of the predator–prey limit cycle.

2.3 Results

Several papers have calculated R_0 in a periodic environment (Bacaër and Guernaoui, 2006; Wang and Zhao, 2008; Wesley and Allen, 2009, for example). Here, we find $\overline{R_0}$ by using a Floquet theory argument. However, we only need to focus on the infecteds/prevalence equations since the predator–prey cycles are stable in the original Rosenzweig–MacArthur model (1–2). The details of this argument are in Appendix 2.A. However, it is worth noting that all $\overline{R_0}$'s can be found directly by using the method in Bacaër and Guernaoui (2006, eq.(31)).

2.3.1 Diseased predators

Figure 2-1(a) shows when a disease establishes in an oscillating predator host, as a function of transmissibility, β. For low transmissibility, the disease is not endemic and only disease-free predator–prey oscillations are stable. At $R_0^* = 1$, an unstable endemic equilibrium bifurcates from the unstable disease-free predator–prey equilibrium. For some region after this (the grey region), we have stable disease-free oscillations with an unstable endemic equilibrium, i.e. the disease is not endemic despite $R_0^* > 1$. At $\overline{R_0} = 1$, a stable endemic limit cycle bifurcates from the stable disease-free predator–prey limit cycle. Beyond this, the disease is endemic in oscillation until the stable oscillations and unstable equilibrium collide at a Hopf bifurcation, giving rise to a stable endemic equilibrium.

The crucial point of Figure 2-1(a) is that the system remains disease-free (zero prevalence) in a parameter range well beyond $R_0^* > 1$, where R_0^* is the equilibrium-based basic reproductive number $R_0^* = \frac{\beta P^*}{m+\mu}$ and P^* is the predator density at the disease-free predator–prey equilibrium. This means that the system remains disease-free for a larger parameter range because of the oscillatory dynamics.

Figure 2-1(b) demonstrates that this difference can be attributed to the difference in the time-averaged density of the predator between the equilibrium and oscillations (a corollary of results in Armstrong and McGehee (1980)). A disease is endemic only when the time-averaged basic reproductive number $\overline{R_0} = \frac{\beta \overline{P}}{m+\mu} \geq 1$, where $\overline{P}$ is the time-average predator density for the disease-free predator–prey oscillations (see

Appendix 2.A). The dotted line representing $R_0(\beta) = 1$ gives the invasion condition for a disease, i.e. the critical host density required for the disease to establish. This means that a disease can only become endemic if the time-averaged predator density is above the dotted line. Note that the dotted line intersects both the (unstable) predator–prey equilibrium and the time-average of the predator–prey oscillations at the transcritical bifurcations where the disease becomes endemic. This is consistent with the fact that R_0^* and $\overline{R_0}$ differ only because the (time-averaged) host densities of the disease-free equilibrium and oscillations are different.

2.3.2 Diseased prey

Figure 2-2(a) demonstrates that the (stable) endemic oscillations bifurcate from the disease-free predator–prey oscillations before the (unstable) endemic equilibrium bifurcates from the disease-free equilibrium[2]. This contrasts with Figure 2-1(a) where the oscillations bifurcate after the unstable equilibrium bifurcates. Hence there is a region (the grey region) where the disease is endemic in oscillations despite $R_0^* < 1$. This means that a disease in the prey host becomes endemic at a smaller transmissibility (β) than expected from the standard calculation of the equilibrium-based basic reproductive number $R_0^* = \frac{\beta N^*}{\mu + \frac{P^*}{h+N^*} + rN^*}$, which can be simplified to $R_0^* = \frac{\beta N^*}{\mu + r}$ where N^* and P^* are the respective prey and predator densities at the disease-free predator–prey equilibrium. Instead, the invasion criterion is $\overline{R_0} = 1$, where $\overline{R_0} = \frac{\beta \overline{N}}{\mu + (\frac{P}{h+N}) + r\overline{N}} = \frac{\beta \overline{N}}{\mu + r}$ is the time-averaged basic reproductive number (see Appendix 2.A). Since the predator–prey oscillations have a larger time-averaged prey density than the equilibrium (Armstrong and McGehee, 1980), $\overline{R_0}$ has a smaller threshold value of β to become endemic. This means the disease will find it "easier" to become endemic because of the oscillatory dynamics. The dotted line in Figure 2-2(b) demonstrates that this change in critical β can be solely attributed to the difference between N^* and $\overline{N}$.

2.3.3 Summary

In this section, we have described the difference between the equilibrium-based basic reproductive number R_0^* and the time-averaged basic reproductive number $\overline{R_0}$ for predator–prey oscillations. In all cases we have that $R_0 = \overline{R_0}$. At equilibrium, $R_0 = \overline{R_0} = R_0^*$. However, in oscillations, we generally have $R_0 = \overline{R_0} \neq R_0^*$.

---

[2]Figure 2-2(a) also demonstrates that both predator and disease in prey can co-exist at equilibrium, contradicting the principle of competitive exclusion. This point is explained in much more detail in Chapter 4.

On a side issue, both the diseased predator and diseased prey models demonstrate that the disease can stabilise an oscillating predator–prey system by increasing total host mortality (for a sufficiently large μ and β), in a manner similar to that in Hilker and Schmitz (2008).

2.4 Extensions

2.4.1 Disease alters density dependent mortality in prey host

Previously, infected prey experienced the same density dependence as susceptible prey. We will now change this assumption by letting infected prey experience a different level of density dependence than susceptible prey. Henceforth, we will assume that susceptible prey have a density dependent mortality term of rSN (since the carrying capacity has been scaled to one), whereas infected prey have a density dependent term $rcIN$ (see Appendix 2.A). Here, c is a coefficient that defines the density dependent mortality infected prey experience relative to susceptible prey. If $c = 1$, then the total density dependent mortality becomes rN^2, which is the same as in the original diseased prey model.

While this formulation accounts for different competitive pressures experienced by susceptible and infected individuals, it implies that both susceptibles and infecteds exert the same competitive strength on an individual they interact with. This is a simplifying assumption and in general is not true. In fact, Hochberg (1991) argues that there are four different terms of density dependence in an SI model; the density dependence that (i) susceptibles inflict on susceptibles (called α_{SS}), (ii) susceptibles inflict on infecteds (α_{IS}), (iii) infecteds inflict on susceptibles (α_{SI}) and (iv) infecteds inflict on infecteds (α_{II}). However, since we can assume that there are negligibly few infected individuals when finding R_0^* or $\overline{R_0}$, the density dependent mortalities caused by infected individuals (cases (iii) and (iv)) are negligible on the calculation of R_0^* and $\overline{R_0}$. This means that R_0^* and $\overline{R_0}$ found here are the same as those in a full four-case density dependent model, where $r = \alpha_{SS}$ and $rc = \alpha_{IS}$.

Now, incorporating this assumption into the diseased prey model, we get:

$$\frac{dN}{dt} = rN\left(1 - N\left((1 - i_N) + c\,i_N\right)\right) - \frac{NP}{h + N} - \mu N i_N, \qquad (2.9)$$

$$\frac{di_N}{dt} = i_N\left((\beta N - \mu - rN(c - 1))(1 - i_N) - r\right), \qquad (2.10)$$

$$\frac{dP}{dt} = \frac{NP}{h + N} - mP. \qquad (2.11)$$

In Appendix 2.A, we demonstrate that:

$$\overline{R_0} = \frac{\beta \overline{N}}{\mu + r + r(c - 1)\overline{N}}, \qquad (2.12)$$

as well as $R_0^* = \frac{\beta N^*}{\mu + r + r(c-1)N^*}$.

If $c \neq 1$, then the denominator of $\overline{R_0}$ depends on $\overline{N}$ and we get an overall expression for $\overline{R_0}$ that is hyperbolic rather than linear in $\overline{N}$. If we assume that infecteds suffer more from density dependent mortality than susceptibles (because they are at a disadvantage in competition), then we have $c > 1$. The expression for $\overline{R_0}$ is then much like a Holling type II functional response. This means that $\overline{R_0}$ still monotonically increases with respect to $\overline{N}$, but it saturates to $\overline{R_0}_{max} = \frac{\beta}{r(c-1)}$. A corollary of this is that the disease can never be endemic if $\beta < r(c - 1)$. However, saturation happens beyond all feasible values of $\overline{N}$; consequently, we have $\overline{R_0}$ is 'sublinear' with respect to $\overline{N}$ (Figure 2-3).

Now suppose $c < 1$, i.e. infected prey are better competitors than susceptible prey. (While this assumption seems unrealistic at first glance, Sieber et al, 2013, find that this is possible if density dependence is due to exploitative competition where infecteds take up less resources. If infecteds take up less resources, one would expect that infecteds would have a smaller reproductive rate than susceptibles. Here, however, both populations have the same birth rate. Hence this may not be compatible with $c < 1$.) Notice that although $\overline{R_0}$ does have an asymptote and can be negative for large enough $\overline{N}$, such values of $\overline{N}$ can never be attained since $\overline{N}$ is bounded above by the disease-free carrying capacity, i.e. $\overline{N} \leq 1$. This means that $\overline{R_0}$ is 'superlinear' and monotonically increasing for all feasible values of $\overline{N}$ (Figure 2-3).

Using $\frac{\partial}{\partial i_N}\left(\frac{dN}{dt}\right)$, we get that N increases with i_N if $\mu + r(c - 1)N < 0$. In particular, if $\mu < r(1 - c)$, the prey host at disease-free carrying capacity (i.e. no predators) will increase in density as the disease establishes in the population. This means a disease that reduces density dependent mortality can benefit the infected host if this reduction is greater than the additional disease-induced mortality. If this is the case (which at the moment is hypothetical), the disease will increase the total host population.

2.4.2 Frequency dependent transmission

One key assumption in all the previous models in this chapter is density dependent transmission. Incorporating frequency dependent transmission into the model (9-11), the prevalence equation becomes:

$$\frac{di_N}{dt} = i_N((\beta - \mu - rN(c-1))(1 - i_N) - r). \tag{2.13}$$

The only difference between this and the previous prevalence equation is that βN has become just β. Using the same arguments as before, we get that $R_0^* = \frac{\beta}{\mu + r + r(c-1)N^*}$ and $\overline{R_0} = \frac{\beta}{\mu + r + r(c-1)\overline{N}}$. If $c = 1$, i.e. we are working with the frequency dependent transmission version of the original diseased prey model, we have that $R_0^* = \overline{R_0} = \frac{\beta}{\mu + r}$. This means that the basic reproductive number is independent of host density, whether oscillatory or not. However, if $c > 1$, we have that $\overline{R_0}$ *is monotonically decreasing with host density* $\overline{N}$. This means that disease is endemic when the population is sufficiently small, i.e. $\overline{N} < \frac{\beta - \mu - r}{r(c-1)}$. If $c < 1$, then $\overline{R_0}$ is monotonically increasing with host density. Here, the disease is endemic if the population is sufficiently large, i.e. $\overline{N} > \frac{\beta - \mu - r}{r(1-c)}$.

2.5 Discussion

We have demonstrated that the conditions for a disease to become endemic in a host involved in a predator–prey relationship depend on the time-averaged host density. Rosenzweig–MacArthur predator–prey dynamics are used to show this. Oscillations in such a model have a greater time-averaged prey density and lower time-averaged predator density compared to the corresponding (unstable) equilibrium. This means that predator–prey oscillations make a disease easier to become endemic in a prey host and harder to become endemic in a predator host.

These explanations could also explain the differing basic reproductive numbers observed in Kooi et al (2011), and make some progress towards explaining the basic reproductive number argument from Hadeler and Freedman (1989). The latter is not straight–forward since the disease in their model infects both the prey and predator and only by cross-infection (i.e. infected prey infect susceptible predators and infected predators infect susceptible prey), which complicates the pattern of transmission (see Appendix 2.B for a model description). However, Figure 2-4(a) demonstrates that the disease is not endemic when the hosts cycle despite having an equilibrium-based basic reproductive number greater than one, i.e. $R_0^* > 1$ (like the diseased predator model).

Likewise, Figure 2-4(b) shows that the disease is endemic when the hosts cycle despite having an equilibrium-based basic reproductive number less than one (like the diseased prey model). This means that the equilibrium-based basic reproductive number does not give either an upper nor lower bound for when a disease is endemic in predator–prey oscillations. With two infected compartments, the model in Hadeler and Freedman (1989) is considerably more complicated than the diseased predators or diseased prey models. In another model with two infected compartments (Bacaër, 2007, a malaria model with seasonality in the vector), it was shown that the actual endemic threshold is based on the time-averaged reproductive number with a correction based on the size of the oscillations. Assuming something similar occurs here, the difference in endemic thresholds between predator–prey oscillations and equilibria in Hadeler and Freedman (1989) can largely be explained by the difference in the time-averages, but this difference alone does not give the full picture.

This can have major consequences for disease management and epidemiology. Firstly, it undermines the idea that the equilibrium-based basic reproductive number determines whether a disease would invade deterministically. This somehow resembles the scenario of a backward bifurcation, where a disease may persist (depending on initial conditions or the "history" of the population) even though $R_0 < 1$. Conversely, other bifurcations like saddle–node bifurcations or homoclinic bifurcations can lead to the disappearance of disease even though $R_0 > 1$, but this typically involves host extinction as well (Hilker et al, 2009; Hilker, 2010). Consequently, if oscillations exist in the disease-free predator–prey system, care must be taken when using reproductive number arguments based on equilibria as one can not assume that they are the same for oscillations (like those in Hilker and Schmitz, 2008; Das et al, 2011).

Secondly, there can be profound consequences for the eradication of diseases within predators. A common strategy to help eradicate a disease from a wildlife host is indiscriminate culling or harvesting of the host. For example, hunting/harvesting/culling has been used for controlling chronic wasting disease in some species of deer and elk (Williams et al, 2002), bovine tuberculosis in badgers (Woodroffe et al, 2002) and facial tumour disease in Tasmanian devils (Beeton and McCallum, 2011). However, harvesting/indiscriminate culling corresponds to effectively increasing the constant per-capita death rate. Applying this to a predator population will not decrease, but rather increase the time-average predator density, if the system is cyclic. (This phenomenon is called the 'hydra effect' Abrams, 2009; Sieber and Hilker, 2012). Hence, harvesting will increase disease prevalence in predators and is therefore counter-productive as a control approach.

By contrast, a management action that can be recommended on the basis of this chapter is to enforce endogenous oscillations in an otherwise stable population. The oscillations could bring the time-averaged basic reproductive number $\overline{R_0}$ below one, even though without oscillations R_0^* is greater that one, resulting in long term disease eradication. One such way of forcing oscillations is to utilise the *paradox of enrichment* by increasing the prey's carrying capacity, which will destabilise the predator–prey system.

Lastly, for prey as a host population, a disease will spread more easily under predator–prey oscillations than at equilibrium, thus making eradication harder. Actions that stabilise predator–prey oscillations such as reducing the prey's carrying capacity or increasing the predators death rate can combat this. In particular, indiscriminate culling or harvesting of predators can help eradicate a disease of the prey by stabilising the predator–prey oscillations. This contradicts the 'keeping the herds healthy' hypothesis in Packer et al (2003), where predator removal is suggested to result in more infections in the prey.

The effect of shifting the threshold for the establishment of disease described in this chapter is only due to the difference of the time-averaged host density. Hence, assumptions about the disease (e.g. increased mortality, reduced fertility, vertical transmission or host manipulation) should not change this. Consequently, the difference between R_0^* and $\overline{R_0}$ is largely independent of model assumptions. In fact, the phenomenon reported here does not depend on the predator–prey dynamics itself, but on the fact that the host is oscillating at a different time-averaged density when compared to the equivalent equilibrium density.

One important assumption made in the diseased prey model is that susceptible and infected prey are equally good intra-specific competitors. However, this assumption is likely to be unrealistic in many cases. In the Extensions, using different strengths of density dependence for susceptibles and infecteds, we demonstrate that although the relationship between time-averaged host density and the time-averaged basic reproductive number is no longer linear, they still monotonically increase with each other. This suggests that density dependence does not alter the rule that higher time-averaged densities have higher values of $\overline{R_0}$.

There is one curious result in the case where infected individuals experience significantly less density dependence than susceptibles ($c \ll 1$); in this case, the disease can increase host density. Here, the reduction in density dependent mortality more than offsets the additional disease-induced mortality, giving a total reduction in host mortality. In particular, this means that infection will result in increasing the carrying

capacity of the host population beyond that of a disease-free host population (the per capita growth rate $(r - \mu i_N)$ still decreases with prevalence). This scenario of a disease increasing rather than decreasing the host carrying capacity challenges the typically detrimental impact associated with diseases. We have not searched for any empirical evidence for this theoretical prediction, but we believe this could be an interesting over-looked indirect effect of infectious diseases.

However, there is one crucial assumption throughout this chapter; namely density dependent disease transmission. For a frequency dependent disease, the basic reproductive number would be independent of host density, whether time-averaged or otherwise. If we put together frequency dependent transmission and infected individuals experiencing greater density dependent mortality, we get that the basic reproductive number R_0 is a monotonically decreasing function of host density. This means that the disease is endemic if the host population is below some threshold density. This is contrary to typical epidemiological models where a disease is endemic when above some threshold density.

Frequency dependent transmission and density dependent mortality are common in epidemiological and ecological systems, respectively. Hence, it seems reasonable that a maximum viable host density should exist in some wildlife diseases. In these cases, attempts to eradicate a disease by reducing the (time-averaged) host density (e.g. by indiscriminate culling) could actually help keep a disease endemic. A more general discussion of this effect is in preparation.

The diseased predator model also exhibits bistability and saddle–node bifurcations (Chapter 3, i.e. Bate and Hilker, 2013a; Hurtado et al, 2014), which further undermine the use of basic reproductive numbers in determining the long term dynamics of an eco-epidemiological system.

In summary, density dependent diseases can only become endemic in an oscillating predator–prey system if the time-averaged density of the disease free oscillation is large enough. The time-averaged density is different from the equilibrium-based density that the disease-free oscillations cycle around. This means endemicity can not be determined by the equilibrium-based basic reproductive number. These results can have major consequences on disease management and conservation in oscillating populations.

Acknowledgements

2.A Model formulation and calculation of $\overline{R_0}$

For all models, the equilibrium-based basic reproductive number R_0^* can be found from $\overline{R_0}$ by setting the time-averaged densities ($\overline{N}$ or $\overline{P}$) as the equilibrium value (since the time-average of something at equilibrium is the equilibrium). The converse is generally not true; for example $(P^2)^* = P^{*2}$ but generally $\overline{P^2} \neq (\overline{P})^2$. This example is equivalent to the variance of one data point against (infinitely) many data points, where variance is zero in the former, but variance is non-zero in the latter unless P is constant.

Diseased predator

Incorporating the assumptions in the main text for a disease in the predators, we get:

$$\frac{dN}{dt} = rN(1-N) - \frac{N(S+I)}{h+N}, \tag{2.14}$$

$$\frac{dS}{dt} = \frac{N(S+I)}{h+N} - mS - \beta SI, \tag{2.15}$$

$$\frac{dI}{dt} = \beta SI - (m+\mu)I. \tag{2.16}$$

From an eco-epidemiological point of view, one key question is what a disease does to the host population. This is not entirely clear when the host is split into two different classes. Hence, we will gather all predators, whether susceptible or infected, into one class. This is done by replacing the equation for $\frac{dS}{dt}$ with $\frac{dP}{dt} = \frac{d(S+I)}{dt}$. Consequently, we have:

$$\frac{dP}{dt} = \frac{NP}{h+N} - mP - \mu I. \tag{2.17}$$

From this, we establish that the disease only adds an additional mortality term to the host population. On top of this, by replacing infected predators with disease prevalence, we get the diseased predator equations (3–5) in the main text.

Along the predator–prey limit cycle, if we integrate over the period T of the limit cycle, then the cycle is back where it has started. The same is true if we take the 'per-capita' of the limit cycle. This means that both $\int_0^T \frac{1}{P}\frac{dP}{dt}dt = 0$ and $\int_0^T \frac{1}{N}\frac{dN}{dt}dt = 0$

by the Fundamental Theorem of Calculus, noting that $\frac{1}{P}\frac{dP}{dt} = \frac{d(\ln P)}{dt}$. Armed with this information we get:

$$\overline{R_0} = \frac{\frac{1}{T}\int_0^T \beta P\,dt}{\mu + m} = \frac{\beta \overline{P}}{\mu + m} \tag{2.18}$$

which can be derived from $\frac{1}{T}\int_0^T \frac{1}{I}\frac{dI}{dt}\,dt = \frac{1}{T}\int_0^T \frac{d(\ln I)}{dt}\,dt = 0$ where I is negligibly small.

There is an equivalent formulation of $\overline{R_0}$ from the prevalence equation (5) which can be found by substituting $m = \overline{\frac{N}{h+N}}$ $\left(\text{from } \frac{1}{T}\int_0^T \frac{1}{P}\frac{dP}{dt}\,dt = 0, \text{ where } I\ (i_P) \text{ is negligi-}\right.$ bly small$\Big)$ into the denominator of the above $\overline{R_0}$. However, this formulation is a more complicated formulation of $\overline{R_0}$ and therefore has been omitted.

Diseased prey

Following the modelling assumptions in the main text for a disease in the prey, we get:

$$\frac{dS}{dt} = r(S+I)(1-S) - \frac{SP}{h+(S+I)} - \beta SI, \tag{2.19}$$

$$\frac{dI}{dt} = \beta SI - \frac{IP}{h+(S+I)} - (\mu + r(S+I))I, \tag{2.20}$$

$$\frac{dP}{dt} = \frac{(S+I)P}{h+(S+I)} - mP. \tag{2.21}$$

Recall that there is no vertical transmission, i.e. infected individuals reproduce into the S-class with the same per-capita birth rate r as susceptible individuals. Moreover, both susceptible and infected individuals experience density-dependent mortality (described by the parameter r since the carrying capacity has been scaled to one) and mortality due to predation, but no density-independent mortality.

Like with the diseased predator model, it is more convenient to work with N instead of S. Consequently, we have:

$$\frac{dN}{dt} = rN(1-N) - \frac{NP}{h+N} - \mu I, \tag{2.22}$$

Again, by replacing infected prey with disease prevalence, we get the diseased prey equations (6–8) in the main text.

Just like for the diseased predator results, we integrate over the period T of the limit cycle for the 'per capita' of the limit cycle. Using $\frac{1}{T}\int_0^T \frac{1}{I}\frac{dI}{dt}\,dt = \frac{1}{T}\int_0^T \frac{d(\ln I)}{dt}\,dt = 0$, where I is negligibly small, we get that:

$$\overline{R_0} = \frac{\frac{1}{T}\int_0^T \beta N dt}{\mu + \frac{1}{T}\int_0^T \left(\frac{P}{h+N} + rN\right) dt} = \frac{\beta \overline{N}}{\mu + \overline{\left(\frac{P}{h+N}\right)} + r\overline{N}}. \tag{2.23}$$

By using $r = \overline{\left(\frac{P}{h+N}\right)} + r\overline{N}$ $\left(\text{from } \frac{1}{T}\int_0^T \frac{1}{N}\frac{dN}{dt}dt = 0 \text{ where } I\,(i_N) \text{ is negligibly small}\right)$, $\overline{R_0}$ can be greatly simplified to:

$$\overline{R_0} = \frac{\frac{1}{T}\int_0^T \beta N dt}{\mu + r} = \frac{\beta \overline{N}}{\mu + r}. \tag{2.24}$$

This formulation demonstrates that $\overline{R_0}$ is in fact linear with $\overline{N}$, something that could not be seen from the original formulation of $\overline{R_0}$. It is also the formulation of $\overline{R_0}$ that can be found directly from the prevalence equation (7) found in the main text.

Density dependent mortality

Here, we will allow infected prey to be weaker (or stronger) intra-specific competitors than susceptible prey, and see the effect this has on $\overline{R_0}$ and its relationship with $\overline{N}$.

Starting with the diseased prey model, suppose that infecteds experience density dependence differently to susceptibles. Doing so, we have that the infected population follows:

$$\frac{dI}{dt} = \beta(N-I)I - rcNI - \mu I - \frac{IP}{h+N}, \tag{2.25}$$

where rc is reflects the density dependence infecteds suffer. The corresponding N, i_N, P equations are given in the Extensions section of the main text (9-11).

Working with the infected population equation (or its logarithm), and assuming that I is negligibly small, we get:

$$\overline{R_0} = \frac{\frac{1}{T}\int_0^T \beta N dt}{\mu + \frac{1}{T}\int_0^T \frac{P}{h+N} + rcN dt} = \frac{\beta \overline{N}}{\mu + \overline{\left(\frac{P}{h+N}\right)} + rc\overline{N}}. \tag{2.26}$$

This in itself is not enlightening. However, by substituting $\frac{1}{T}\int_0^T \frac{1}{N}\frac{dN}{dt}dt = 0$ where I (i_N) is negligibly small or by using the prevalence equation we get:

$$\overline{R_0} = \frac{\frac{1}{T}\int_0^T \beta N dt}{\mu + r(1 - \frac{1}{T}\int_0^T N dt) + rc\frac{1}{T}\int_0^T N dt} = \frac{\beta \overline{N}}{\mu + r + r(c-1)\overline{N}}. \tag{2.27}$$

Linking back to the original diseased prey model (when $c = 1$), we had that $\overline{R_0}$ is linear (with respect to $\overline{N}$). This means that the original $\overline{R_0}$ is the transition between the sublinear ($c > 1$) and superlinear ($c < 1$) cases, which makes sense.

2.B   Disease in both predators and prey

The model is from Hadeler and Freedman (1989). It has notable differences to the other models in this chapter beyond just being a disease infecting both predators and prey. Disease transmission is interspecific only, where susceptible predators become infected by feeding on infected prey, and susceptible prey are infected by infected predators. However, the disease-free dynamics are the same (up to rescaling) as the models considered in this chapter, and thus have the same type of oscillations.

Keeping the original notation from Hadeler and Freedman (1989), we have:

$$\frac{dx_0}{dt} = ax\left(1 - \frac{x_0}{K}\right) - \frac{x_0}{A + x_0 + \rho x_1}y - \beta x_0 y_1, \tag{2.28}$$

$$\frac{dy_0}{dt} = -c\frac{B}{B+A}y_0 + c\frac{x_0 + \rho x_1}{A + x_0 + \rho x_1}y - \kappa\frac{\rho x_1}{A + x_0 + \rho x_1}y_0, \tag{2.29}$$

$$\frac{dx_1}{dt} = \beta y_1 x_0 - \frac{axx_1}{K} - \frac{\rho x_1}{A + x_0 + \rho x_1}y, \tag{2.30}$$

$$\frac{dy_1}{dt} = -c\frac{B}{B+A}y_1 + \kappa\frac{\rho x_1}{A + x_0 + \rho x_1}y_0, \tag{2.31}$$

where $x = x_0 + x_1$ is the total prey density, x_0 is the susceptible prey density and x_1 is the infected prey density. Likewise, $y = y_0 + y_1$ is the total predator density, y_0 is the susceptible predator density and y_1 is the infected predator density. Many of the parameters have abstract definitions chosen for analytical simplicity; but some parameters do have important definitions. For example, ρ is the vulnerability to predation of infected prey relative to the susceptible prey (Hadeler and Freedman (1989) stipulated that $\rho > 1$, a restriction we will ignore here), κ is the transmissibility from feeding on infected prey, β is the transmissibility of the disease from infected predator to prey, K is the carrying capacity of the prey, and B is the prey density at the disease-free predator–prey equilibrium (when $B < K$).

In this model, oscillatory disease-free predator–prey dynamics occurs when $B < (K - A)/2$. Likewise, the condition where the (equilibrium-based) basic reproductive number $R_0^* = 1$ is:

$$\beta\kappa = \frac{cB}{A+B}\frac{ax^*(A+x^*)+\rho Ky^*}{\rho Kx^*y^*} = \frac{cB}{A+B}\frac{B+\rho(K-B)}{B\rho(K-B)} \tag{2.32}$$

where (x^*, y^*) is the disease-free (unstable) equilibrium.

(a)

(b)
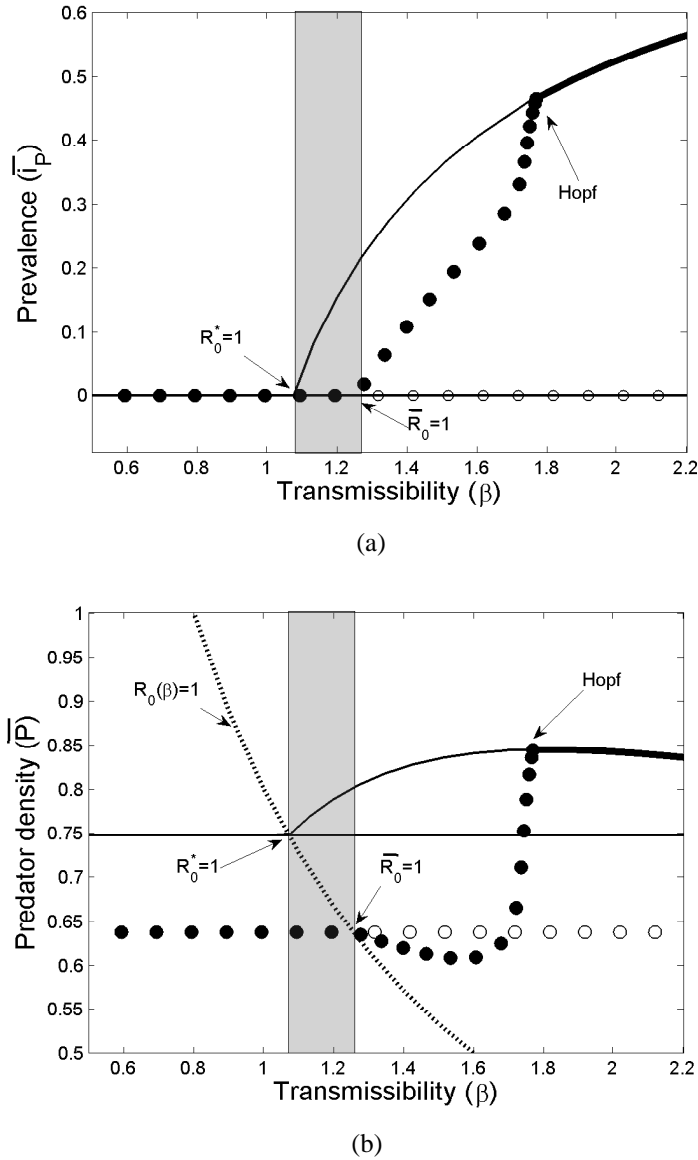
Figure 2-1: *Diseased predators model: Time-averaged bifurcation diagram of (a) prevalence and (b) predator (host) density, with respect to the disease transmission parameter β. The grey region highlights where the disease is* not *endemic despite the equilibrium-based reproductive number being greater than one, i.e. $i_P = 0$ and $R_0^* > 1$. Thick lines mean stable equilibria, thin lines mean unstable equilibria, black (white) circles are time-averages of stable (unstable) oscillations. The dotted line in (b) represents $R_0(\beta) = 1$ and goes through both $R_0^* = 1$ and $\overline{R_0} = 1$, demonstrating that host time-averaged density alone explains the difference in disease invasion. (Parameter values: $\mu = 0.5$, $r = 2$, $h = 0.3$ and $m = 0.3$)*
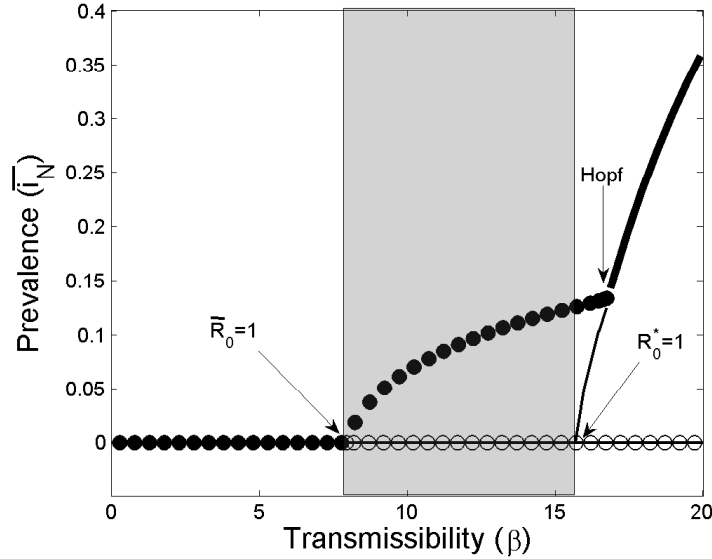
(a)
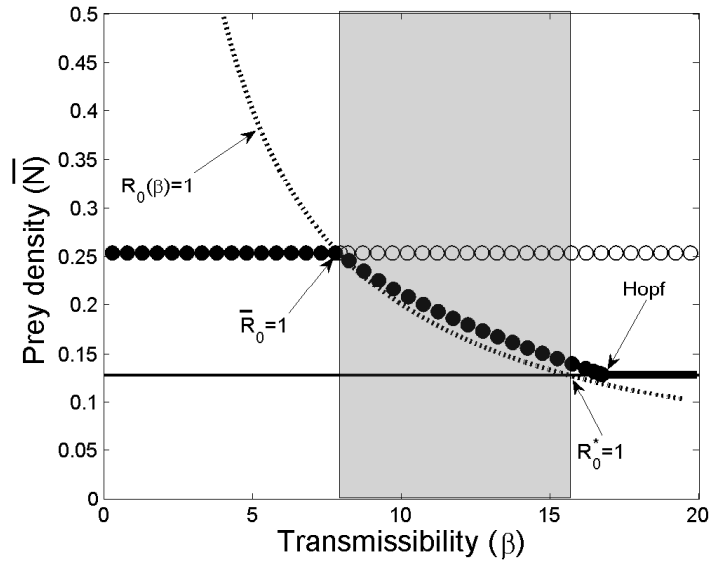
(b)

Figure 2-2: *Diseased prey model: Time-averaged bifurcation diagram of (a) prevalence and (b) prey (host) density, with respect to the disease transmission parameter β. The grey region highlights where the disease is endemic despite the equilibrium-based reproductive number being less than one, i.e. $\overline{i_N} > 0$ and $R_0^* < 1$. The lines and circles have the same meaning as those in Figure 2-1. (Parameter values: $\mu = 1$, $r = 1$, $h = 0.3$ and $m = 0.3$)*
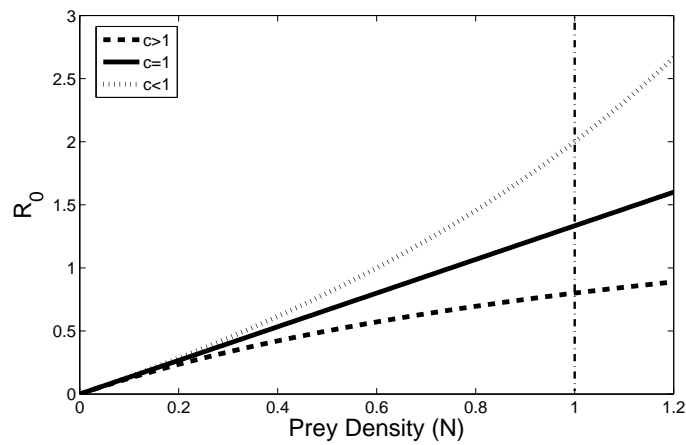
Figure 2-3: *Density dependent mortality: plots of R_0 as a function of host density. This figure demonstrates, with respect to N, R_0 is sublinear for $c > 1$, linear for $c = 1$ and superlinear for $c < 1$. Replace R_0 and N with R_0^* and N^* or $\overline{R_0}$ and $\overline{N}$ to get the equivalent figure of R_0^* and $\overline{R_0}$, respectively. The vertical line represents the disease-free carrying capacity of the prey. Parameter values: $\beta = 2$, $\mu = 0.5$, $r = 1$, $c = 2$ (sublinear) and $c = 0.5$ (superlinear).*
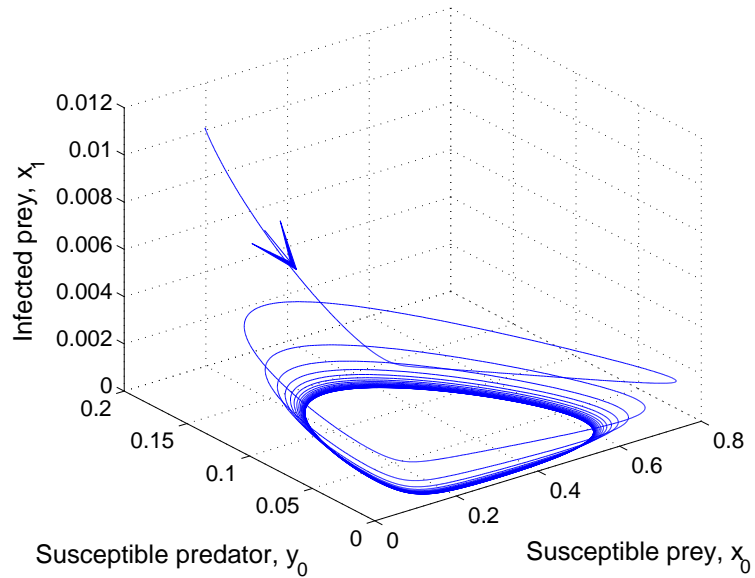
(a)
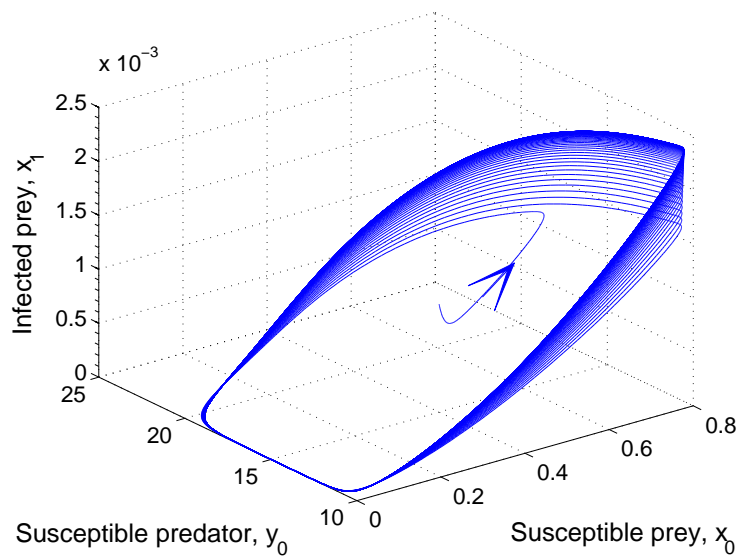
(b)

Figure 2-4: *Disease in both predator and prey: State space diagrams of (a) a disease that does not become endemic in the prey (likewise predator) despite $R_0^* > 1$ ($R_0^* = 1.26$) and (b) a disease that becomes endemic in the prey (likewise predator) despite $R_0^* < 1$ ($R_0^* = 0.8055$). For model details/equations, see Appendix 2.B. Parameter values: (a) $\beta = 3$, $a = 0.1$ and $\rho = 1$, (b) $\beta = 1.4$, $a = 50$ and $\rho = 10$. Other parameters: $K = \kappa = c = 1$ and $A = B = 0.3$.*

Chapter 3

Complex dynamics in an eco-epidemiological model[1]

Abstract

The presence of infectious diseases can dramatically change the dynamics of ecological systems. By studying an SI-type disease in the predator population of a Rosenzweig–MacArthur model, we find a wealth of complex dynamics that do not exist in the absence of the disease. Numerical solutions indicate the existence of saddle–node and subcritical Hopf bifurcations; turning points and branching in periodic solutions; and a period-doubling cascade into chaos. This means that there are regions of bistability, in which the disease can have both a stabilising and destabilising effect. We also find tristability, which involves an endemic torus (or limit cycle), an endemic equilibrium and a disease-free limit cycle. The endemic torus seems to disappear via a homoclinic orbit. Notably, some of these dynamics occur when the basic reproduction number is less than one, and endemic situations would not be expected at all. The multistable regimes render the eco-epidemic system very sensitive to perturbations and facilitate a number of regime shifts, some of which we find to be irreversible.

3.1   Introduction

Complex dynamics like bistability, quasiperiodicity and chaos have been found in isolation in many ecological, epidemiological and eco-epidemiological models. Such

---

[1]This chapter has previously been published in Bulletin of Mathematical Biology (Bate and Hilker, 2013a) and is reproduced here with kind permission from Springer Science+Business Media

complex dynamics mean that small changes to parameters or initial conditions can have large effects on the biological system in the long term. In this chapter, two relatively simple eco-epidemiological models are investigated; both models are of Rosenzweig–MacArthur predator–prey type with an SI disease in the predator with different forces of infection. Within these models, a multitude of different forms of bistability are found, as well as a torus bifurcation, a period-doubling cascade into chaos and even an example of tristability. This diversity of complex dynamics has rarely been seen in one investigation.

Some of these complex dynamics have been discovered in ecology. For example, May (1974) demonstrated that simple discrete-time single-species models can exhibit chaos. However, in continuous-time models, three species are needed to produce more complex dynamics than just equilibria and limit cycles (Seydel, 1988). Gilpin (1979) found the first example of chaos in a continuous-time ecological model while investigating a one-predator–two-prey model, whereas Hastings and Powell (1991) found chaos in a three-species food chain. Bistability is something that has long been established in ecology. One famous example of bistability is the two-species Lotka–Volterra competition model. Likewise, in epidemiology, there exist backward bifurcations with saddle–node bifurcations in several models creating bistability between endemic and disease-free equilibria (van den Driessche and Watmough, 2002).

Within the field of eco-epidemiology, there are a few studies that demonstrate some of these complex dynamics. Hilker and Malchow (2006) found a 'strange periodic' attractor, which seems to be a toric transient that lasts for a substantial time period. Sieber and Hilker (2011) go further than Hilker and Malchow (2006) by demonstrating that chaos, bistability and attractor crises can also occur. The first eco-epidemiological paper to show chaos is Upadhyay et al (2008), using an existing model (Chattopadhyay and Bairagi, 2001), presumably via a cascade of period-doubling bifurcations. Stiefs et al (2009) demonstrate that quasi-periodicity and chaos exist in a generalised predator–prey model with an SIRS disease in the predator, although the focus of the complex dynamics is on cases with saturating forces of infection. Siekmann et al (2010) found bistability when adding a free-living virus stage to models of a predator–prey system with disease in the prey. Kooi et al (2011) found period-doubling cascades into chaos, bistability and transcritical bifurcations of limit cycles. However, the existence of chaos in this model is not surprising, since the model is the same as the three-species Rosenzweig–MacArthur food chain model that was found to be chaotic in Hastings and Powell (1991).

In this chapter, we explore two relatively simple eco-epidemiological models and

demonstrate that a multitude of complex dynamics occurs. Such an array of complex dynamics has rarely been seen before. In Section 3.2, the models are introduced and explained, whereas Section 3.3 is a discussion on the steady states of these models and their stability. Together, these two Sections give the background (the 'basic' dynamics) for the main results in Section 3.4. These main results include bistability of limit cycles, turning points of limit cycles, a period-doubling cascade into chaos, tristability and a stable torus and its homoclinic destruction. All these results are a consequence of the disease since they do not occur in the disease-free predator–prey system.

3.2 The models

We will introduce two similar models, one of which is the model in Hilker and Schmitz (2008) and uses frequency dependent transmission. The other model is the diseased predator model in Chapter 2, i.e. Bate and Hilker (2013b), which is the analogue with density dependent transmission. We will start by describing their similarities before working on each model individually.

For both models, prey density X grows logistically to a carrying capacity K in the absence of predators. In the absence of prey, the predators die out exponentially. Predation is based on a Holling type II functional response and the predator's numerical response is proportional to total predation. Predators are infected by an SI disease, i.e. infection is for life and there is no immunity. Susceptible and infected predators are denoted by the densities S and I, respectively. All predators are born susceptible; there is no vertical transmission from infected mother to offspring. Infected predators suffer an additional disease-induced death rate, but otherwise behave in the same way as susceptible predators.

Starting with a prey–susceptible predator–infected predator model formulation, we will reformulate the models in terms of the total predator and prey populations and the prevalence of the disease in the predator population, i.e. the fraction of predators that are infected. This scaling is used to demonstrate the effect of the disease on the predator in the predator–prey system, something that is not immediately clear when the predator population is in two classes.

3.2.1   Density dependent transmission (DD model)

Incorporating all these assumptions with a density dependent force of infection gives:

$$\frac{dX}{dT} = bX\left(1 - \frac{X}{K}\right) - \frac{aX(S+I)}{H+X}, \tag{3.1}$$

$$\frac{dS}{dT} = \frac{eaX(S+I)}{H+X} - dS - \sigma SI, \tag{3.2}$$

$$\frac{dI}{dT} = \sigma SI - (d+\alpha)I, \tag{3.3}$$

where b is the per capita growth rate of the prey when rare, K the carrying capacity of the prey, H the half-saturation population density, a the maximum predation rate per predator per prey, e the biomass conversion constant, d the natural per capita death rate of the predator, α the disease-induced per capita death rate of the predator and σ the transmissibility coefficient.

Setting $Y = S + I$ as the total predator density and $i = \frac{I}{Y}$ to be the prevalence, i.e. the proportion of infected predators, we get:

$$\frac{dX}{dT} = bX\left(1 - \frac{X}{K}\right) - \frac{aXY}{H+X}, \tag{3.4}$$

$$\frac{dY}{dT} = \frac{eaXY}{H+X} - dY - \alpha Yi, \tag{3.5}$$

$$\frac{di}{dT} = i\left((\sigma Y - \alpha)(1-i) - \frac{eaX}{H+X}\right). \tag{3.6}$$

To reduce the number of parameters, we can rescale using $X = NK$, $Y = eKP$ and $T = \frac{t}{ea}$ to get:

$$\frac{dN}{dt} = rN(1-N) - \frac{NP}{h+N}, \tag{3.7}$$

$$\frac{dP}{dt} = \frac{NP}{h+N} - mP - \mu Pi, \tag{3.8}$$

$$\frac{di}{dt} = i\left((\beta P - \mu)(1-i) - \frac{N}{h+N}\right), \tag{3.9}$$

where $r = \frac{b}{ea}$, $h = \frac{H}{K}$, $m = \frac{d}{ea}$, $\mu = \frac{\alpha}{ea}$ and $\beta = \frac{\sigma K}{a}$. This model is the diseased predator model in Bate and Hilker (Chapter 2 (2.3-2.5, p14), i.e. 2013b)

3.2.2 Frequency dependent transmission (FD model)

Using the same argument, we arrive at the frequency dependent model, the same model as that in Hilker and Schmitz (2008). The parameters are the same as in the density dependent model except that the transmissibility carries a different unit and its dimensionless analogue is rescaled to $\beta = \frac{\sigma}{ea}$. This means that:

$$\frac{dX}{dT} = bX\left(1 - \frac{X}{K}\right) - \frac{aX(S+I)}{H+X}, \tag{3.10}$$

$$\frac{dS}{dT} = \frac{eaX(S+I)}{H+X} - dS - \sigma\frac{SI}{S+I}, \tag{3.11}$$

$$\frac{dI}{dT} = \sigma\frac{SI}{S+I} - (d+\alpha)I, \tag{3.12}$$

becomes:

$$\frac{dN}{dt} = rN(1-N) - \frac{NP}{h+N}, \tag{3.13}$$

$$\frac{dP}{dt} = \frac{NP}{h+N} - mP - \mu Pi, \tag{3.14}$$

$$\frac{di}{dt} = i\left((\beta - \mu)(1-i) - \frac{N}{h+N}\right). \tag{3.15}$$

Notice that (13–15) are almost identical to (7–9), the difference being that (9) has a βP term whereas (15) has a β term.

3.3 Steady states and stability

In this section, we will give a brief summary of the steady states and their stability. For more details, see Appendix 3.A.

For both models, we have the extinction steady state $(0,0,0)$ and the prey-only disease-free steady state $(1,0,0)$. The former is always unstable, whereas the latter is stable when the natural mortality rate of the predators is too high (i.e. $m > \frac{1}{h+1}$). Additionally, the FD model has a disease-induced predator extinction steady state $(1,0,i^*)^2$, where $i^* = 1 - \frac{1}{(\beta-\mu)(1+h)}$. This occurs when the total mortality rate (natural plus disease-induced) of the predators is too high (i.e. $m + \mu i^* > \frac{1}{h+1}$). Notice that this can never happen if $m + \mu < \frac{1}{h+1}$.

---

[2]The disease-induced extinction steady state is a singularity in the original (N,S,I) model. However, in the original model, it represents a disease that can persist (deterministically) in even the smallest host populations, i.e. $\lim_{S+I \to 0} \frac{I}{S+I} = i^* > 0$, allowing the disease to be a driving force in host extinction. This phenomenon would be lost or hidden without rescaling to (N,P,i) (Hilker and Schmitz, 2008).

There can be two other steady states; the disease-free predator–prey steady state $(N^*, P^*, 0)$ and the coexistent (predator–prey–disease) steady state (N^*, P^*, i^*). There is a transcritical bifurcation between these at $R_0^* = 1$ (the equilibrium-based basic reproductive number, Bate and Hilker, 2013b). For the FD model, the coexistent steady state is always unique when it exists. However, for the DD model, there can be up to two coexistent steady states. This opens up the possibility of saddle–node and backward bifurcations of the coexistent steady states.

Finding all the steady states does not give the full story. The underlying predator–prey system is the Rosenzweig–MacArthur model (1963), which is well-known for having oscillatory dynamics caused by a Hopf bifurcation. Hence, by continuity, oscillations should occur in the predator–prey–disease system. Given the existence of stable oscillations, numerical results will be necessary. All bifurcation diagrams are plotted in MATLAB, mostly using data from the continuation software XPPAUT or multiple runs of 'ode45' or 'ode15s' in MATLAB. Equations in MATLAB are 'log transformed' to prevent numerical errors dominating dynamics around zero. MAT-CONT is used for the two-parameter bifurcation diagram in Figure 3-3(a).

3.4 Results

In this section, we will analyse and compare various complex dynamics that have been found in both models when there exist stable predator–prey oscillations in the absence of the disease (so parameters are chosen such that $m < \frac{1-h}{1+h}$). This analysis is largely done by varying the disease transmissibility (β) and the disease-induced death rate (μ). First, we will describe some general results that apply to either model. Then, we will focus on various forms of bistability that can be found in these models. Furthermore, we will demonstrate that the DD model can exhibit tristability, a stable torus and its destruction via a homoclinic bifurcation; whereas the FD model can exhibit chaos via a period-doubling cascade. Lastly, we will describe various forms of regime shifts and hysteresis.

3.4.1 General results

Figure 3-1(a)-(d) are bifurcation diagrams with respect to transmissibility (β) for the FD and DD models, respectively. When transmissibility is small, the disease can not spread fast enough to survive in the long run and thus only disease-free predator–prey oscillations are stable. As transmissibility increases, it will reach a threshold value cor-

responding to $\overline{R_0} = 1$, above which the disease will become endemic in the predator–prey oscillations, giving coexistent oscillations (Figure 3-1(d)). Increasing transmissibility further results in the stabilisation of the coexistent oscillations via a Hopf bifurcation, leading to a stable coexistent equilibrium. The reason for stabilisation is that the total death rate of predators ($m + \mu i^*$) is now large enough to prevent predator–prey oscillations. However, this depends on a sufficiently large disease-induced death rate μ.

In addition to these common effects between the two models, there are aspects that only exist in one of the models.

For the FD model, a disease-induced extinction of the predators can occur when transmissibility (β) (and disease-induced death rate μ) are particularly large (Figure 3-1(a)). This is not possible in the DD model since the disease can not survive when the density of predators becomes small, whereas the disease in the FD model can persist at any predator density, provided transmissibility is sufficiently large.

For the DD model (Figure 3-1(b)), there is a difference between the transcritical bifurcation in the (stable) predator–prey oscillations ($\overline{R_0} = 1$) and the transcritical bifurcation in the (unstable) predator–prey equilibrium ($R_0^* = 1$). This means that the disease has a different endemic threshold in predator–prey oscillations than at equilibrium (Figure 3-1(d)). This difference in thresholds occurs because the time-averaged predator density for predator–prey oscillations is smaller than the predator density for the (unstable) predator–prey equilibrium in Rosenzweig–MacArthur predator–prey models. In the FD model, the thresholds at equilibrium and in oscillations are the same since the thresholds are independent of predator density, i.e. $R_0^* = \overline{R_0} = \frac{\beta}{m+\mu}$. The difference between the thresholds $R_0^* = 1$ and $\overline{R_0} = 1$ has been explored in more detail in Bate and Hilker (2013b). As we will find out in the next subsection, this difference can lead to an interesting form of bistability between the endemic equilibrium and disease-free predator–prey oscillations in the DD model.

3.4.2   Various forms of bistability

In this subsection, we will demonstrate the birth of bistability via a cusp bifurcation of limit cycles and a generalised Hopf bifurcation in both the DD and FD models. We then discuss various forms of bistability, including bistability between endemic and disease-free states in the DD model.

Figure 3-2(a) is a bifurcation diagram with respect to transmissibility (β) for the DD model, like Figure 3-1(b), but with a slightly increased disease-induced death

rate ($\mu = 0.53$ instead of $\mu = 0.5$ in Figure 3-1(b)). Both figures are quite similar with respect to the overall pattern from low to high transmissibility (β) of disease-free oscillations to coexistent oscillations to coexistent equilibria. There is, however, one major difference; namely, there are two turning points of limit cycles in the coexistent oscillations branch. Zooming in around the turning points makes this difference much clearer (Figure 3-2(b)). Due to these two turning points of limit cycles, there are parameter regions with three coexistent limit cycles; the inner and outer limit cycles are stable (black circles in Figure 3-2(b)), whereas the middle limit cycle (the one that joins the two turning points of limit cycles) is unstable (white circles in Figure 3-2(b)). Thus there is bistability between two different limit cycles.

Figure 3-3 demonstrates how two turning points of limit cycles can arise, as well as how this can lead to a subcritical Hopf bifurcation. We start the sequence in Figure 3-3(b)(i) (bottom of Figure 3-3(a)) with a solitary (coexistent) limit cycle just like in Figure 3-1. Increasing μ results in the limit cycle branch being bowed in the middle much like a reverse '$\int$' (Figure 3-3(b)(ii)). Instantaneously, this bowing results in an inflection point, also called a cusp point or bifurcation of the limit cycle (Figure 3-3(b)(iii)). This is shown by the 'CPC' in Figure 3-3(a). Beyond this inflection point there are two turning points (i.e. two saddle–nodes bifurcations) of limit cycles (Figure 3-3(b)(iv)). In between these, there are three limit cycles; one stable limit cycle with small amplitude oscillations, one stable limit cycle with large amplitude oscillations and one unstable limit cycle that is between the other two. Thus there is bistability between two different limit cycles, one with large amplitude and one with small amplitude.

Further increasing μ results in the two turning points spreading apart, and at some point the top/outer limit cycle goes beyond the Hopf bifurcation (when one of the dashed lines moves to the right of the bold Hopf line in Figure 3-3(a)). From this point on, there is some parameter region where there is bistability between the large-amplitude limit cycle and the coexistent steady state. Increasing μ further moves the inner turning point closer to the Hopf bifurcation until they collide resulting in a generalised Hopf bifurcation (Figure 3-3(b)(v)). This generalised Hopf bifurcation is marked 'GH' in Figure 3-3(a). Increasing μ beyond this, there is a subcritical Hopf bifurcation and only one turning point (Figure 3-3(b)(vi)). In this case, there is bistability only between the outer coexistent limit cycle and the coexistent equilibrium.

This bifurcation sequence occurs in both the DD and FD models (see caption of Figure 3). Consequently, both models can exhibit bistability between either two coexistent oscillations (one with large-amplitude and one with small-amplitude) or between

a coexistent oscillation and a coexistent equilibrium. There is another form of bistability that, to the authors' knowledge, can only occur in the DD model: bistability between the coexistent equilibrium (or small-amplitude coexistent oscillations) and disease-free oscillations. This occurs when the Hopf bifurcation is to the left of the transcritical bifurcation of limit cycles at $\overline{R_0} = 1$ (Figure 3-4 is an example of this kind of bistability). Bistability in the DD model between coexistent equilibria and either coexistent or disease-free oscillations model has also been found in Hurtado et al (2014), although they dismiss such bistability occurring in the FD model.

3.4.3 Torus bifurcations and tristability

Figure 3-4 illustrates many phenomena not shown previously in this chapter:

1. There is a saddle–node bifurcation of the coexistent equilibrium.

2. There is bistability between disease-free oscillations and coexistent equilibria. Normally, this bistability occurs when the Hopf bifurcation is to the left of the transcritical bifurcation of limit cycles. However, if the Hopf bifurcation is on the lower 'saddle' branch of equilibria (like in Figure 3-4) this bistability occurs when the saddle–node bifurcation is to the left of the transcritical bifurcation of limit cycles.

3. The saddle–node and Hopf bifurcations have switched positions (previously, the Hopf bifurcation was located on the upper 'node' branch of equilibria, whereas in Figure 3-4, the Hopf bifurcation is located on the lower 'saddle' branch of equilibria). This means that a fold–Hopf bifurcation (sometimes called a zero–Hopf bifurcation) has occurred when the two bifurcations meet.

4. Along the unstable limit cycle arising from the Hopf bifurcation, a torus bifurcation occurs, which stabilises the limit cycle until a turning point of limit cycles is reached.

5. The stable torus created at the torus bifurcation is destroyed by a homoclinic bifurcation as the torus collides with the saddle limit cycle. Between the turning point of limit cycles and the homoclinic destruction of the torus, there is a region of tristability (the grey region of Figure 3-4). Figure 3-5(a) demonstrates this tristability by showing that three different attractors can be obtained just by changing the initial condition, whereas Figure 3-5(b) demonstrates that the toric attractor gives quasiperiodic dynamics.

The cause of the tristability seems to be the combination of (i) the Hopf bifurcation colliding with the saddle–node bifurcation, creating a fold–Hopf bifurcation, and (ii) a generalised Hopf bifurcation leading to the creation of a turning point of limit cycles near the Hopf bifurcation (like in Figure 3-3) occurring soon after the fold–Hopf bifurcation. By varying the disease-induced death rate, μ, and assuming all other parameters are the same as Figure 3-4, tristability occurs for values of μ beyond the fold–Hopf bifurcation ($\mu \approx 0.95$) and the generalised Hopf bifurcation ($\mu \approx 0.97$), i.e. tristability occurs for $\mu \gtrsim 0.97$.

The torus that appears at the (supercritical) torus bifurcation grows until it collides with another invariant set. In Figure 3-4 ($\mu = 2$), the torus breaks down as it seems to collide with the saddle limit cycle to form a homoclinic orbit. (This is clearer in Figure 3-4(b) since in Figure 3-4(a), the torus looks as if it is close to the unstable equilibrium at the homoclinic bifurcation, which is not the case). Figure 3-6(a) and (b) are Poincaré sections before and after this homoclinic bifurcation, respectively, showing the homoclinic destruction of the torus. Figure 3-6(a) shows a closed loop in the Poincaré section, consistent with quasi-periodic dynamics on a stable torus[3], whereas Figure 3-6(b) shows a loop in the Poincaré section that is broken after many iterations, consistent with a long quasi-periodic transient. Figure 3-6(c) is a sketch of the mechanism behind the homoclinic destruction of the torus. The saddle limit cycle (seen as a saddle point in the Poincaré section) and stable torus (seen as a stable limit cycle in the Poincaré section) approach each other (top left of Figure 3-6(c)). Instantaneously, the stable torus and saddle limit cycle collide to form a homoclinic orbit in the Poincaré section (top right of Figure 3-6(c)). Beyond this, although there are quasiperiodic transients, the stable torus no longer exists, leaving just the saddle limit cycle and unstable limit cycle (bottom middle of Figure 3-6(c)). In the case of Figure 3-4, after the homoclinic destruction of the torus, trajectories near the original torus seem to eventually converge to the disease-free predator–prey oscillations, after some quasiperiodic transient.

The existence of a stable torus should not be too much of a surprise. In fact, Kuznetsov (1995, p.300) states that fold–Hopf bifurcations, the interaction between fold (i.e. saddle–node) and Hopf bifurcations, can lead to tori. In the FD model, however, torus bifurcations and tristability have not been found. The reason is that

---

[3]Ulrike Feudel (pers. comms. after publication) mentioned that the kink suggests that this torus has become chaotic as the stable and unstable manifolds twist around each other. This could be investigated using Lyapunov exponents. However, this does not undermine the idea of tristability, nor the existence of tori for parameter values nearer the torus bifurcation. All it does is 'muddy' the transition around the homoclinic bifurcation.

there is no 'fold' in the FD model. Likewise, there is no saddle–node bifurcation to provide a second equilibrium branch which may lead to another set of stable dynamics. Consequently, the frequency dependent model probably does not have either tristability or invariant tori, although we can not exclude these phenomena.

It is worth noting that in this scenario, 'living on the torus' can be a reasonably good scenario for the disease, predator and prey. For $\beta = 27.4$, the minimum values are $N \approx \exp(-3.5)$, $P \approx \exp(-4)$ and $i \approx \exp(-11)$, whereas near the homoclinic orbit at $\beta = 27.54513$ (Figure 3-6(a)) the lows are $N \approx \exp(-5)$, $P \approx \exp(-6)$ and $i \approx \exp(-25)$. For example, if β increases from a region with a stable torus to a region where it has broken down, trajectories near the previously stable torus will now eventually approach (after some quasiperiodic transient) the disease free predator–prey oscillations. These oscillations have much more severe lows for both predator and prey (approximately $\exp(-19)$ and $\exp(-43)$, respectively) which in reality could lead to stochastic extinction of the predator and/or prey.

At $\mu = 1$ (with other parameters the same as Figure 3-4), there is a similar torus/limit cycle tristability (since $\mu \gtrsim 0.97$). However, the parameter region is very small, which also makes it more difficult to numerically investigate how the torus disappears. In this case, the lows of each variable are not as severe as the case of $\mu = 2$ (Figure 3-4). The authors suspect that this breakdown is either the result of the same homoclinic orbit at the saddle limit cycle or the 'hole' of the torus shrinks to nothing, colliding with the unstable (saddle point) steady state it surrounds. Following the breakdown of this torus for $\mu = 1$, after some quasiperiodic transient, the system seems to settle down at the endemic equilibrium, which is different to the $\mu = 2$ (Figure 3-4) case where the disease-free oscillations are approached.

3.4.4   Period-doubling and chaos

In the FD model, increasing the disease-induced death rate (μ), period-doubling bifurcations begin to arise. By the time $\mu = 12$, three period-doubling bifurcations have occurred (Figure 3-7(a)), resulting in the existence of an '8-cycle' (Figure 3-7(b)). Figure 3-8 demonstrates that these period-doubling bifurcations form part of a period-doubling cascade, which results in chaotic dynamics soon after $\mu = 12$.

We also have a region of bistability in Figure 3-7(a), between coexistent limit cycles (including 2-cycles) and coexistent equilibria. This leads to the possibility of bistability between coexistent chaos and coexistent equilibria/small-amplitude limit cycles.

In the DD model, period-doubling bifurcations have not been found. However, we suspect that period-doubling bifurcations and the cascading into chaos phenomenon might exist in the DD model. Additionally, since bistability seems to be at least as common in the DD model, compared with the FD model, bistability between coexistent chaos and coexistent equilibria/small-amplitude limit cycles might also exist in the DD model.

3.4.5 Regime shifts and hystereses

There is one distinct phenomenon common to Figures 3-2, 3-3, 3-4, 3-7; the possibility of regime shifts and hystereses. Regime shifts are large, abrupt, persistent changes in the structure and function of a system (Biggs et al, 2009). Here, we will restrict the definition of regime shifts to that of 'critical transitions' from Scheffer (2009); the drastic change towards another state caused by minor perturbations and/or a gradual change in the system (i.e. parameters), This definition ignores drastic changes caused by large and sudden changes to the system. Using this definition, a regime shift occurs when there is a discontinuity (jump) in stable attractors when varying a particular parameter. Here, there are many different regime shifts because of the existence of saddle–node bifurcations, turning points of limit cycles, bistability, tristability and the homoclinic destruction of a stable torus. We will separate regime shifts into two different classes; (globally) reversible and (globally) irreversible.

A (globally) reversible regime shift is a regime shift such that there is a (possibly complex) sequence of small alterations in the bifurcation parameter that will lead back to the starting point, via a hysteresis loop. Notice that we mention globally, since we are describing recovering to the original state via some potentially long and complicated path and not by a small, local change. An example of a reversible regime is in Figure 3-7; starting just to the left of the turning point of the coexistent oscillations, slowly increasing transmissibility beyond the turning point will mean that the system will eventually approach the coexistent equilibrium after some oscillatory transient. Now that we 'sit' on the endemic equilibrium, reducing transmissibility slowly will not deviate from the equilibrium until the Hopf bifurcation is passed, far below the original transmissibility. Below the Hopf bifurcation, the system will slowly approach the endemic oscillations (possibly a 2-cycle). Once there, slowly increasing the transmissibility will move the system towards the original state near the turning point on the endemic oscillations.

A (globally) irreversible regime shift is a regime shift where there is no such se-

quence of small alterations to get back to the starting point, i.e. there is no hysteresis loop. This means that once the system has moved away from the starting point, it can never return without a dramatically large perturbation away from another stable state. For example, in Figure 3-4, there seems to be no plausible way of approaching the endemic limit cycle/torus via either stable oscillations or equilibria. This means when starting on the stable coexistent limit cycle/torus, slowly decreasing transmissibility below the turning point of coexistent oscillation or increasing transmissibility beyond the homoclinic destruction of the torus would lead to the end of coexistent limit cycle/torus forever.

3.5   Discussion

In this chapter, we explored two relatively simple eco-epidemiological models and found an unusually large variety of complex dynamics. The variety of complex dynamics found in these models, which is summarised in Table 3.1, is much broader than in previous studies in eco-epidemiology and most studies in ecology and epidemiology.

We found that the Hopf bifurcation between the coexistent steady state and the coexistent periodic orbit can become subcritical, via a cusp bifurcation of limit cycles. Consequently, bistability between coexistent oscillations and coexistent equilibria or between two different coexistent oscillations can occur in both the DD and FD models. Combining this with the fact that there is a difference between R_0^* and $\overline{R_0}$ in the DD model (see Chapter 2, i.e. Bate and Hilker, 2013b, for more details), there are also scenarios where there is bistability between a coexistent equilibrium and disease-free predator–prey oscillations. In these scenarios, it is the initial condition that determines whether the disease can become endemic to a stable equilibrium or not. In particular, if the saddle–node bifurcation is biologically realistic, there are scenarios where the disease is endemic (at equilibrium, oscillation or torus, Figure 3-4) despite both R_0^* and $\overline{R_0}$ being less than one. This is reminiscent of a backward bifurcation, a phenomenon found in a few epidemiological models like some in van den Driessche and Watmough (2002).

In the previous paragraph, we concluded that the disease can persist despite both R_0^* and $\overline{R_0}$ being less than one. However, we can say more; Figure 3-4 demonstrates that there can be two stable coexistent states despite both R_0^* and $\overline{R_0}$ being less than one. This goes beyond the usual backward bifurcation since Figure 3-4 demonstrates that the disease can persist in two stable states, one stable state is an equilibrium whereas

the other is (quasi-)oscillatory, despite both R_0^* and $\overline{R_0}$ being less than one.

We demonstrated that period-doubling exists in the FD model. In fact, we have shown that period-doubling bifurcations can cascade into chaos. We have not found period-doubling in the DD model, however, the authors believe that period-doubling bifurcations (and the cascade into chaos) might occur.

One result in this chapter is the existence of hystereses and regime shifts. With all the bistability, tristability and homoclinic orbits, there are many examples of regime shifts. Most of these regime shifts can be reversed via some long and complex sequence of small changes in parameter value. It is worth noting that such sequences may be impractical, not feasible or downright impossible in reality. However, some regime shifts can not be reversed. In particular, we found that the stable coexistent torus/oscillations in Figures 3-4, 3-5, 3-6 are not recoverable when lost without large perturbations.

One aspect that is novel in this chapter is the scenario of tristability. Tristability seems particularly rare in ecological and epidemiological models. The authors are not aware of any previous examples of tristability in eco-epidemiological papers, with only a few works finding bistability (Siekmann et al, 2010; Kooi et al, 2011; Sieber and Hilker, 2011). In fact, the most examples the authors have found of tristability in ecology or epidemiology typically involve one or more Allee effects. For example, Hilker et al (2009) found tristability when adding disease to a population with an Allee effect, whereas González-Olivares and Rojas-Palma (2011) found tristability when combining a predator–prey interaction with a Holling type III functional response and an Allee effect in the prey. Likewise, Berezovskaya et al (2010) found tristability when considering a predator–prey interaction with linear functional response, prey refuge and an Allee effect in the prey. Tristability in these models is not particularly surprising; Allee effects usually imply bistability, so tristability only requires the creation of one unexpected stable equilibrium or limit cycle. An example of tristability that does not involve Allee effects is found in Beardmore and White (2001); here there is an infectious disease in a population with complex social group structure. All these papers have one aspect in common, the tristability is between several equilibria (Beardmore and White, 2001; Hilker et al, 2009) or two equilibria and an oscillation (Hilker et al, 2009; González-Olivares and Rojas-Palma, 2011; Berezovskaya et al, 2010), with one or more of the equilibria being (semi-)trivial. In this chapter, the tristability is between a disease-free (semi-trivial) oscillation and two coexistent states, one equilibrium and one (quasi-)oscillatory. However, both coexistent states, as previously mentioned, are not expected to exist from the usual 'R_0 argument' as both $R_0^* < 1$ and $\overline{R_0} < 1$. On top

of this, the coexistent torus/limit cycle in Figure 6 can not be found by the usual steady state and stability analysis.

We can confirm that a disease with density dependent transmission can have the same stabilising effect as the disease with frequency dependent transmission has on a predator found in Hilker and Schmitz (2008), taking predator–prey oscillations to endemic equilibrium. The reason why this occurs is that the disease increases total host mortality (from mP to $(m + \mu i)P$), which will dampen the boom and bust of Rosenzweig–MacArthur predator–prey dynamics. Also, we have demonstrated that disease in the predators can greatly influence not only predator (host) density, but also interacting species like the prey.

The models used in this chapter are relatively simple for eco-epidemiological models as the disease only increases host mortality. This means infection does not change how effective the predator is at searching, handling and eating prey as well as reproduction. This point is particularly clear in the predator–prey–prevalence equations (7–9) and (13–15), where the disease has no direct influence on total prey density and only influences the predator population via additional mortality. Likewise, the disease is only an SI disease, with no recovery, latency or immunity. Also, the models use the standard frequency dependent and density dependent forces of infection.

These two forces of infection are the two default choices when modelling disease transmission, largely because they are relatively simple and can be mechanistically derived using assumptions based on contact rates. However, in wildlife diseases, there have been mixed results to whether these forces of infections are realistic (McCallum et al, 2001; Ferrari et al, 2011). Despite this, they are still seen as the benchmarks of which all other forces of infection are compared (Begon et al, 2002a).

The summary of results in Table 3.1 shows that density dependent and frequency dependent transmission can yield distinctly different dynamics. Note that tristability and different endemic thresholds between limit cycles and equilibrium are not possible with frequency dependent transmission. On top of this, there are relatively small regions of coexistence between predator and disease in the frequency dependent transmission if the disease-induced mortality (μ) is large. If more complex, non-linear forces of infection were used, one would expect some of the complex dynamics found in these models (especially the density dependent model, since many non-linear forces of infection like those based on power laws or saturating contact rates can be simplified to a density dependent force of infection via parameter or limit assumptions) as well as other complex phenomena. In particular, the endemic thresholds R_0^* and $\overline{R_0}$ would be different for most forces of infection, with frequency dependent transmis-

sion being the main exception. This means that, unlike frequency dependent transmission, most forces of infection could have bistability between endemic and disease-free states. However, both models have bistability and both are suspected to have chaos following a period–doubling cascade, which suggests that such phenomena also exist for a wide range of forces of infection.

There is a caveat to some of these results in this chapter, one that is common with many models that exhibit chaos and complex dynamics; dangerously small population sizes (Berryman and Millstein, 1989; Thomas et al, 1980). Some of the interesting dynamics occur in scenarios of major boom and bust, cases that are likely to cause stochastic extinctions (this problem depends on the predator/prey rescaling; in particular, it depends on the carrying capacity of the prey in the original model, K). In particular, looking at the phase space plots illustrating tristability in Figure 3-5, we can see that the predator–prey oscillations (and to a lesser extent the coexistent torus) get very close to the origin. Although various simulations were investigated, the search was not exhaustive and there may be parameter values that do not result in dramatic boom and bust but still contain similar complex dynamics. For example, the torus at $\mu = 1$ (other parameters are the same as in Figure 3-4) suffers less from the dangerously low populations than the example in Figures 3-4, 3-5, 3-6 where $\mu = 2$. In particular, we only investigated scenarios where disease-free predator–prey oscillations exist. There could be scenarios where complex dynamics like oscillatory dynamics, bi-/tristability and chaos occur when, in the absence of the disease, only stable equilibria exist; but we stress that this has not been investigated in this chapter.

The existence of a torus bifurcation (equivalent to a Neimark–Sacker bifurcation of the Poincaré map) poses many unanswered questions. We have demonstrated one case where the torus seems to be broken by a homoclinic orbit of a saddle–cycle. However, there are many other ways how a torus can bifurcate or disappear. For example, the torus could experience period doubling bifurcations into chaos or there could be phase locking into a periodic orbit. The analysis in this chapter is restricted to just one set of parameter values, largely because of the interesting case of tristability. This means there is much more to explore in relation to the stable torus than is found this chapter.

The results in the FD model are directly comparable with Hilker and Schmitz (2008). Figure 3-1 uses parameter values not too dissimilar to those in Hilker and Schmitz (2008). As we make the disease dynamics 'faster' (i.e. higher disease-induced death rate μ with higher transmissibility β), the system becomes more complex as bistability and period doubling cascades arise. However, increasing μ gives smaller ranges of β where coexistence can occur (complex or not). This makes it less likely for

coexistence to occur for high μ, a point that can be seen in Hilker and Schmitz (2008, Figure 4). In the DD model, we suspect a similar pattern for fast disease dynamics. However, there is no upper limit in transmissibility (β) for endemic coexistence since there is no disease-induced extinction of the predator in the DD model.

In the absence of the disease, the predator–prey interaction can only lead to two types of stable dynamics; stable equilibria and stable oscillations. This means that the bistability, tristability, period-doubling into chaos, stable tori and homoclinic orbits (and much more, see Table 3.1) exist because of the interaction with the disease in the predator. The regimes of multistability imply that the eco-epidemic system may be extremely sensitive to perturbations (e.g. due to stochastic events, control actions like culling or gradual trends in environmental conditions). This can trigger a number of regime shifts, some of which we have identified to be irreversible. The regime shifts may also be accompanied by long-lasting transients of former attractors.

In summary, we can conclude that diseases can greatly influence the dynamics of the host population and other species interacting with the host. In other words, eco-epidemiology can give profoundly different results than just the background ecology. Similarly, predation can make disease dynamics more complicated.

Acknowledgements

3.A   Steady states of FD and DD models

There are two key differences between the DD and FD model. One is the existence of a disease-induced extinction of the predator in the FD model. The other is that there can be only one coexistent steady state in the FD model as the corresponding value of i^* is known; whereas in the DD model, there can be one or two coexistent steady states.

3.A.1   Trivial/semi-trivial steady states

- Both models: $(0,0,0)$ which always exists and is always unstable

- Both models: $(1,0,0)$ which always exists and is stable if $m > \frac{1}{1+h}$, unstable otherwise

	FD model	DD model
Disease stabilisation	✓(Hilker and Schmitz, 2008)	✓(Fig. 3-1(b)-(d))
Different endemic thresholds	✗, $R_0^* = \overline{R_0}$ (Chapter 2, i.e. Bate and Hilker (2013b))	✓, $R_0^* > \overline{R_0}$ (Chapter 2, i.e. Bate and Hilker (2013b))
S–N bifurcation of Eq	✗(Appendix 3.A)	✓(Fig. 3-4)
S–N bifurcation of LC (turning points)	✓(Fig. 3-2,3-3)	✓(Fig. 3-2,3-3)
Subcritical Hopf	✓(Fig. 3-3,3-7(a))	✓(Fig. 3-3)
Cusp bifurcation of LC	✓(Fig. 3-3)	✓(Fig. 3-3)
Bistability ...	✓	✓
... between Co LC and Co Eq	✓(Fig. 3-3,3-7(a))	✓(Fig. 3-3)
... between 2 Co LC	✓(Fig. 3-2,3-3)	✓(Fig. 3-2,3-3)
... between DF LC and Co Eq/LC	✗	✓(Fig. 3-4)
... between Co Chaos and Co Eq/LC	✓? (Fig. 3-7)	✓?
Torus bifurcation	✗?	✓(Fig. 3-4)
Homoclinic bifurcation	✗?	✓, destruction of torus (Fig. 3-4,3-6)
Tristability	✗?	✓, between DF LC, Co Eq and Co LC/Torus (Fig. 3-4,3-5)
Period doubling bifurcation	✓, cascades into chaos, (Fig. 3-7,3-8)	✓?
Regime Shifts and hysteresis	✓, Reversible found only	✓, Reversible and irreversible

Table 3.1: *Summary of complex dynamics found in the DD and FD models: '✓' means found, '✗' means can not occur in this model, '✓?' means that not found in this chapter but we suspect can occur in this model and '✗?' means that we do not believe this can occur but have not completely discounted it. 'Co': Coexistent, 'DF': Disease-free, 'Eq': Equilibria, 'LC': Limit cycles, 'S–N': Saddle–Node.*
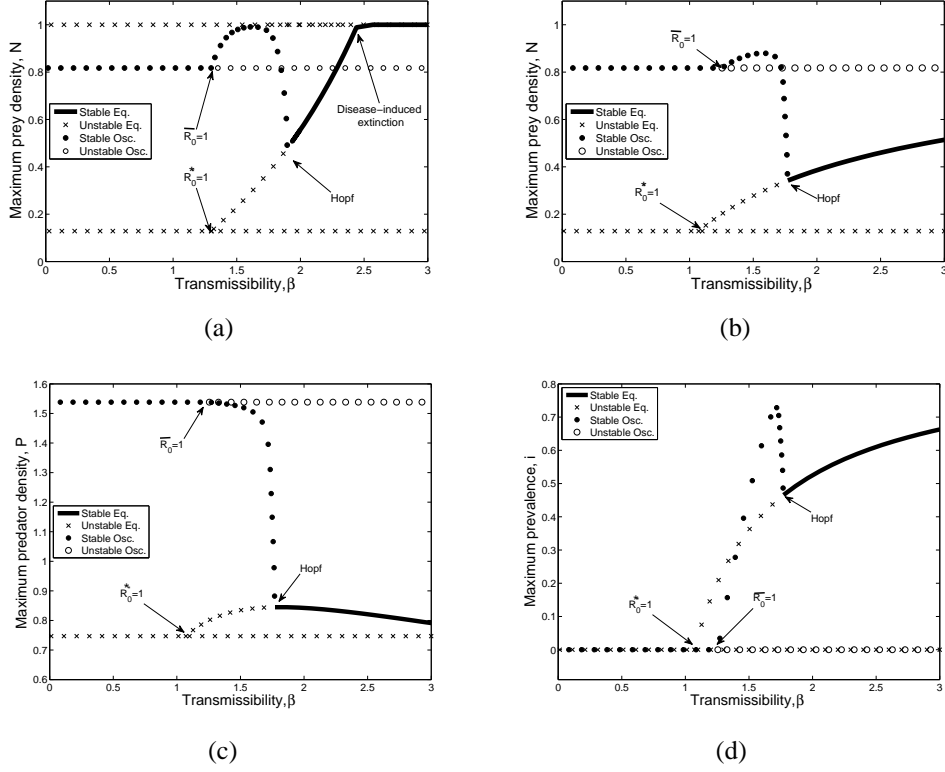
Figure 3-1: *Bifurcation diagrams of (a) the FD model and (b),(c),(d) the DD model, demonstrating the progression (with increasing transmissibility) from disease-free oscillations to endemic oscillations to an endemic equilibrium and, in (a) only, to disease-induced extinction of the predators. (a) and (b) show the (maximum) prey density (N) with respect to transmissibility (β), whereas (c) and (d) show maximum predator density and maximum prevalance, respectively. The trivial steady states have been omitted as well as the prey only steady state in (b). (b) is the same as Figure 2-1 in Chapter 2, i.e. Bate and Hilker (2013b) (but without the time-averaging), whereas (a) is comparable to Figure 2(a) in Hilker and Schmitz (2008) (but with different parameter values). Parameter values: (a) $\mu = 1$, $r = 1$, $h = 0.3$ and $m = 0.3$ (FD model); (b),(c),(d) $\mu = 0.5$, $r = 2$, $h = 0.3$ and $m = 0.3$ (DD model).*

- Both models: $(N^*, P^*, 0)$, where $N^* = \frac{hm}{1-m}$ and $P^* = r(h+N^*)(1-N^*)$. This exists when $m < \frac{1}{1+h}(< 1)$. It is stable if $N^* > \frac{1-h}{2}$ (equivalently $m > \frac{1-h}{1+h}$ (Hopf bifurcation)) and $R_0^* < 1$, where R_0^* equals $\frac{\beta P^*}{m+\mu}$ (DD model) and $\frac{\beta}{m+\mu}$ (FD model).

- FD model only: $(1,0,i^*)$ where $i^* = 1 - \frac{1}{(\beta-\mu)(1+h)}$. This exists when $\beta - \mu > \frac{1}{1+h}$ and is stable if $m + \mu i^* > \frac{1}{1+h}$, unstable otherwise.

- (FD model only: $(0,0,1)$. This is always unstable.)

- (FD model only: $(0,0,i^*)$. i^* is unspecified. This only exists when $\beta = \mu$, which is not generally true. This is always unstable.)

3.A.2 Coexistent steady state(s)

DD model

The coexistent equilibria for the DD model are of the form (N^*, P^*, i^*), where $N^* = \frac{h(m+\mu i^*)}{1-(m+\mu i^*)}$, $P^* = r(h+N^*)(1-N^*)$ and $i^* = 1 - \frac{N^*}{h+N^*}\frac{1}{\beta P^* - \mu} = 1 - \frac{m+\mu i^*}{\beta P^* - \mu} = \frac{\mu(1-i^*)-m+\beta P^*}{\beta P^* - \mu}$.
This exists when $i^* < \frac{1-m}{\mu}$ ($N^* > 0$), $i^* < \frac{1}{\mu(h+1)} - \frac{m}{\mu}$ ($N^* < 1$, i.e. $P^* > 0$), $P^* > \frac{\mu}{\beta}$
(for $i^* < 1$) and $P^* > \frac{\mu+m}{\beta}$ (for $i^* > 0$).

The strongest of these conditions are $i^* < \frac{1}{\mu(h+1)} - \frac{m}{\mu}$ and $P^* > \frac{\mu+m}{\beta}$, which are
the conditions that $R_i^p > 1$ (the predators' reproductive number given an infection is
present) and $R_0^* > 1$, (the diseases' reproductive number).

It is not clear whether (N^*, P^*, i^*) has only one solution. Consequently, this must
be solved. For tidiness, let $D = m + \mu i^*$. Starting
with $\frac{D-m}{\mu}$ ($= i^*$), we get:

$$\frac{D-m}{\mu} = 1 - \frac{D}{\beta P - \mu} \tag{3.16}$$

$$= 1 - \frac{D}{\beta r(h+N)(1-N) - \mu} \tag{3.17}$$

$$= 1 - \frac{D}{\beta r(h + \frac{hD}{1-D})(1 - \frac{hD}{1-D}) - \mu} \tag{3.18}$$

$$= 1 - \frac{D(1-D)^2}{\beta rh(1-D-hD) - \mu(1-D)^2}. \tag{3.19}$$

After some further rearrangement, we get:

$$0 = \left(\frac{D-m}{\mu} - 1\right)\beta rh(1-D-hD) + (m+\mu)(1-D)^2 \tag{3.20}$$

This is clearly quadratic with respect to D and thus i^*. D can only be biologically
realistic if $D \in (m, m+\mu)$ (i.e $i^* \in (0,1)$). This means there are at most two feasible
coexistent solutions.

The stability is not fully investigated. However, when these steady states exist,
no other steady state is stable. Also, when there are two viable coexistent steady
states, they will be connected to a nearby saddle–node bifurcation, so only one steady
state should be stable. Given this, we expect would that either one of the coexistent
equilibria is stable or there is some stable periodic solution.

FD model

The coexistent steady state for the FD model is (N^*, P^*, i^*) where $N^* = \frac{h(m+\mu i^*)}{1-(m+\mu i^*)}$, $P^* = r(h+N^*)(1-N^*)$ and $i^* = 1 - \frac{\mu+m}{\beta}$. This exists when $\beta > \mu + m$ ($i^* > 0$), $i^* < \frac{1-m}{\mu}$ ($N^* > 0$), $i^* < \frac{1}{\mu(h+1)} - \frac{m}{\mu}$ ($N^* < 1$, i.e. $P^* > 0$). Like the DD model, the two strongest conditions are $i^* < \frac{1}{\mu(h+1)} - \frac{m}{\mu}$ and $\beta > \mu + m$. In this case, there is only one coexistent steady state if it exists.

The stability is not fully investigated. However, when this steady state exists, no other steady state is stable. Given this, we would expect that either one of the coexistent equilibria is stable or there is some stable periodic solution.
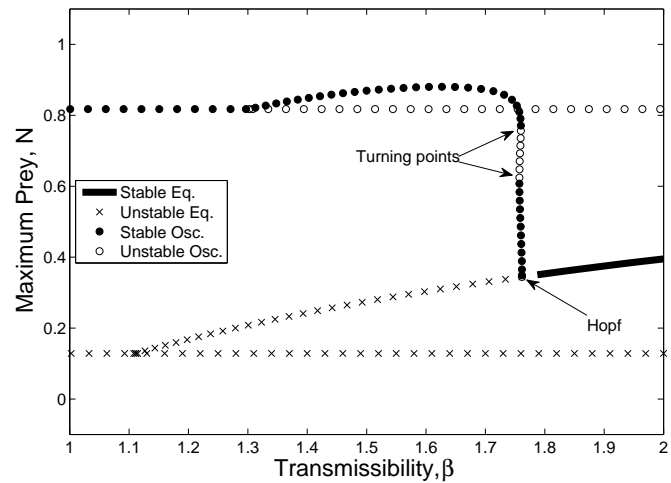
(a)
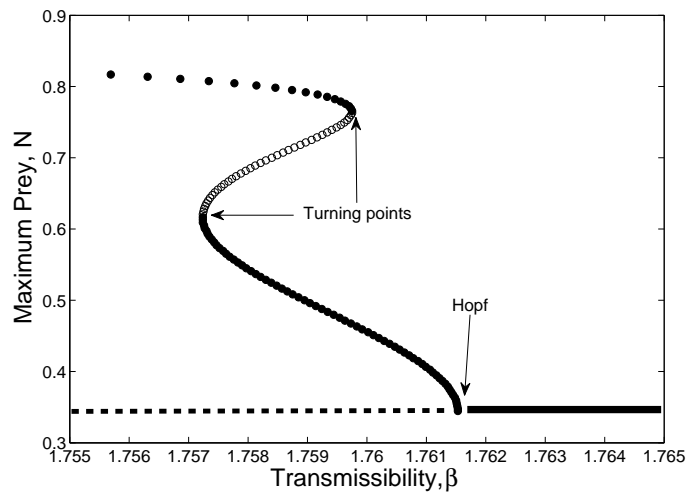
(b)

Figure 3-2: *Bistability between two limit cycles in the DD model. (a) demonstrates that bistability occurs for values of β between the two turning points of limit cycles, whereas (b) zooms in on the turning points of the limit cycles. There is also similar bistability in the FD model. In (b), the disease-free oscillations are not shown and stable/unstable equilibria have been drawn in for clarity, with the dashed line representing unstable equilibrium. μ = 0.53. Other parameters are the same as Figure 3-1(b)*

.
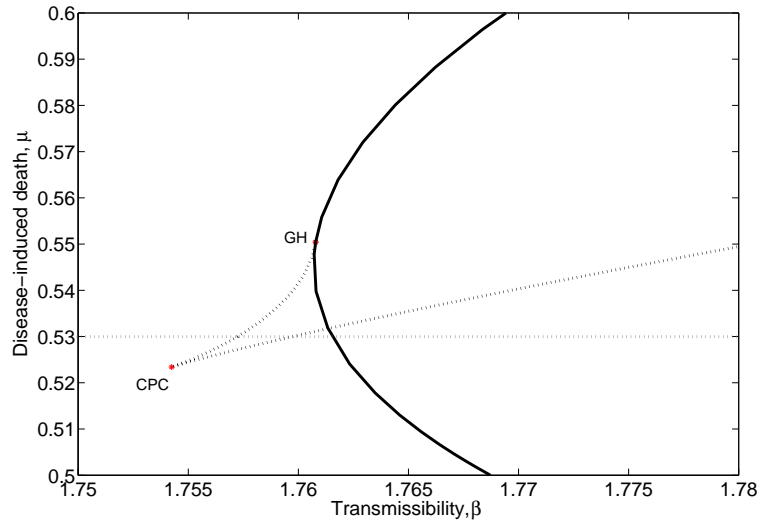
(a)
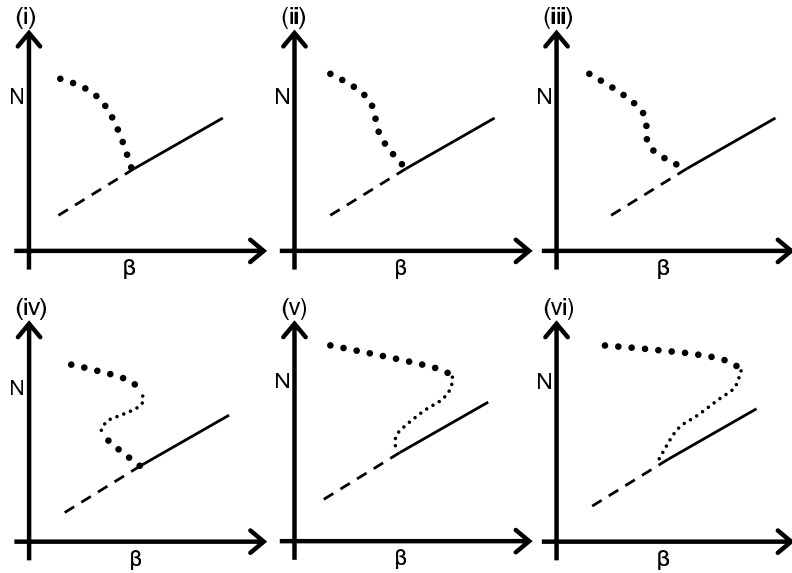
(b)

Figure 3-3: *The birth of bistability: (a) is a two-parameter bifurcation diagram with varying transmissibility (β) and disease-induced death rate (μ). This demonstrates that the bistability in Figure 3-2 is the result of a cusp bifurcation of turning points of limit cycles between Figure 3-1(b) and Figure 3-2 (marked 'CPC' for Cusp Point of Cycles). Further increases of μ lead to bistability between an equilibrium and a limit cycle (once beyond the generalised Hopf bifurcation, marked 'GH'). For (a), the thick dashed lines represent the turning points of limit cycles, the bold line represents the Hopf bifurcation, and the grey dashed horizontal line highlights where Figure 3-2 fits in. (b) is a sequence of sketched bifurcation diagrams with respect to transmissibility (β) for increasing disease-induced death rate (μ). For (b), large black circles stand for stable (endemic) oscillations, and small black circles stand for unstable (endemic) oscillations. Starting with a stable limit cycle (i) (μ = 0.5, see Figure 3-1(b)), the system progresses to the limit cycle beginning to 'bow' (ii) (μ = 0.52); to an inflection point in the limit cycle (cusp point) (iii) (μ ≈ 0.5235); to two stable limit cycles and one unstable limit cycle (iv) (μ = 0.53, see Figure 3-2); to a generalised Hopf bifurcation (v) (μ ≈ 0.55); to a subcritical Hopf bifurcation with one stable and one unstable endemic cycle (vi) (μ = 0.6). A similar progression occurs in the FD model: μ = 1 (see Figure 3-1(a)) (i), μ = 2.4 (ii), μ ≈ 2.47 (iii), μ = 3 (iv), μ ≈ 3.35 (v) and μ = 3.5 (vi). Other parameters. DD model: same as Figure 3-1(b). FD model: same as Figure 3-1(a).*

65
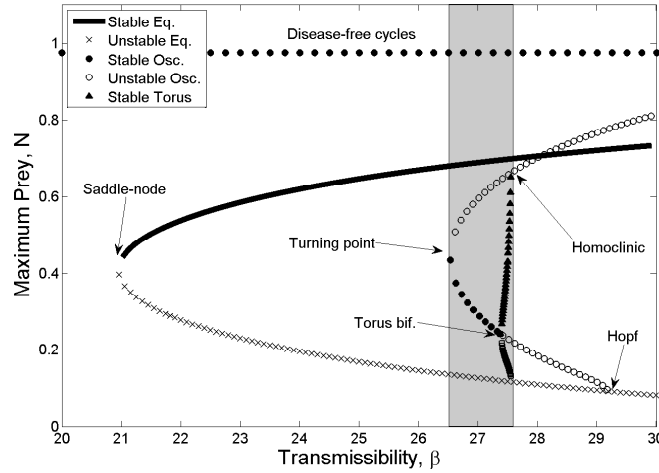
(a)
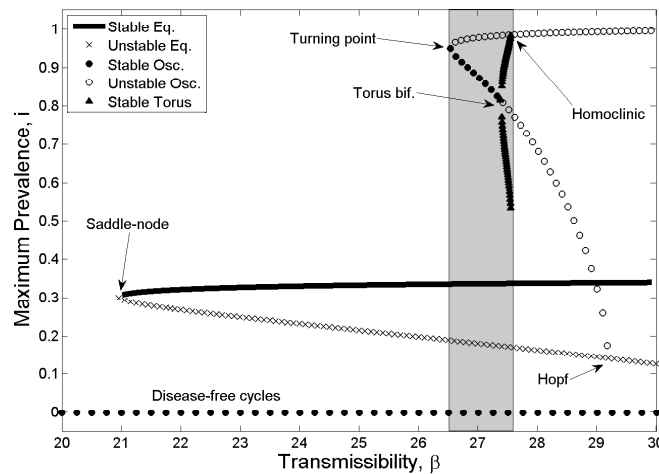
(b)

Figure 3-4: *Tristability and torus bifurcations in the DD model: Bifurcation diagrams of (a) maximum prey density (N) and (b) maximum prevalence, with respect to transmissibility (β) focused around the Hopf and saddle–node bifurcations. The grey region highlights a region of tristability between disease-free predator–prey oscillations, a coexistent equilibrium and coexistent limit cycle or torus. In this figure, both $R_0^* < 1$ and $\overline{R_0} < 1$, yet there are two endemic states in the grey region. Parameter values: $\mu = 2$, $r = 0.5$, $h = 0.1$ and $m = 0.2$. The disease-free predator–prey equilibrium is omitted; it is a horizontal line near the horizontal-axis (N = 0.025). The parameter region where the disease invades the predator–prey oscillation has been omitted.*
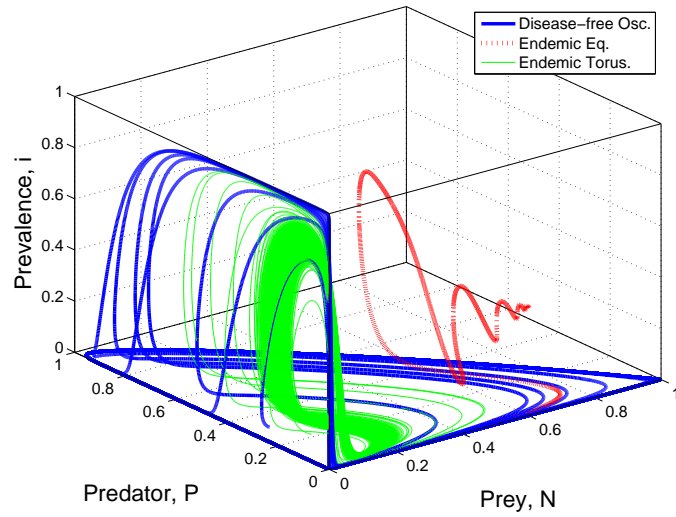
(a)
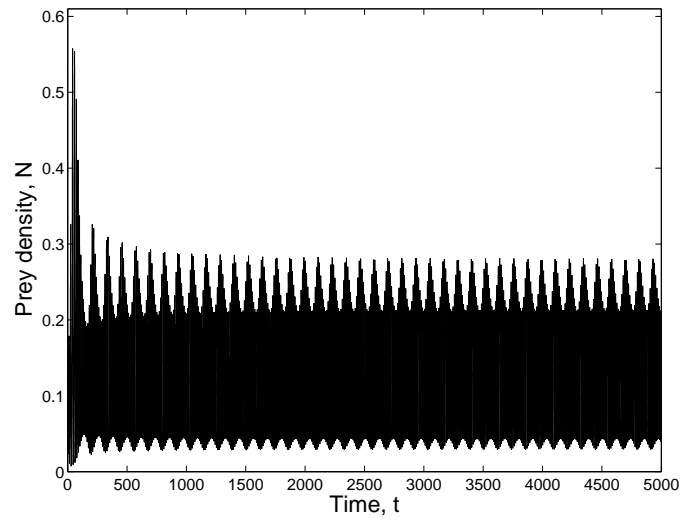
(b)

Figure 3-5: *(a) Phase portrait illustrating tristability in the DD model and (b) a time profile of the coexistent torus with respect to prey density (N). Initial conditions are (0.05,0.3,0.01) (disease-free oscillations), (0.5,0.01,0.01) (coexistent equilibrium) and (0.1,0.2,0.01) (coexistent torus). $\beta = 27.4$. Other parameters are the same as Figure 3-4.*
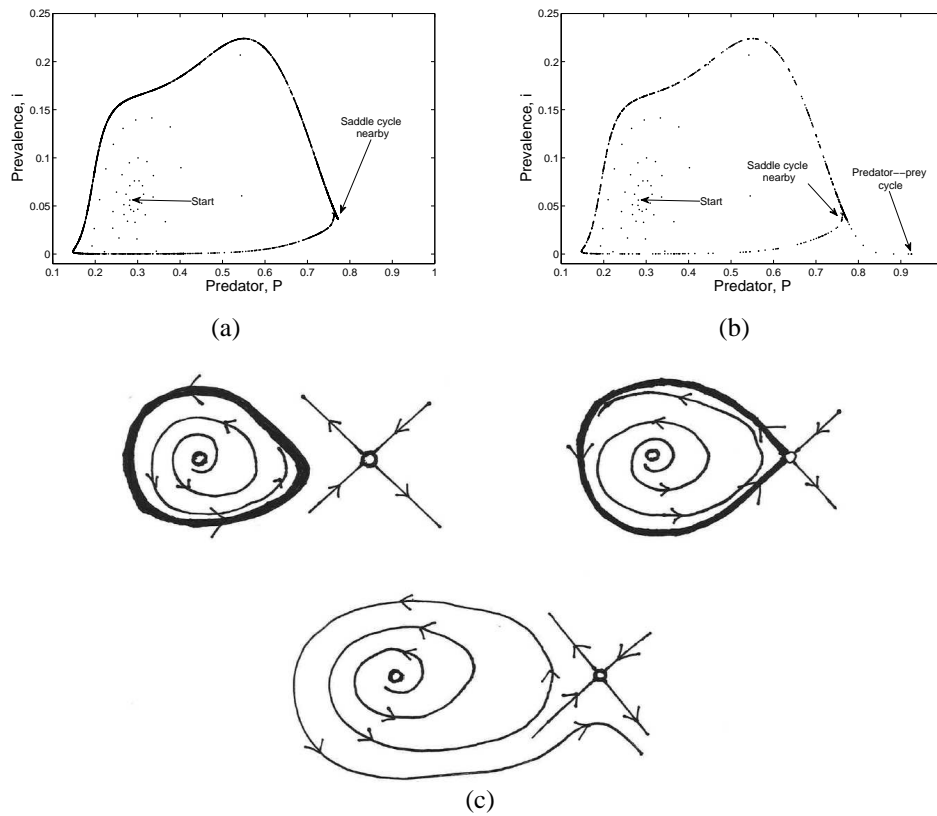
Figure 3-6: *Poincaré sections demonstrating the destruction of the torus in Figure 3-4 in the DD model: (a) just before the homoclinic destruction of the torus ($\beta = 27.54513$), (b) just after the homoclinic destruction of the torus ($\beta = 27.54514$). Notice the curve in the Poincaré section (torus) is sparser in (b) since the system follows the cycle several times in a transient phase before going to the predator–prey oscillations. The Poincaré section is of trajectories hitting the $N = 0.12$ plane from above. (c) is a sketch of the creation and destruction of the homoclinic orbit in the Poincaré section, where the white circles represent unstable (or saddle) limit cycles, thick lines represent the stable torus, and the thin lines with arrows represent either the trajectories, or the stable/unstable manifolds of the saddle-limit cycle. Other parameters are the same as Figure 3-4.*
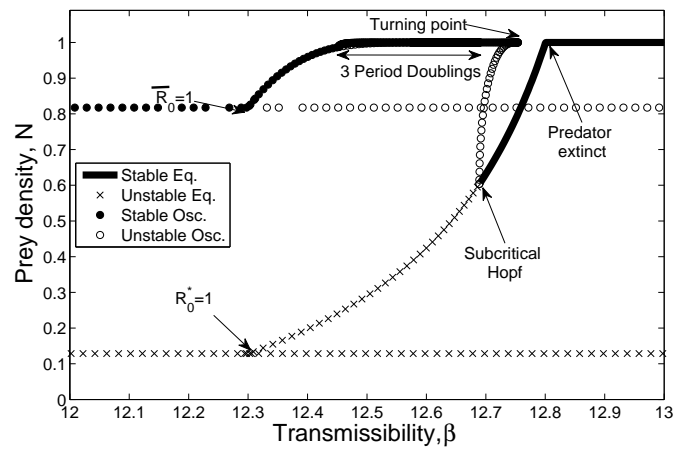
(a)
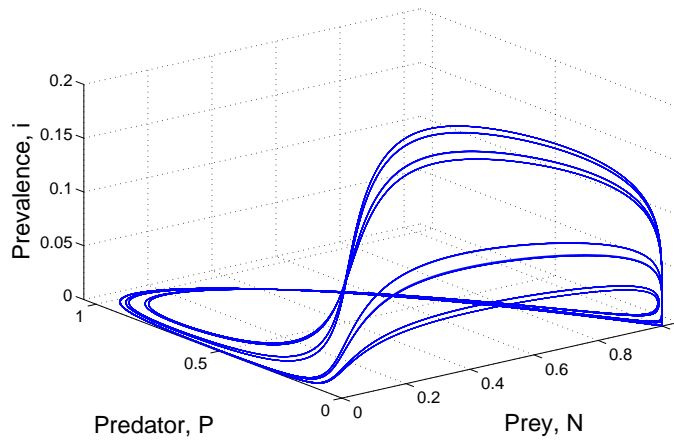
(b)

Figure 3-7: *Period-doubling in the FD model: (a) Bifurcation diagram with respect to β where $\mu = 12$. Three period-doubling bifurcations have occurred, although this is not clear as all branches are very close to each other. To confirm the existence of three period doubling bifurcations, (b) shows a phase portrait of the resulting 8-cycle at $\beta = 12.62 (= \mu + 0.62)$. Other parameters are the same as Figure 3-1(a).*
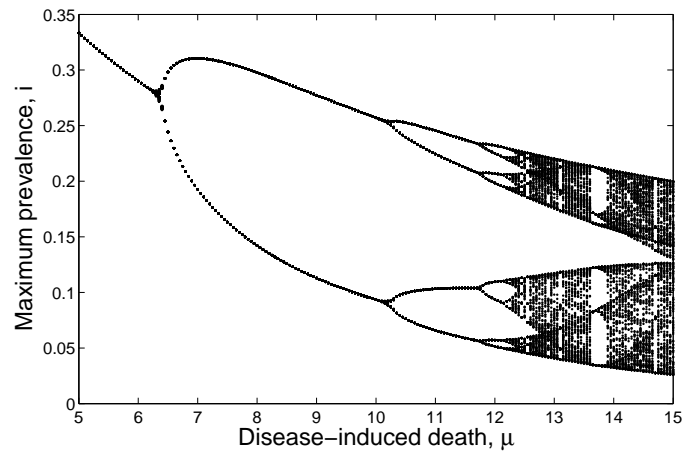
Figure 3-8: *Period-doubling cascade into chaos in the FD model. Bifurcation diagram of (local) maximum prevalence with respect to μ, where β varies with μ along the line β = μ + 0.62. Other parameters are the same as Figures 3-1(a) and 3-7. The initial condition $(N, P, i) = (1, 0.1, 0.01)$ was used.*

Chapter 4

Disease in group-defending prey can benefit predators[1]

Abstract

Infectious diseases have the capacity to influence not only the host population but also interacting species like predators. In particular, they can reduce host densities, which can have knock-on effects on predators. Here, we consider how an infectious disease in the prey affects the predator–prey relationship where the prey exhibit some kind of group defence against the predator (using a Holling type IV functional response). We find that the disease can reduce prey densities to levels where the group defence is weaker. This weakened group defence allows predators to survive in many scenarios where they could not without the disease.

4.1   Introduction

Group-defending prey pose many difficulties for predators to overcome. Large groups of prey can dazzle and confuse predators, making it difficult for predators to focus on and pick out individual prey from the group. Large groups of prey have many eyes that improve vigilance, reducing the element of surprise often necessary for successful attack. On top of this, large groups of prey may even mob attack, potentially harming predators.

There are many examples of group defence (see Krause and Ruxton, 2002). As

---

[1]This chapter has previously been published in Theoretical Ecology (Bate and Hilker, 2014) and is reproduced here with kind permission from Springer Science+Business Media B.V.

early as 1920, Allen suggests that a school of sardines can confuse Great Northern loons, whereas Miller (1922) suggests a flock of Bush tits has many eyes to spot hawks and will respond with a 'confusion chorus'. More recently, Japanese honeybees have been reported to mob attack foraging hornets by forming a 'hot defensive ball' around the hornet (Ono et al, 1995).

There have been several attempts to mathematically model group defence, the first being Freedman and Wolkowicz (1986). The most common and among the simplest method of incorporating group defence in a predator–prey model is by using Holling type IV functional responses (sometimes called Monod–Haldane functional responses, a term with origins in microbiology, Andrews, 1968). Such functional responses behave much like a Holling type II functional response, especially for small prey densities. However, instead of saturating at large prey densities, the functional response will become negatively sloped. That is, the predation rate per predator decreases for larger prey densities as a consequence of group defence. From this, it is worth noting that Holling type IV functional responses usually result in an upper threshold of prey density, beyond which the predator can not survive. This can be seen as a strong group defence. There are other ways of modelling group defence. For example, Ajraldi et al (2011) and Venturino (2011a) recently suggested a 'square-root' functional response for predators of herding prey, particularly for the herding of large mammals. Their argument centres around the idea that predators can only attack those prey along the perimeter of a herd. Such functional responses neglect the other aspects of group defence like predator confusion, but also these functional responses grow particularly high for small prey densities (with infinite gradient at zero). Likewise, Geritz and Gyllenberg (2013) developed a model for group defence where predators capture only individual prey and not those in groups. These individual prey can join and leave groups. This results in a functional response that is proportional to the number of individual prey which increases monotonically (sublinearly) with total prey density.

The combination of group defence and disease has rarely been considered, either theoretically (Venturino, 2011a, being an exception) or empirically. However, diseases have the capacity to weaken not only the infected individuals, but also the group defences. This weakening can be simply because the disease reduces the size of the group via disease-induced mortality. However, a weaker group defence could also be the result of infected individuals not being as good at contributing to the group defence. For example, Seppälä et al (2008) show that rainbow trout infected with eye flukes have different shoaling behaviour to those without eye flukes; and although infected and susceptible fish were not mixed, one would expect that infected fish would not

co-ordinate well with susceptibles of the shoal, potentially breaking down the whole group defence. In short, there is much prospect for diseases to undermine group defence effort by prey.

Diseases and predators are competing for the same prey hosts. In many models, both the disease and predator can coexist at equilibrium. However, such coexistence between predator and disease is the result of infected prey being more vulnerable to predation than susceptible prey. In particular, equilibrial coexistence can not occur in models where predators do not discriminate between susceptible and infected prey with respect to the predators' functional response (Siekmann et al, 2010; Hilker and Malchow, 2006). This is because discriminate predation is reminiscent of intraguild predation (with susceptible prey as resource, infected prey as intraguild predator and the predator as top predator), whereas indiscriminate predation can be rescaled to exploitative competition (see Sieber and Hilker, 2011), where predator and prevalence (the proportion of infected prey in the prey population) do not interact directly but both prey on the same prey host.

In ecology, it has long been established (Gause, 1934) that two species competing for a common resource can not coexist at equilibrium (called the 'principle of competitive exclusion'; Hardin, 1960). In short, exploitative competition means extinction of one or more predators. There are factors that undermine this principle; for example, it does not hold if there is any direct interaction between two predators like competition. In particular, coexistence can occur if one of the predators preys on the other predator, i.e. we have intraguild predation. Another counterexample is that coexistence can occur if all populations are oscillating, e.g. due to a Holling type II functional response (McGehee and Armstrong, 1977). Likewise, Chesson (2000) demonstrates that coexistence can occur if there is some spatial heterogeneity. Another, often overlooked counterexample is that one or more of the predators are restricted by some sort of density dependence (Gurney and Nisbet, 1998, pp.166–167). In this case, coexistence can occur if the density dependent predator can survive at prey levels set by the other predator.

In this chapter, we find that a disease and predator can coexist on the same prey host, contradicting the principle of competitive exclusion. On top of that, if we assume that the prey exhibit some group defence, we find that the disease can benefit the predator by reducing prey densities to more manageable levels for the predator. In particular, we find two cases where an endemic disease can prevent the predator becoming extinct; one case is where the disease reduces the prey density below a critical threshold; the other is that the disease reverses a homoclinic bifurcation, bringing

coexistent oscillations from what was the certain extinction of the predator.

4.2 Model derivation

In this section, we will construct two models with predators, susceptible prey and infected prey where the prey exhibit group defence. But before we proceed, we need to carefully derive appropriate functional responses.

4.2.1 The functional response

When modelling group defence for the prey, Holling type IV functional responses of the form equivalent to $\frac{aN}{1+bN+cN^2}$ (or the simplification $\frac{aN}{1+cN^2}$) are often used (Freedman and Wolkowicz, 1986; Ruan and Xiao, 2001; Kot, 2001, chap. 9). Usually, they are used without any mechanistic derivation or justification. Such Holling type IV functional responses can be derived from a Holling type II functional response, $\frac{aN}{1+ahN}$, where a is the attack rate, h is the handling time and N is the prey density. One way of deriving a Holling type IV is by assuming that the attack rate a decreases with respect to N inverse-quadratically, i.e. $a(N) = \frac{a_0}{1+bN^2}$ (Koen-Alonso, 2007). Another derivation assumes that the handling time is linearly increasing with respect to N, i.e. $h(N) = h_0 + h_N N$. (There have been a few other attempts to derive a Holling Type IV, for example, Collings (1997) derives it by assuming both a linearly increasing handling time and an inverse-linear attack rate, which is not a simple argument.) The second derivation based on linear handling times will be used here, largely because it is a simpler argument. The handling time formulation is apt if we assume that time taken to attack and catch a prey increases linearly with respect to prey density. This increased handling time can be considered due to group defence and the additional time it takes to separate and subdue prey at higher prey densities. The time to eat and digest prey is still independent of prey density.

This single-prey Holling type IV functional response does not take into account that the prey is structured because of an infectious disease. We need to derive a two-prey Holling type IV functional response where the two classes of prey are susceptible, S, and infected, I. This can be done by considering the following two-prey Holling type II functional response for susceptible prey, derived using a standard time-management argument (Holling, 1959; Murdoch, 1972):

$$f_S(S,I) = \frac{a_S S}{1 + a_S h_S S + a_I h_I I}.$$

Here, a_S and a_I are the attack rates on the susceptibles and infecteds, respectively. Likewise, h_S and h_I are the handling times on the susceptibles and infecteds, respectively. The infected prey have an equivalent $f_I(S,I)$, which has the numerator $a_I I$.

Now we can assume, as with the one-prey case, that the handling times are density dependent. Thus, we have $h_S(S,I) = h_{S0} + h_{SS}S + h_{SI}I$ and $h_I(S,I) = h_{I0} + h_{IS}S + h_{II}I$, where h_{S0} and h_{I0} are the density independent handling times of the susceptible and infected prey, respectively; h_{SS} and h_{IS} are the density dependent (with respect to susceptible prey) handling times of susceptible and infected prey, respectively; whereas h_{SI} and h_{II} are the density dependent (with respect to infected prey) handling times of susceptible and infected prey, respectively. These formulations take into account that although infected and susceptible prey are seen as different classes of prey, they contribute to the same group defence. In general, all these parameters can be different. For example, imagine a diseased fish that can not follow the rest of the school, potentially leading to ineffective school movement and compromised group defence, or a diseased meerkat that is not as capable at spotting threats when acting as sentry for the clan, leaving the clan at greater risk. Both of these examples suggest that $h_{SS} \neq h_{SI}$. Likewise, infected prey can be easier to catch, subdue and eaten by predator once spotted, suggesting that $h_{SS} \neq h_{IS}$ and $h_{SI} \neq h_{II}$.

By incorporating these density dependent handling times, we get the following two-prey Holling type IV functional response for the susceptible prey:

$$f_S(S,I) = \frac{a_S S}{1 + a_S h_{S0}S + a_I h_{I0}I + a_S h_{SS}S^2 + (a_S h_{SI} + a_I h_{IS})SI + a_I h_{II}I^2}.$$

Likewise, the functional response for the infected prey is:

$$f_I(S,I) = \frac{a_I I}{1 + a_S h_{S0}S + a_I h_{I0}I + a_S h_{SS}S^2 + (a_S h_{SI} + a_I h_{IS})SI + a_I h_{II}I^2}.$$

If susceptible and infected prey do not contribute to the same group defence, but instead contribute to their own group defence, then we would have that $h_{SI} = 0$ and $h_{IS} = 0$. In this case, we would have a functional response comparable to that of two distinct species under a common predator, both with their own group defence.

4.2.2   Other model assumptions

We consider an SI disease in the prey where disease transmission is either frequency dependent ($\beta(S,I) = \frac{\beta SI}{S+I}$) or density dependent ($\beta(S,I) = \beta SI$), where β is the transmissibility coefficient. All prey are born susceptible, i.e. there is no vertical trans-

mission. We assume (for now at least) that infecteds have different fertility, increased density independent mortality and different strengths of competition when compared to susceptible prey. Additionally, predators grow linearly with respect to the predation and die at a constant per capita rate.

$$\frac{dS}{dt} = b_S S + b_I I - mS - c_{SS} S^2 - c_{SI} SI - f_S(S,I)P - \beta(S,I), \qquad (4.1)$$

$$\frac{dI}{dt} = \beta(S,I) - (m+\mu)I - c_{IS} IS - c_{II} I^2 - f_I(S,I)P, \qquad (4.2)$$

$$\frac{dP}{dt} = (\gamma_S f_S(S,I) + \gamma_I f_I(S,I) - d)P. \qquad (4.3)$$

Here, b_S and b_I are the per capita birth rates and γ_S and γ_I are conversion efficiencies from consuming susceptible and infected prey, respectively. c_{SS} and c_{SI} represent density dependent mortalities that susceptibles experience when encountering other susceptible and infected prey, respectively. Likewise, c_{IS} and c_{II} represent density dependent mortalities that infected prey experience when encountering other susceptible and infected prey, respectively. Together, c_{SS}, c_{SI}, c_{IS} and c_{II} represent intra/interspecific competition. m is the natural per capita (density independent) death rate of the prey, μ is the disease-induced per capita death rate of the prey and d is the per capita death rate of the predator and μ is the disease-induced per capita death rate.

4.2.3 Simplified model

The full model (4.1)–(4.3) is rather complex, with twenty parameters in a three dimensional system. To mitigate this, we simplify the model as much as possible as a starting point. We can always, in the future, consider more complicated versions once the simpler model is fully understood.

The simplifying assumptions are as follows: $b_S = b_I(:=b)$, $c_{SS} = c_{SI} = c_{IS} = c_{II}(:=c)$, $\gamma_S = \gamma_I(:=\gamma)$, $a_S = a_I(:=a)$, $h_{S0} = h_{I0}(:=h_0)$ and $h_{SS} = h_{SI} = h_{IS} = h_{II}(:= h_N)$. These assumptions essentially can be summarised by saying that infected and susceptible prey only differ by additional mortality for infected prey ($\mu > 0$); that susceptible and infected prey have the same birth rates, are equally good competitors and have equal attack rates, handling times and conversion. By implementing these assumptions, we can not only gather terms but also collapse the functional responses

to a single-prey form:

$$\frac{dS}{dt} = b(S+I) - mS - cS(S+I) - \frac{aSP}{1+ah_0(S+I)+ah_N(S+I)^2} - \beta(S,I), \quad (4.4)$$

$$\frac{dI}{dt} = \beta(S,I) - (m+\mu)I - cI(S+I) - \frac{aIP}{1+ah_0(S+I)+ah_N(S+I)^2}, \quad (4.5)$$

$$\frac{dP}{dt} = P\left(\frac{\gamma a(S+I)}{1+ah_0(S+I)+ah_N(S+I)^2} - d\right). \quad (4.6)$$

Working with total prey $N = S+I$ instead of susceptible prey and prevalence $i = \frac{I}{N}$, i.e. the proportion of infected prey in the prey population, instead of infected prey:

$$\frac{dN}{dt} = (b-m)N - \mu i N - cN^2 - \frac{aNP}{1+ah_0 N+ah_N N^2}, \quad (4.7)$$

$$\frac{di}{dt} = i\left(\left(\frac{\beta(N,i)}{Ni(1-i)} - \mu\right)(1-i) - b\right), \quad (4.8)$$

$$\frac{dP}{dt} = P\left(\frac{\gamma a N}{1+ah_0 N+ah_N N^2} - d\right). \quad (4.9)$$

For frequency dependent transmission, $\beta(N,i) = \beta Ni(1-i)$, whereas for density dependent transmission, $\beta(N,i) = \beta N^2 i(1-i)$.

To reduce the number of parameters further, we non-dimensionalise the system. Let us rescale time such that the predator's death rate becomes one ($t = \frac{1}{d}T$). Predator density is rescaled such that the numerator of the functional response becomes one ($P = \frac{d}{a}y$). Prey density is rescaled such that the numerator of the predator's numerical response is scaled to one ($N = \frac{d}{\gamma a}x$). Then, for frequency dependent transmission, equations (4.7)–(4.9) become:

$$\frac{dx}{dT} = (b'-m')x - \mu' i x - c'x^2 - \frac{xy}{1+H_0 x+H_x x^2}, \quad (4.10)$$

$$\frac{di}{dT} = i((\beta'-\mu')(1-i) - b'), \quad (4.11)$$

$$\frac{dy}{dT} = y\left(\frac{x}{1+H_0 x+H_x x^2} - 1\right). \quad (4.12)$$

The new parameters are the scaled prey birth ($b' = \frac{b}{d}$) and death ($m' = \frac{m}{d}$) rates, scaled disease-induced death rate ($\mu' = \frac{\mu}{d}$), scaled density dependent mortality ($c' = \frac{c}{\gamma a}$), scaled transmissibility ($\beta' = \frac{\beta}{d}$) and the scaled density independent ($H_0 = \frac{h_0 d}{\gamma}$) and density dependent ($H_x = \frac{h_N d^2}{a\gamma^2}$) handling time.

For density dependent transmission, the only difference from equations (4.10)–

(4.12) is that the prevalence equation (4.11) becomes:

$$\frac{di}{dt} = i((\beta' x - \mu')(1 - i) - b'), \tag{4.13}$$

where $\beta' = \frac{\beta}{\gamma a}$.

For simplicity of notation, we will drop the dashes. From now on, we will only work with the non-dimensionalised parameters, so there should be no confusion of notation.

These models are comparable with existing models; in particular, setting $m = 0$ and $H_x = 0$, we obtain the diseased-prey model in Chapter 2, i.e. Bate and Hilker (2013b). Also, with this scaling, we have reduced the model from an intraguild predation model to something resembling exploitative competition, as there is no direct interaction between predators and disease prevalence (cf Sieber and Hilker, 2011). In fact, for density dependent transmission, the model is exploitative competition.

Now, for the frequency dependent model, by defining functions $f(x) = \frac{x}{h(x)}$ (functional response), $g(x) = b - m - cx$ (per capita growth rate of prey in absence of predators and disease), $h(x) = 1 + H_0 x + H_x x^2$ (the denominator of the functional response, or in other words, the total time predators spend searching and handling prey relative to search time) and $p(i) = (\beta - \mu)(1 - i) - b$ (per capita growth in prevalence), we get:

$$\frac{dx}{dT} = f(x)[(g(x) - \mu i)h(x) - y], \tag{4.14}$$

$$\frac{di}{dT} = i\, p(i), \tag{4.15}$$

$$\frac{dy}{dT} = y(f(x) - 1). \tag{4.16}$$

For the density dependent model, $p(i)$ becomes:

$$p(x, i) = (\beta x - \mu)(1 - i) - b. \tag{4.17}$$

With such functions, we can use analysis similar to that in Kot (2001, chap. 9) to establish the existence and stability of steady states with relatively clear notation. In the rest of the chapter, we will always assume the prey can grow in the absence of predator and disease, i.e. $g(0) > 0$ (equivalently, $b > m$).

4.3 Disease-free predator–prey dynamics

Ignoring the disease, the predator–prey model is equivalent to the model in Freedman and Wolkowicz (1986) and Kot (2001, chap. 9). Since these are existing results, we will summarise and classify them into various scenarios here. However, for completeness, some of the steady state and nullcline analysis is explained in Appendices 4.A and 4.B.

There are three different main scenarios that can be derived from the steady states:

- Scenario 1: There is no coexistent steady state. The prey-only steady state is stable. This can be split into (1A) no real solutions or (1B) only negative solutions for the coexistent steady states. A phase plane of Scenario 1B (top left of Figure 4-1) has two vertical predator nullclines that do not intercept the humped prey nullcline in the positive quadrant.

- Scenario 2: One coexistent steady state exists. It is either (2A) stable or (2B) unstable and is the centre of some stable limit cycle. This depends on the slope of the prey nullcline, which is given by the sign of $\frac{\partial y}{\partial x}(x^*) := y'(x)$. Phase planes of Scenarios 2A and 2B show that one of the predator nullclines intercepts the humped prey nullcline in the positive quadrant, resulting in one predator–prey equilibrium and an unstable prey-only steady state. If the interception occurs while the prey nullcline is negatively sloped (i.e. to the right of the maximum in the prey nullcline), the predator–prey equilibrium is stable (Scenario 2A (top middle of Figure 4-1)); whereas, if the interception occurs while the prey nullcline is positively sloped (i.e. to the left of the maximum in the prey nullcline), the predator–prey equilibrium is unstable and there is a stable predator–prey limit cycle (Scenario 2B (top right of Figure 4-1)).

- Scenario 3: Two coexistent steady states exist. The coexistent steady state with the lower prey density is either (3A) stable or (3B) unstable and is the centre of some limit cycle. Again, this depends on the slope of the prey nullcline, which is given by the sign of $y'(x)$. The stable steady state/limit cycle is bistable with the prey-only steady state, where the higher prey density coexistent steady state forms part of a separatrix. In the phase planes of Scenarios 3A and 3B (Figure 4-1 bottom left and middle, respectively), both predator nullclines intercept the humped prey nullcline, resulting in two predator–prey steady states. The prey-only steady state is stable and the 'right' coexistent steady state (i.e. the coexistent steady state with the larger prey density) is always unstable (saddle

point). The difference between Scenarios 3A and 3B is the same as the difference between Scenarios 2A and 2B; the stability of the 'left' coexistent steady state (i.e. the coexistent steady state with the smaller prey density) and the existence of a limit cycle depend on where the interception is relative to the maximum of the prey nullcline.

Scenarios 1 and 2 can be said to be the cases where group defence is weak since these scenarios are also possible for a Holling type II functional response (i.e. the Rosenzweig–MacArthur model). In Scenario 3, group defence is strong enough to dominate dynamics for larger prey densities. This is expressed by the stability of the prey-only equilibrium and the bistability, which is not possible in the Rosenzweig–MacArthur model. Note that the dynamics associated with Holling Type II functional responses are still dominant for smaller prey densities.

This list does not give all the information; there is also a global bifurcation. Freedman and Wolkowicz (1986) and Kot (2001, chap. 9) demonstrate that the limit cycle in Scenario 3B can collide with the saddle point to form a homoclinic orbit. Beyond this homoclinic bifurcation, the limit cycle disappears and the prey-only steady state is the only stable steady state, like Scenario 1. Consequently, we have another scenario:

- Scenario 4: Two coexistent steady states exist, neither are stable. No limit cycle exists due to a homoclinic bifurcation. Only the prey-only steady state is stable. In the phase plane of Scenarios 4 (Figure 4-1 bottom right), both predator nullclines intercept the humped prey nullcline, resulting in two predator–prey steady states.

Scenario 4 means that there is no stable coexistence. There may be, however, coexistent oscillatory transients dynamics near the homoclinic bifurcation for some initial conditions, meaning that the eventual extinction of the predator would not be apparent in short to medium time scales. Figure 4-2 demonstrates this homoclinic bifurcation with a phase plane 'before' (left) and 'after' (right) the homoclinic bifurcation. In the left panel, we are in Scenario 3B, with the stable coexistent limit cycle and saddle point are very close. The right panel is in Scenario 4, where the limit cycle has disappeared after colliding with the saddle point, leaving the prey-only steady state as the only stable attractor, despite there being two coexistent steady states. Scenario 4 essentially means that the usual predator–prey oscillations from the Rosenzweig–MacArthur model can not be fully contained in the region where prey densities are small enough for group defence to be weak, and instead encroaches into regions where group defence dominates.

4.4 Results: Frequency dependent transmission

In the previous section, we set the scene by describing the predator–prey model in the absence of infection. Now we can incorporate a disease in the prey population. In this section, we will analyse the frequency dependent model (4.14–4.16), and we will then tackle the more complicated case of density dependent transmission in the next section.

4.4.1 Coexistence between disease and predator

Observing that the prevalence equation (4.15) is completely independent from both the predator and prey (since $p(i) = (\beta - \mu)(1 - i) - b$), we can separate the prevalence equation. From the prevalence equation, we have that the disease-free state ($i^* = 0$) is stable if $p(0) = \beta - \mu - b < 0$. Otherwise, if $p(0) > 0$, the disease-free state is unstable, the disease will be endemic and disease prevalence will approach $i^* = 1 - \frac{b}{\beta - \mu}$.

For the remainder of this section, we will assume that the prevalence is at the equilibrium $i^* = 1 - \frac{b}{\beta - \mu}$. Armed with this quasi-stationary assumption, we can treat prevalence as a constant, reducing the frequency dependent model (4.14–4.16) to the following 2D model:

$$\frac{dx}{dT} = f(x)[(g(x) - \mu i^*)h(x) - y], \tag{4.18}$$

$$\frac{dy}{dT} = y(f(x) - 1). \tag{4.19}$$

This model is the same as the disease-free predator–prey model, except that there is an additional disease-induced mortality in the prey. This additional term only alters the 'humped' non-trivial prey nullcline defined by $y(x) = (g(x) - \mu i^*)h(x)$.

Figure 4-3 demonstrates how this nullcline is changed. Increasing prevalence alters two key points of the humped nullcline; (i) the intercept with the horizontal-axis (the prey-only steady state) is moved left, i.e. prevalence reduces the prey-only steady state, and (ii) the maximum of the nullcline $y(x)$ is moved left, i.e. occurs at lower prey densities.

4.4.2 Loss of stability of the prey–only steady state

As prevalence increases, prey density at the prey-only steady state is reduced. This reduction in prey carrying capacity by the disease can become beneficial for the predator

as it can shift the predator–prey system from Scenario 3 to Scenario 2, like in Figure 4-3. This shift is important since Scenario 3 means bistability involving a prey-only steady state, whereas Scenario 2 means the predator will always survive. In this case, the disease can help the predator survive under conditions where it can not survive without the disease due to unmanageable prey densities. The presence of the disease does reduce predator density at the stable coexistent equilibrium, though, but the loss of extinction risk at high prey densities is significant (i.e. the disease can render group defence ineffective).

4.4.3   Stabilisation of limit cycles

The shift of the maximum of the nullcline $y(x)$ to the left reduces or eliminates limit cycles (Figure 4-3). In the disease-free predator–prey system, limit cycles only occur if the maximum of the nullcline $y(x)$ is to the right (i.e. at a higher prey density) of the coexistent steady state with the lower prey density. By shifting this maximum beyond the lower steady state, the limit cycle is eliminated and a stable steady state is formed. Thus, we have that Scenario 2B/3B becomes Scenario 2A/3A. This means that increasing prevalence should take Scenario 3B to Scenario 2A via either Scenario 3A or via Scenario 2B.

4.4.4   Disease reversing global bifurcation

As we previously stated, there are significant parameter regions in the predator–prey model where the prey-only steady state is the only attractor despite the existence of two coexistent steady states (Scenario 4). In these regions, the predator can not survive in the long run, independent of the initial condition. However, the presence of a disease infecting the prey can reverse this homoclinic bifurcation and give rise to a stable predator–prey–disease limit cycle. This means that the disease can facilitate coexistence where it was impossible without the disease.

4.4.5   Overall pattern

Figure 4-4 demonstrates this reversal of a homoclinic bifurcation. In the absence of the disease ($i^* = 0$), the predator can not survive, despite there being two predator–prey steady states. As the prevalence increases, the prey-only steady state decreases. If disease-induced mortality is sufficiently high, the disease can bring the prey steady state close to the predator–prey saddle point. At the same time, increased prevalence

will reduce the slope of the prey nullcline and shift the maximum to the left. Together, with sufficiently large prevalence, a stable limit cycle will appear as the homoclinic bifurcation is reversed. We have suddenly moved from Scenario 4 to 3B. In this region, the predator can survive with the right initial condition. However, if we increase prevalence further, the prey-only steady state will lose stability as it collides with the predator–prey saddle point in a transcritical bifurcation (like in Figure 4-3). After this transcritical bifurcation, we will move to Scenario 2B where the predator will survive no matter what the initial condition. The next transition occurs when the predator–prey limit cycle is stabilised by a Hopf bifurcation (like in Figure 4-3), leading to Scenario 2A. Increasing prevalence further ($i^* > 0.6$), the predator–prey steady state will collide with the prey-only steady state in a transcritical bifurcation, resulting in the loss of the predator–prey steady state and a stable prey-only steady state (Scenario 1). And finally, if prevalence (and disease-induced mortality, μ) is sufficiently high ($i^* > 0.75$), the disease can wipe out the prey population (i.e. if $b < m + \mu$). This host extinction is a trademark of frequency dependent diseases and can not happen in density dependent diseases (see next section).

4.4.6 Summary

For a frequency dependent disease, the prevalence equation is independent of prey or predator densities. Consequently, the prevalence can be assumed to be fixed. With this in mind, we find that the disease can coexist with the predator (Scenarios 2 and 3). On top of this, the disease can help the predator by (a) keeping prey densities below densities where prey group defence is strong; (b) stabilising predator–prey cycles (preventing large booms and busts of predator and prey populations) and (c) reversing the homoclinic bifurcation, thus preventing the eventual extinction of the predator. In particular, Figure 4-4 demonstrates that with increasing prevalence, we can go from a prey-only steady state (Scenario 4) to bistability between the prey-only steady state and a predator–prey limit cycle (Scenario 3B) to a predator-prey limit cycle (Scenario 2B) to a predator–prey steady state (Scenario 2A) to prey-only steady state (Scenario 1) to diseased-induced extinction of the prey (and predator, of course).

4.5 Results: Density dependent transmission

Unlike in the frequency dependent model, we can not separate the disease from the predator–prey dynamics in the density dependent model (4.14), (4.16) and (4.17). This

means that 2D phase plane analysis used in the disease-free and frequency dependent models can not give the whole story. In particular, it does not provide much insight into the existence of more complex dynamics like chaos and quasi-periodic dynamics. However, such phase plane analysis is still very enlightening as a similar pattern of progressing from Scenario 4 to Scenario 1 occurs.

Firstly, both oscillatory and equilibrial coexistence between predator and disease prevalence also occur in the density dependent model. This coexistence is more interesting and complex than in the frequency dependent model as the predator–prevalence–prey equations are in the form of exploitative competition; thus this coexistence contradicts the principle of competitive exclusion.

The coexistence is facilitated by the mixture of density dependent terms (i.e. the '$1-i$' terms) and density independent terms (in this case, 'b') in the per-capita growth rate for prevalence $p(x,i)$. This means that the prevalence nullsurface (the points of (x,y,i) such that $p(x,i)=0$) is not fixed to a particular value of prey density but instead exists for a range of prey densities. Since the predator nullplanes have fixed prey densities, if one or more of these prey densities lie within the range of prey densities for the prevalence nullsurface, coexistence will occur (subject to positive predator densities and prevalence).

Secondly, the same scenarios and transitions occur in the density dependent model as in the frequency dependent model. For example, Figure 4-5 demonstrates that increasing transmissibility (as a proxy for prevalence and thus Figure 4-5 is equivalent to Figure 4-4) goes through the same transitions, from Scenario 4 to Scenario 3B to Scenario 2B to Scenario 2A, as Figure 4-4 (except for Scenario 1, which occurs for levels of transmissibility well beyond the range of Figure 4-5, and disease-induced extinction, which can not happen in the density dependent model).

One novelty is that prevalence does not always increase with transmissibility (Figure 4-5(b)). In particular, the loss of stability for the disease–prey steady state at the transition between Scenarios 3B and 2B results in massive reduction of prevalence (although the predator–prey–disease limit cycle will have short periods where prevalence is higher than the disease–prey steady state).

Lastly, complex dynamics can occur. In the 2D predator–prey and frequency dependent models, the possible stable dynamics are limit cycles and equilibria only. In 3D systems like the density dependent model, many more phenomena can be found within regions of Scenarios 2B and 3B. An example of such complex dynamics is Figure 4-6.

In Figure 4-6, there are several complex dynamics. After the reversal of the ho-

moclinic orbit (at approximately $\beta = 0.6$), the species coexist on a '2-cycle' (note that both predators and prey exhibit two local maxima and minima each, whereas the prevalence, not shown here, exhibits only one local maximum and minimum each). At approximately $\beta = 1$, one branch of the attractor suddenly disappears as one of the maxima collides with one of the minima. Note that this branch emerges again in form of a chaotic attractor, as the remaining branch has undergone a cascade of period doubling bifurcations. At around $\beta = 1.8$, the system stabilises via a period halving cascade. But for parameter values in between, the bifurcation diagram displays a number of different attractor crises, in which branches of the attractor merge and split, or significantly change in size out of the blue. This suite of attractor crises is indicative of global bifurcations and in some way a more complex analogue of the homoclinic bifurcation known from the disease-free 2D predator-prey model. The non-local phenomena characteristic of the Holling-type IV predator–prey model therefore persist, in increased variety, also in the 3D model with disease. Hence, group defence tends to induce sudden catastrophic changes in the qualitative dynamics.

4.6 Discussion

In this chapter, we consider how an infectious disease in the prey affects the predator–prey relationship where the prey exhibits some kind of group defence against the predator. We find that the disease can reduce prey densities to levels where the group defence is not as strong. This allows predators to survive in scenarios where they could not without the disease.

In the absence of the disease, there are three scenarios where the predator can not survive; prey-only steady with no other unstable steady states (Scenario 1), bistability between prey-only steady state and predator-prey steady state/oscillations (Scenario 3, survival depends on the starting point) and a prey-only steady state with two unstable predator–prey steady states (Scenario 4). The disease can help the predator survive in the latter two cases. Firstly, the disease can reduce the prey carrying capacity to densities more manageable for the predator, moving from bistability between a prey-only steady state and a predator–prey steady state/limit cycle to where only the predator–prey steady state/limit cycle is stable. On top of this, the disease can reverse a homoclinic bifurcation, going from just a prey-only steady state to bistability between the prey-only steady state and the predator–prey limit cycle. This is due to the disease dampening the predator–prey oscillations, keeping prey densities too small for group defence to dominate. Combining these two phenomena together, we do have

cases that, with the disease, only the predator–prey steady state/limit cycles are stable, whereas in the absence of the disease, only the prey-only steady state exists. In this case, the disease is helping the predator survive for all initial conditions where it could not survive in the diseases absence.

Typically, both the predator and disease are in competition for prey hosts. In several models, this competition leads to only one of the predator or disease persisting, i.e. the predator/disease manages to keep prey/host density low enough that the disease/predator population will eventually die out (for example, Hilker and Malchow, 2006; Siekmann et al, 2010, although coexistence can occur if all populations oscillate). Here, in both the density dependent and frequency dependent model, there is a stable predator–prey–disease equilibrium. This was also true in the diseased prey models in Chapter 2, i.e. Bate and Hilker (2013b), and several extension models in Table 6 of Anderson and May (1986), although this was not elaborated in either paper. This is novel in itself, especially for the density dependent model, since the principle of competitive exclusion states that two consumers can not share a resource. Previously, counterexamples are the result of temporal heterogeneity (Armstrong and McGehee, 1980, for example, via predator–predator–prey oscillations) or spatial heterogeneity (Chesson, 2000). Here, we have steady state coexistence, which is largely independent of the choice of functional response (for example, using linear and Holling type II functional responses would also have steady state coexistence). In particular, it is independent of group defence; however, with group defence, we find that the disease not only coexists with predators, it can help predators survive where they could not without the disease.

The counterexample of the principle of competitive exclusion found in the density dependent model occurs because there is a mix of density dependent and density independent terms in the prevalence equation (4.17). Gurney and Nisbet (1998, pp.166–167) found that adding a density dependent mortality (a quadratic term) to one of the predators allowed both predators to coexist at equilibrium. This can be generalised to other forms of density dependence like predator interference (by using a Beddington–DeAngelis functional response) in one or both predators. The reason that density dependence defies competitive exclusion is that it gives the predator a range of prey densities under which it can be at equilibrium, and if the other consumer can also survive at steady state in this range, coexistence can occur. Without density dependence, the range is a point which means coexistence generally can not occur. The same density dependence argument occurs in the density dependent model, in the prevalence equation (4.17), since the mixture of density dependent $((\beta x - \mu)(1-i))$ and density

independent (b) terms means that prevalence can be static for a range of x.

There are several key assumptions in this model that lead to coexistence of both the disease and predator. For example, if infected prey are completely sterile, then the b term in prevalence equation (4.17) becomes $b(1-i)$. With this, the prevalence equation can only be static for $i^* = 0, 1$ unless prey density is $x^* = \frac{\mu + b}{\beta}$, which is generally not true. Since $i^* = 1$ means all prey are infected and sterile (leading to the extinction of the prey and predator), equilibrial coexistence between predator and disease can not occur in general. Likewise, the lack of vertical transmission also allows for coexistence (for example, in Hilker and Malchow, 2006; Siekmann et al, 2010, there is perfect vertical transmission, an assumption that leads to the lack of equilibrial coexistence).

For the frequency dependent model, coexistence of predator and disease is not as profound as is the case in the density dependent model. The prevalence equation 4.15 shows that the prevalence–prey equations follow amensalism (disease prevalence has a negative effect on prey growth but disease prevalence does not gain from higher prey densities) and not exploitation. Consequently, the principle of competitive exclusion does not apply for frequency dependent transmission.

Venturino (2011a) tackled group defence from a different perspective, leading to significantly different result. Instead of a non-monotonic functional response like the Holling Type IV used in this chapter, he uses square root functional response. This choice of functional response is based on the idea that predators can only take prey on the outskirt of the herd and thus the functional response should be proportional to the perimeter of the herd. However, Venturino (2011a) assumes this only applies to susceptible prey since infected prey are assumed to leave the herd and thus experience a linear functional response. The resulting dynamics are less complicated in their model, only equilibria and limit cycles seem to occur with no bistability. Coexistence between predator and prey can occur as well as cases where the disease helps the predator survive. In this chapter, bistability occurs in Scenario 3 and more complex dynamics can occur in the density dependent model.

Previous eco-epidemiological models have demonstrated equilibrial coexistence between predator and disease for the prey host invariably, but those models can not be simplified to a exploitative competition model. Instead, they can only be simplified to an intraguild predation or food chain model (in particular Venturino, 2011a). As such, coexistence between predator and disease is expected. There is one model that looks like exploitative competition and has coexistence (Das et al, 2009), but this coexistence occurs because the predator grows logistically in the absence of prey, so implicitly the predator has another resource.

For brevity, we have not looked into the case where the prey nullcline has both a maximum and a minimum (see Appendix 4.B). In this case, steady states with low prey density are stable, likewise for high prey density (i.e. Scenarios 2A and 3A), but for moderate densities, the steady state is unstable (i.e. Scenarios 2B, 3B and 4). Given this nullcline will probably flatten, move to the left and eventually lose both extrema as we increase prevalence/virulence, it seems plausible that there may be some prevalence region where we are in Scenario 4 whereas without the disease we would be in Scenario 3A or 3B. However, further increases in prevalence/virulence would reverse this and go through the usual pattern from Scenario 4 to Scenario 3 to Scenario 2 and so forth.

In this chapter, we derive a general 'two species' Holling type IV functional response incorporating a handling time that is linear with respect to prey density to a Holling type II functional response. This formulation, although straightforward, seems novel as multispecies Holling type IV functional responses are rarely considered and single species Holling type IV functional responses are usually stated and not derived and explained. In particular, assuming that handling time is a linear function of prey density seems to be the simplest assumption in deriving a single species Holling type IV functional response.

For simplicity, we assumed that the infected prey and susceptible prey are equivalent. Although the full model is cumbersome, future investigations could relax some of these simplifying assumption. For example, we could assume that infected prey may contribute less to the group defence. The authors suspect that if a disease does weaken group defence by more than just reducing host density, the disease could even further benefit the predator by increasing predator density and not just by eliminating extinction risk. In particular, if the disease is trophically transmitted (we have direct transmission in this chapter), it may be beneficial for the disease if the infected prey break down group defence to aid transmission to predators. This should depend on relative importance for the disease of the effect on prey to predator transmission as well as the greater predator numbers and lower prey numbers caused by the breakdown of group defence. However, by doing so, the resulting eco-epidemiological system would almost certainly result in more complicated intraguild predation.

To conclude, we find that predator and disease can coexist at steady state, contradicting the principle of competition. On top of this, in some cases where group defence in the prey is prominent, coexistence between prey and predator can often benefit from the presence of the disease, either by reversing a homoclinic bifurcation or by reducing the prey density below a group defence threshold.

Acknowledgements

4.A Steady state analysis

4.A.1 Disease-free model

From steady state analysis, we have the following conditions for each Scenario (assuming $b > m$):

- Scenario 1: There is no coexistent steady state. Prey-only steady state is stable. (1A)$H_0 > 1$ or $(H_0 - 1)^2 - 4H_x < 0$ (no real solutions), (1B)$H_0 < 1$, $(H_0 - 1)^2 - 4H_x > 0$, $\frac{b-m}{c} < \frac{(1-H_0) \pm \sqrt{(H_0-1)^2 - 4H_x}}{2H_x}$ (two negative solutions).

- Scenario 2: One coexistent steady state exists. It is either (2A) stable or (2B) the centre of some stable limit cycle (depending on the sign of $y'(x^*)$) $\left(H_0 < 1, \right.$
  $\left. (H_0 - 1)^2 - 4H_x > 0, \frac{(1-H_0) - \sqrt{(H_0-1)^2 - 4H_x}}{2H_x} < \frac{b-m}{c} < \frac{(1-H_0) + \sqrt{(H_0-1)^2 - 4H_x}}{2H_x} \right)$ (one positive and one negative solution)

- Scenario 3: Two coexistent steady state exists. The coexistent steady state with the lower prey density is either (3A) stable or (3B) the centre of some limit cycle (depending on the sign of $y'(x^*)$). This is bistable with the prey-only steady state, where the higher prey density coexistent steady state acting as a separatrix. $\left(H_0 < 1, (H_0 - 1)^2 - 4H_x > 0, \frac{(1-H_0) \pm \sqrt{(H_0-1)^2 - 4H_x}}{2H_x} < \frac{b-m}{c} \right)$ (two positive solutions)

4.A.2 Frequency dependent model

The conditions are the same for the frequency dependent model as for the disease-free model except you must substitute m with $m + \mu i^*$, where $i^* = \max\left(0, 1 - \frac{b}{\beta - \mu} \right)$. Note that if $b < m + \mu i^*$, then the disease will cause the extinction of both predator and prey.

4.A.3 Density dependent model

There are the following steady states (x^*, y^*, i^*):

- $(0,0,0)$ always exists and is stable if $b < m$

- $(x^*, 0, 0)$, where $x^* = \frac{b-m}{c}$. This exists when $b > m$ and is stable when $f(x^*) < 1$ (i.e. predators can not survive) and $\frac{\beta x^*}{\mu + b} < 1$ (i.e. disease can not spread)

- $(x^*, 0, i^*)$ where x^*, i^* solve $p(x^*, i^*) = 0$ and $g(x^*) = \mu i^*$. This exists when $x^* > 0$ and $i^* > 0$ $\left(\text{i.e. } b > m \text{ and } \frac{\beta x^*}{\mu + b} > 1\right)$. It is stable if $f(x^*) < 1$ (i.e. predators can not survive)

- $(x^*, y^*, 0)$, where x^* solves $f(x^*) = 1$ $\left(\text{i.e. } x^* = \frac{(1 - H_0) \pm \sqrt{(H_0 - 1)^2 - 4H_x}}{2H_x}\right)$ and $y^* = g(x^*)h(x^*)$. This exists if $x^* > 0$ and $g(x^*) > 0$ $\left(\text{i.e. } H_0 < 1, (H_0 - 1)^2 - 4H_x > 0\right.$ and $x^* < \frac{b-m}{c}$. This means there can be up to two such steady states . It is stable if $\frac{\beta x^*}{\mu + m} < 1$ (i.e. disease can not invade), $f'(x^*) > 0$ and $h(x^*)g'(x^*) + h'(x^*)g(x^*) := y'(x^*) < 0$. If $f'(x^*) < 0$, then this steady state is a saddle point, whereas if $f'(x^*) > 0$ and $y'(x^*) > 0$, we have that the steady state in unstable and is surrounded by a stable limit cycle. The sign of $f'(x^*)$ depends on the relative values of x^* (when two steady states occur); the smaller x^* has $f'(x^*) > 0$, whereas the larger x^* has $f'(x^*) < 0$.

- (x^*, y^*, i^*), where x^* solves $f(x^*) = 1$ $\left(\text{i.e. } x^* = \frac{(1 - H_0) \pm \sqrt{(H_0 - 1)^2 - 4H_x}}{2H_x}\right)$, i^* solves $p(x^*, i^*) = 0$ and $y^* = (g(x^*) - \mu i^*)h(x^*)$. This exists if $x^* > 0$ (i.e. $H_0 < 1$ and $(H_0 - 1)^2 - 4H_x > 0$), $i^* > 0$ $\left(\text{i.e. } \frac{\beta x^*}{\mu + m} > 1\right)$ and $y^* > 0$ (i.e. $g(x^*) > \mu i^*$). This means that there can be up to two steady states. By using qualitative stability criteria on the Jacobian at these steady states, we have that the system is definitely stable when $f'(x^*) > 0$ and $\frac{\partial y^*}{dx^*}(x^*, i^*) < 0$. Likewise, if $f'(x^*) < 0$, then the Jacobian has a positive determinant which means the steady state is unstable. If $\frac{\partial y^*}{dx^*}(x^*, i^*) > \frac{i(\beta x^* - \mu)}{f(x^*)}$, then the Jacobian has a positive trace which means the steady state is unstable. Consequently, we only do not know the stability for the region $f'(x^*) > 0$ and $0 < \frac{\partial y^*}{dx^*}(x^*, i^*) < \frac{i(\beta x^* - \mu)}{f(x^*)}$, presumably there is a Hopf bifurcation within this region (like the disease free case). Like the predator–prey case, there can be up to two steady states.

This steady state analysis can be summarised into the same scenarios as before, but some of the criteria have not been fully analysed. In particular, the Hopf bifurcation separating Scenario 2A/3A and 2B/3B has not been found.

4.B   Phase plane analysis

To complement the steady state analysis, we can use phase plane analysis to derive and demonstrate the different Scenarios (Figures 4-1 and 4-2). For simplicity, we will use nullclines to refer to both the nullclines of the predator–prey system and nullplanes/-surfaces of both the frequency and density dependent models.

There are up to three different predator nullclines. The predator-free nullcline ($y = 0$) always exists. The other two nullclines are the roots (if they exist) of the quadratic equation derived from $f(x) = 1$. These roots are always positive when they exist.

There are two different prey nullclines; one is the prey-free nullcline ($x = 0$), the other nullcline is derived from $y = h(x)(g(x) - \mu i)$. The latter nullcline is in fact cubic with respect to x. Assuming that $b > m + \mu i$, then the intercept at $x = 0$ is positive, and there is one intercept with $y = 0$ at $g(x) = \mu' i$. Given that the nullcline is cubic with respect to x, there can be up to two local extrema. Thus the nullcline can have:

- no realistic (positive) extrema ($y'(0) < 0$ and $y'(x)$ has no positive (or real) roots).

- two realistic (positive) extrema ($y'(0) < 0$ and $y'(x)$ has two positive roots). These extrema are one local minimum and one local maximum, the minimum occurs at lower prey density than the maximum. The region between these two extreme has a positive slope $y'(x) > 0$.

- only one positive local maximum ($y'(0) > 0$)

For simplicity, we will consider the third type of (disease-free) nullclines. The first case will not have a limit cycle, as $y'(x) < 0$ for all $x > 0$. This means only Scenarios 1, 2A and 3A can occur. The second case is a little more complex than the third case, but the same arguments still apply. In fact, the only difference is that for small prey densities (lower than the local minimum), $y'(x) < 0$ and thus steady states can be stable here. In between the maximum and minimum, limit cycles are likely to occur. This formulation does not add any new scenarios but may change the order of scenario changes when we increase prevalence. In particular, it seems plausible that the disease may destabilise the predator–prey equilibrium if the disease moves the minimum to a lower prey density than the lower predator nullcline (i.e. going from Scenario 2A to Scenario 2B or from Scenario 3A to Scenario 3B or 4).

There are at most two disease nullclines, the disease-free nullcline $i = 0$ and the endemic nullcline $p(i, x) = 0$. In the frequency dependent model, the endemic nullcline is $i = 1 - \frac{b}{\beta - \mu}$.
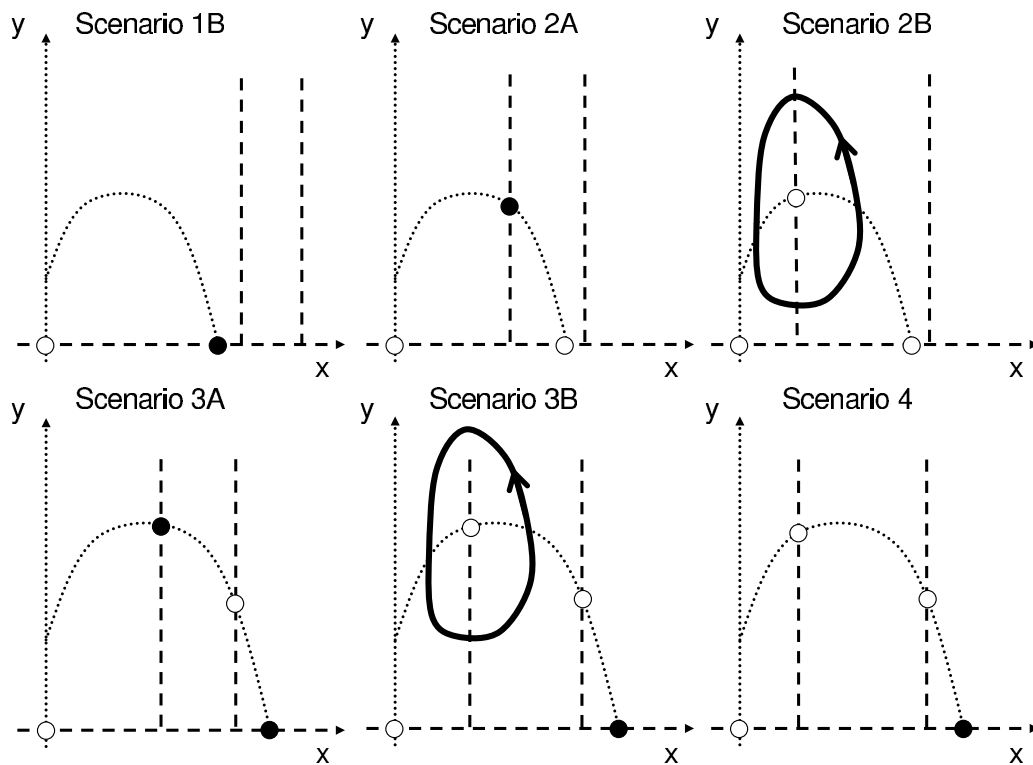
Figure 4-1: *Sketched phase planes of different scenarios from the disease-free predator–prey model with group defence. These scenarios are: a stable prey-only equilibrium with no coexistent equilibrium (Scenario 1B, top left); one stable coexistent equilibrium (Scenario 2A, top middle); one unstable coexistent equilibrium surrounded by a stable coexistent limit cycle (Scenario 2B, top right); bistability between a coexistent equilibrium and prey only equilibrium (Scenario 3A, bottom left); bistability between a coexistent limit cycle surrounding an unstable coexistent equilibrium and a prey-only equilibrium (Scenario 3B, bottom middle); and finally a stable prey-only equilibrium with two unstable equilibria and no limit cycle (Scenario 4, bottom right). The dashed lines represent predator nullclines, the dotted lines represent prey nullclines, the white circles represent unstable steady states, the black circles represent stable steady states and the loop represents a stable limit cycle.*
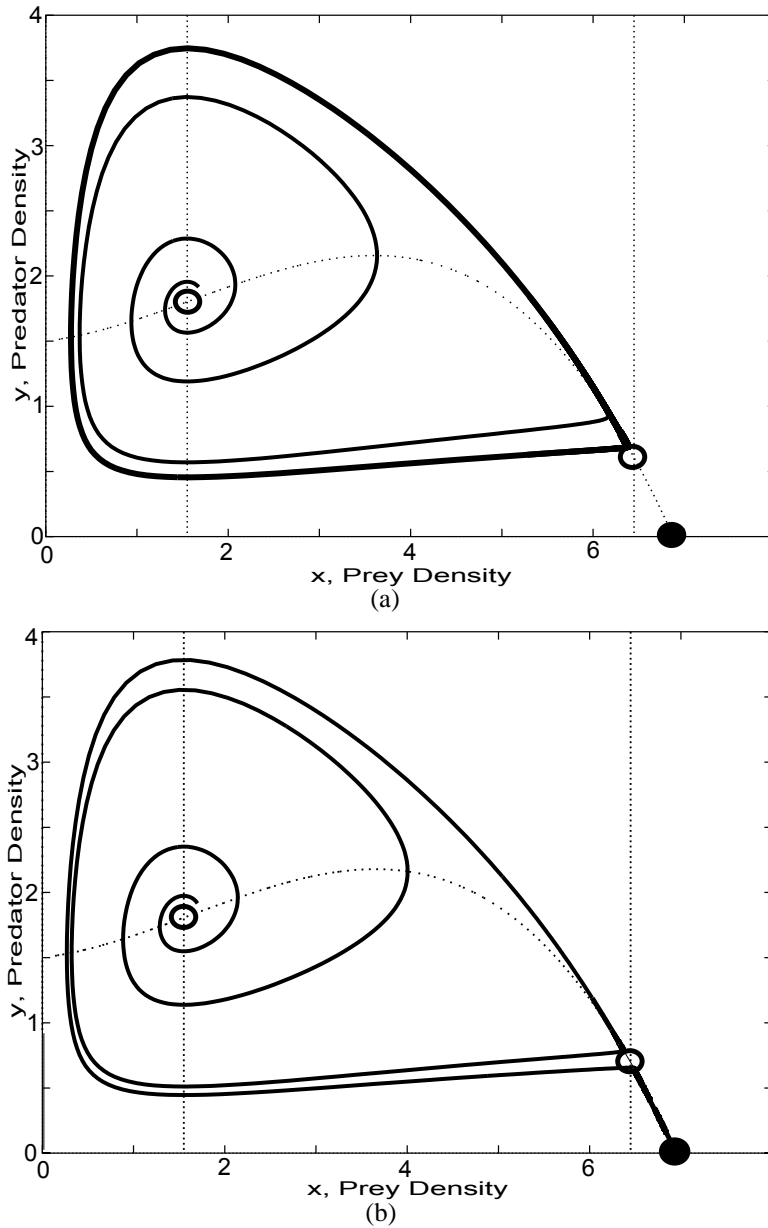
Figure 4-2: *Phase planes demonstrating the existence of a homoclinic bifurcation and the resulting destruction of the stable limit cycle in the disease-free model. (a) is a phase plane with bistability between a stable predator–prey limit cycle and a prey-only equilibrium (Scenario 3B), where the stable predator–prey limit cycle is close to the predator–prey saddle point (c = 0.218); whereas (b) is a phase plane with no stable limit cycle after a homoclinic bifurcation (c = 0.216). Here, all trajectories eventually approach the prey-only steady state despite there being two coexistent steady states (Scenario 4). The dashed lines represent nullclines. Other parameters: $H_0 = 0.2$, $H_x = 0.1$, $b = 2$, $m = 0.5$*
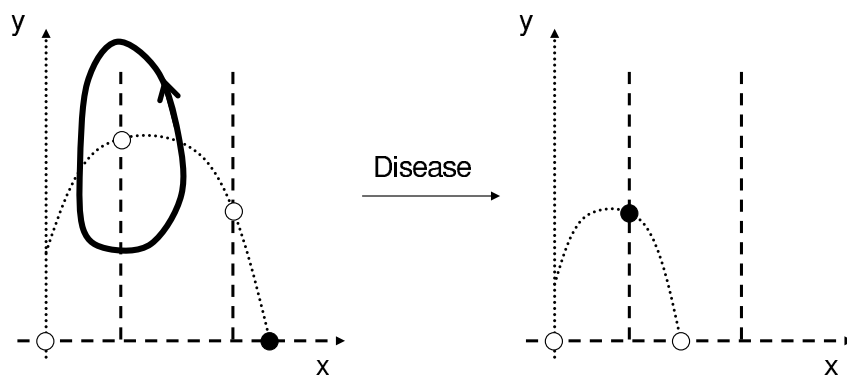
Figure 4-3: *Impact of disease on group defence in the frequency dependent model: sketch of the predator–prey phase plane with nullclines and equilibria where x is prey density and y is predator density. Left hand figure is without disease. Here, there is bistability between the prey-only equilibrium and a predator–prey oscillation, where the predator can not survive 'beyond' the separatrix saddle–point (unstable) equilibrium (Scenario 3B). Including the disease has no effect on the predator nullclines, but it 'lowers' the prey nullcline and moves the maximum to the left and down (right hand figure). These changes stabilise the predator–prey oscillations and result in the prey-only steady state losing stability. Consequently, with the disease, we have a stable predator–prey equilibrium (Scenario 2A). The lines and circles have the same meaning as Figure 4-1.*
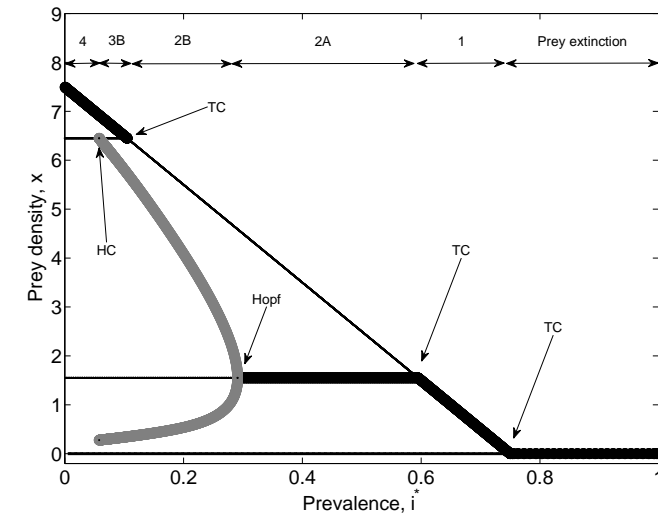
(a)
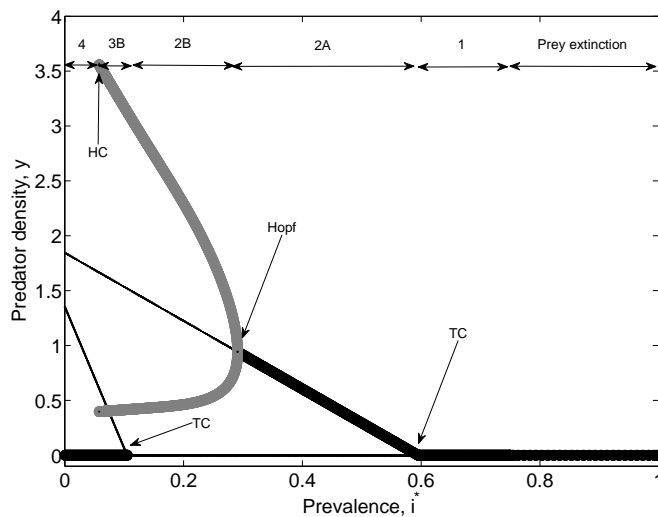
(b)

Figure 4-4: *Frequency dependent model: Bifurcation diagrams of (a) prey density and (b) predator density, with respect to prevalence equilibrium i^*, showing the progression of Scenarios as prevalence increases. As prevalence is assumed to be static, we can treat it as a control parameter. In the absence of disease ($i^* = 0$), only the prey-only steady state is stable but two predator–prey steady states exist (Scenario 4). However, as we increase prevalence, we go from Scenario 4 to Scenario 3B (bistability between predator–prey oscillations and prey-only steady state) to Scenario 2B (only the predator–prey oscillations are stable) to Scenario 2A (only the predator–prey steady state is stable) to Scenario 1 (only the prey-only steady state is stable) to prey extinction. Thick black lines represent stable equilibria, thick grey lines represent stable oscillations and thin black lines represent unstable equilibria. 'TC', 'HC' and 'Hopf' stand for transcritical, homoclinic and Hopf bifurcation, respectively. Other parameters: $H_0 = 0.2$, $H_x = 0.1$, $b = 2$, $m = 0.5$, $c = 0.2$ $\mu = 2$. Figures produced using MATLAB, using data from continuation software XPPAUT.*

(a)

(b)

(c)
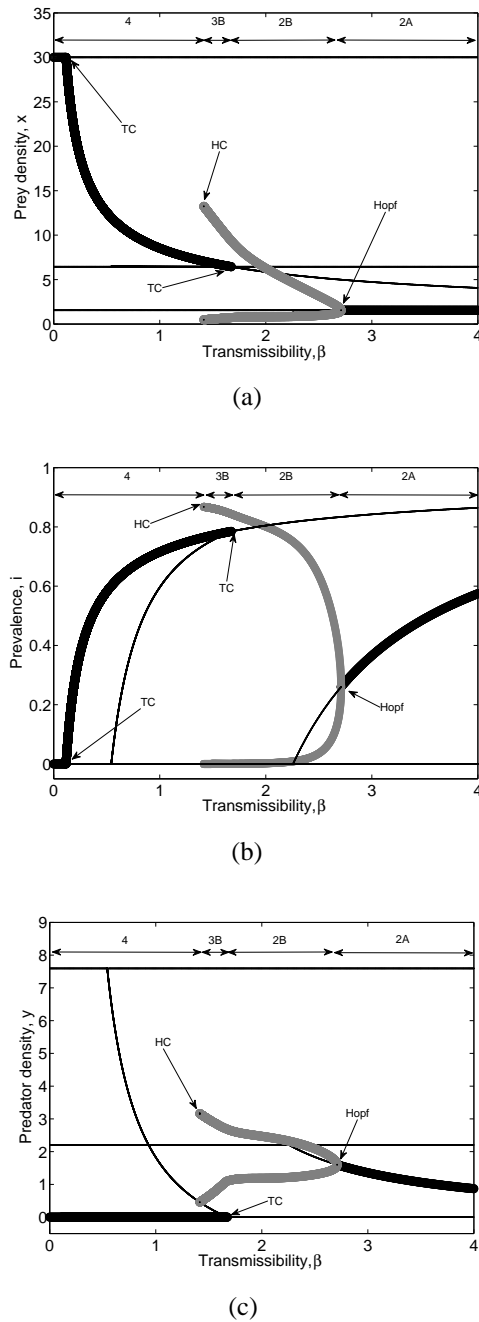
Figure 4-5: *Density dependent model: Bifurcation diagrams of (a) prey density, (b) prevalence and (c) predator density, with respect to transmissibility β. Together they show the progression from a stable prey-only (or prey–disease) steady state with two other predator–prey (or predator–prey–disease steady states) (Scenario 4); to bistability between a coexistent limit cycle and prey–disease equilibrium (Scenario 3B); to a coexistent limit cycle (Scenario 2B); to a coexistent steady state (Scenario 2A). The stable limit cycle numerically breaks down at 'HC'. The labels and lines have the same meaning as Figure 4-4. The trivial (no prey) steady state has been omitted. Parameter values $\mu = 1.5$, $c = 0.05$, $b = 2$, $m = 0.5$, $H_0 = 0.2$ and $H_x = 0.1$.*
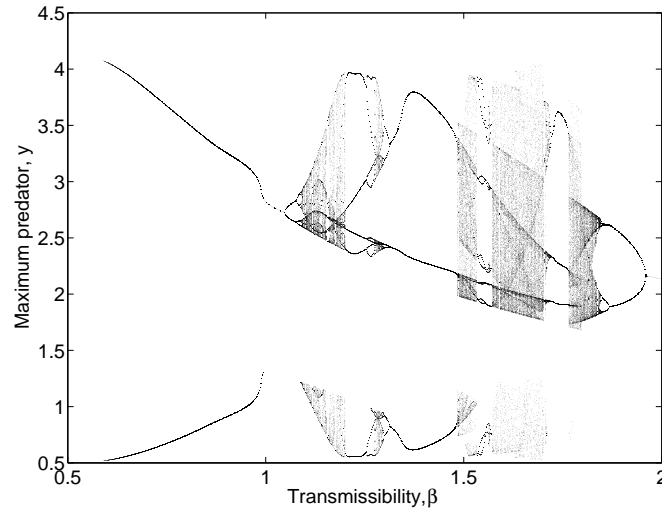
(a)
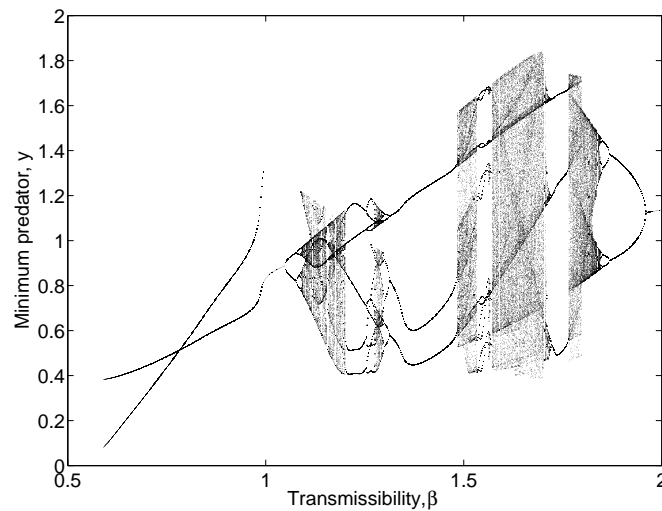
(b)

Figure 4-6: *Complex dynamics in the density dependent model: Bifurcation diagrams of (a) (local) maximum predator density and (b) (local) minimum predator density, with respect to transmissibility. For $\beta \lesssim 0.6$, we are in Scenario IV and the predator can not survive. At $\beta \approx 0.6$, a two-cycle (with respect to the predator) appears (i.e. there are two local maxima and minima). At around $\beta = 1$, one of the local maxima collides with a local minima, resulting in the loss of both. Soon afterwards, a period doubling cascade occurs, resulting in chaos. After this, the second branch of maxima and mimuma reappears, but this time as a chaotic attractor. In the interval $\beta \in (1,2)$, a series of attractor crises occur. Parameter values: $\mu = 1.5$, $c = 0.2$, $b = 2$, $m = 0.5$, $H_0 = 0.2$ and $H_x = 0.1$. Using the initial condition $(x,y,i) = (0.5, 0.5, 0.1)$, we find the numerical solution (by using MATLAB's 'ode45' and the log-transform of equations (4.14)–(4.16), subject to equation (4.17), to avoid numerical errors around zero) for time up to $T = 7000$ and then discard transients (all data up to $T = 4000$).*

Chapter 5

Preytaxis and travelling waves in an eco-epidemiological model

Abstract

We investigate the effects preytaxis has on the wavespeed of several different invasion scenarios in an eco-epidemiological system. In general, preytaxis cannot slow down predator or disease invasions and there are scenarios where preytaxis speeds up predator or disease invasions. For example, in the absence of disease, positive preytaxis results in an increased wavespeed of predators invading prey, whereas negative preytaxis has no effect on the wavespeed, but the wavefront is shallower. On top of this, negative preytaxis can induce spatiotemporal oscillations and/or chaos behind the invasion front, phenomena normally only seen when the steady state is unstable. In the presence of disease, the predator wave can have a different response to attractive susceptible and attractive infected prey. In particular, we found a case where attractive infected prey increases the predators' wavespeed by a disproportionately large amount compared to attractive susceptible prey since a predator invasion has a larger impact on the infected population. When we consider a disease invading a predator–prey steady state, we found some counter-intuitive results. For example, if infected prey attract predators, then the infection wave will move a little faster. Likewise, repulsive susceptible prey can also increase the infection wave's wavespeed. These results suggest that overlooked phenomena like preytaxis can have a major effect on the interactions of predators, prey and diseases.

5.1   Introduction

In previous chapters, we have ignored spatial effects. This means that we have assumed that the populations are averaged over space. However, usually population distributions are not uniform. In particular, biological invasions are inherently local events and not global. For a species (or infection) to successfully invade, it must first be introduced, then establish locally and then spread (Petrovskii and Li, 2006), usually in the form of a travelling wave. There are many examples of predator invasions that are considered to have spread like a travelling wave. The Colorado Potato Beetle spread rapidly across mainland Europe during the mid 20th century (Johnson, 1967; Begon et al, 2002b), damaging potato crops as it spread. Red Foxes have spread across much of mainland Australia over the last 140 years after being introduced in south Victoria around 1871, with major impact on birds and medium-sized mammals (Dickman, 1996). Likewise, there are many epidemics that also moved like a travelling wave, from the Black Death during 14th Century Europe to the spread of rabies across continental Europe (Murray, 2003; Shigesada and Kawasaki, 1997; Langer, 1964, Chapter 13). Other famous invasions that have moved like travelling waves are the Muskrat invasion of Europe (Skellam, 1951; Britton, 2003) and the Grey Squirrel invasion of the British Isles, which has had a massive impact on the native Red Squirrel (Middleton, 1930; Lloyd, 1983; Tompkins et al, 2003; Bell et al, 2009).

Most models that involve spatial movement assume that prey and predators (especially when using PDEs) move by diffusion only. This means that predators and prey move in a random manner with no bias or external stimuli. However, movement is often not random. In particular, there are many external factors that attract or repel prey and predators, be it chemical attractant/repellent gradients (chemotaxis), gradients of oxygen (aerotaxis) or gradients of prey density (preytaxis).

The term 'preytaxis' was first coined in Kareiva and Odell (1987), where they modelled movement patterns of foraging Ladybirds. There are two schools of thought for modelling preytaxis; there are those who incorporate a flux in the predator that is dependent on gradients of prey density (Kareiva and Odell, 1987; Grünbaum, 1998; Lee et al, 2008, 2009; Ainseba et al, 2008), and those who incorporate preytaxis in a separate predator velocity equation where predators accelerate according to prey gradients (with some diffusion term to harmonise predator velocities with neighbours) (Arditi et al, 2001; Sapoukhina et al, 2003; Chakraborty et al, 2007). In other words, the former consider preytaxis as the predators' velocity is proportional to prey gradients (a formulation akin to other classical taxis models like chemotaxis), whereas the later

consider preytaxis as the predators' acceleration is proportional to prey gradients. This difference seems to be largely down to whether you feel it is reasonable to assume that predators can adjust their velocity instantaneously with changes in prey gradients, although I believe there are more caveats to the latter formation. For example, suppose that prey density has fixed gradient for all time over a large domain. In the former, the predators will move at a constant velocity. In the latter, assuming no spatial heterogeneity in velocity as an initial condition, the predators will move with constant acceleration, leading to unrealistic velocities if the domain/prey density gradient is large enough.

These two different schools of modelling preytaxis seem to give different results. In the former, (positive) preytaxis always has a stabilising effect, limiting spatiotemporal oscillations and chaos (Lee et al, 2009), whereas the latter form of preytaxis can only have a stabilising effect for intermediate values of (positive) preytaxis, i.e. strong preytaxis can induce spatiotemporal chaos and oscillations (Sapoukhina et al, 2003). This difference may be attributed to the fact that there is some 'inertia' in the latter formation, predators that have reached the peak of prey density no longer accelerate but still have velocity and thus can overshoot. In this chapter, the former, flux-based method, is used, largely because of its relative simplicity and tangibility and that instantaneous velocity changes in predators seems a reasonable simplifying assumption.

In previous preytaxis papers, the focus has largely been about pattern formation (Chakraborty et al, 2007; Ainseba et al, 2008; Lee et al, 2009) or on the effect preytaxis has for pest control (Sapoukhina et al, 2003; Lee et al, 2008). Given this, studies of preytaxis are relatively limited and a qualitative study of how preytaxis alters predator invasions, the corresponding travelling waves and their wavespeeds has not been investigated, although Ainseba et al (2008) found that predators with preytaxis and diffusion can fill a 2D domain faster than with diffusion alone.

There are no preytaxis papers that consider the impact a disease has on a preytactic predator–prey interaction. In fact, in eco-epidemiology, there have been only a handful of papers that have considered spatial interactions. Most of these spatial eco-epidemiological papers consider infections within plankton communities (Malchow et al, 2004, 2005; Hilker et al, 2006; Sieber et al, 2007; Siekmann et al, 2008). There are other papers considering a general predator–prey–disease system with spatial effects, but they discretise space by using lattices (Su et al, 2009) and cellular automata instead of PDEs (Su et al, 2008; Su and Hui, 2011; Ferreri and Venturino, 2013).

In this chapter, we will develop a spatial eco-epidemiological model that incorporates the random (diffusive) movement of predators and prey as well as predators

moving along susceptible and infected prey gradients (preytaxis). Following that, we will consider the results of various invasion scenarios, with a particular focus on how preytaxis affects the resulting travelling wave and its wavespeed.

5.2 Model derivation

Consider a model with susceptible prey, infected prey and predators, denoted by the densities s, i and p, respectively. Firstly, we will define the non-spatial parameters. Let b be the per-capita birth rate for prey and let m and d be the natural per-capita death rates for prey and predators, respectively. Let c be the coefficient for density dependent mortality caused by competition among prey, which results in logistic growth for the prey. We also assume that infection does not alter the host's per capita birth rate b and competition coefficient c. β is the transmissibility of the disease (in this case, the transmissibility term for density dependent transmission; we will later briefly consider frequency dependent transmission). a_S and a_I are the attack rates of the predator on susceptible and infected prey, respectively. Likewise, h_S and h_I are the handling times of the predator when attacking susceptible and infected prey, respectively. μ is the additional per-capita disease-induced mortality for infected prey. And lastly, e is a conversion coefficient of predators from eating prey. In short, the model is similar to the model in Chapter 4 (i.e. Bate and Hilker, 2014) but with no group defence parameter.

Now, we will assume that susceptible prey, infected prey and predators experience diffusion with coefficients D_S, D_I and D_P, respectively. On top of diffusion, we assume that predators move along prey gradients. This means that the preytaxis flux is $pF_S\frac{\partial s}{\partial x}$ and $pF_I\frac{\partial i}{\partial x}$ for susceptible and infected prey, respectively. This form of preytaxis is chosen because it is a relatively simple form that includes a different preytaxis terms for infected and susceptible prey.

$$\frac{\partial s}{\partial t} = D_S\frac{\partial^2 s}{\partial x^2} + b(s+i) - ms - cs(s+i) - \beta si - \frac{a_S sp}{1+a_S h_S s + a_I h_I i}, \qquad (5.1)$$

$$\frac{\partial i}{\partial t} = D_I\frac{\partial^2 i}{\partial x^2} + \beta si - (m+\mu)i - ci(s+i) - \frac{a_I ip}{1+a_S h_S s + a_I h_I i}, \qquad (5.2)$$

$$\frac{\partial p}{\partial t} = D_P\frac{\partial^2 p}{\partial x^2} - \frac{\partial}{\partial x}\left(pF_S\frac{\partial s}{\partial x} + pF_I\frac{\partial i}{\partial x}\right) + \frac{ep(a_S s + a_I i)}{1+a_S h_S s + a_I h_I i} - dp. \qquad (5.3)$$

We will assume zero flux boundary conditions on the boundaries of spatial domain $[0,L]$, i.e. $\frac{\partial s}{\partial x}(0,t) = \frac{\partial s}{\partial x}(L,t) = 0$, $\frac{\partial i}{\partial x}(0,t) = \frac{\partial i}{\partial x}(L,t) = 0$ and $\frac{\partial p}{\partial x}(0,t) = \frac{\partial p}{\partial x}(L,t) = 0$

for all times t, where L is the width of the domain. Now, we can non-dimensionalise to simplify and reduce the number of parameters. Let $t = \tau T$, $s = \gamma S$, $p = \delta P$ and $x = \chi X$. Then, we choose τ such that the per-capita predator death rate is one ($\tau = \frac{1}{d}$), χ such that the susceptible prey diffusion is set to one ($\chi^2 = \frac{D_S}{d}$), δ such that the coefficient of numerator of the susceptible prey functional response (attack rate) becomes one ($\delta = \frac{d}{a_S}$) and γ such that the coefficient for susceptible prey predation in the predators' numerical response is set to one ($\gamma = \frac{d}{ea_S}$). Given this, we have:

$$\frac{\partial S}{\partial T} = \frac{\partial^2 S}{\partial X^2} + b'(S+I) - m'S - c'S(S+I) - \beta'SI - \frac{SP}{1 + h_S'S + a_R h_I'I}, \tag{5.4}$$

$$\frac{\partial I}{\partial T} = D_R \frac{\partial^2 I}{\partial X^2} + \beta'SI - (m' + \mu')I - c'I(S+I) - \frac{a_R IP}{1 + h_S'S + a_R h_I'I}, \tag{5.5}$$

$$\frac{\partial P}{\partial T} = D_P' \frac{\partial^2 P}{\partial X^2} - \frac{\partial}{\partial X}\left(PF_S' \frac{\partial S}{\partial X} + PF_I' \frac{\partial I}{\partial X} \right) + \frac{P(S + a_R I)}{1 + h_S'S + a_R h_I'I} - P. \tag{5.6}$$

where $b' = \frac{b}{d}$, $m' = \frac{m}{d}$, $c' = \frac{c}{ea_S}$, $\beta' = \frac{\beta}{ea_S}$, $h_S' = \frac{dh_S}{e}$, $a_R = \frac{a_I}{a_S}$ (relative attack rate), $h_I' = \frac{dh_S}{e}$, $D_R = \frac{D_I}{D_S}$, $\mu' = \frac{\mu}{d}$, $D_P' = \frac{D_P}{D_S}$, $F_S' = \frac{dF_S}{ea_S D_S}$ and $F_I' = \frac{dF_I}{ea_S D_S}$. Likewise, from the boundary conditions, we have that $L' = \frac{L\sqrt{d}}{\sqrt{D_S}}$.

To simplify terminology, we will drop all the primes. Now, we will replace susceptible prey with a total prey class, $N = S + I$. Unlike in previous chapters, we will leave the infected class alone and will not consider the prevalence equation. The reason for this is that the prevalence equation would have considerably more complex diffusion and preytaxis terms.

$$\frac{\partial N}{\partial T} = \frac{\partial^2 N}{\partial X^2} + (D_R - 1)\frac{\partial^2 I}{\partial X^2} + bN - mN - cN^2 - \mu I - \frac{(N + (a_R - 1)I)P}{1 + h_S N + (a_R h_I - h_S)I}, \tag{5.7}$$

$$\frac{\partial I}{\partial T} = D_R \frac{\partial^2 I}{\partial X^2} + \beta(N - I)I - (m + \mu)I - cIN - \frac{a_R IP}{1 + h_S N + (a_R h_I - h_S)I}, \tag{5.8}$$

$$\frac{\partial P}{\partial T} = D_P \frac{\partial^2 P}{\partial X^2} - \frac{\partial}{\partial X}\left(PF_S \frac{\partial N}{\partial X} + P(F_I - F_S)\frac{\partial I}{\partial X} \right) + \frac{P(N + (a_R - 1)I)}{1 + h_S N + (a_R h_I - h_S)I} - P. \tag{5.9}$$

Let $f(N, I) = \frac{N + (a_R - 1)I}{1 + h_S N + (a_R h_I - h_S)I}$, $g(N) = b - m - cN$, $k(N, I) = \beta(N - I) - (m + \mu) -$

cN and $f_I(N,I) = \frac{a_R}{1+h_S N+(a_R h_I - h_S)I}$. Then these equations can be written as:

$$\frac{\partial N}{\partial T} = \frac{\partial^2 N}{\partial X^2} + (D_R - 1)\frac{\partial^2 I}{\partial X^2} + Ng(N) - \mu I - f(N,I)P, \qquad (5.10)$$

$$\frac{\partial I}{\partial T} = D_R \frac{\partial^2 I}{\partial X^2} + I(k(N,I) - f_I(N,I)P), \qquad (5.11)$$

$$\frac{\partial P}{\partial T} = D_P \frac{\partial^2 P}{\partial X^2} - \frac{\partial}{\partial X}\left(PF_S \frac{\partial N}{\partial X} + P(F_I - F_S)\frac{\partial I}{\partial X}\right) + P(f(N,I) - 1). \qquad (5.12)$$

The zero flux boundary conditions are $\frac{\partial N}{\partial X}(0,T) = \frac{\partial N}{\partial X}(L,T) = 0$, $\frac{\partial I}{\partial X}(0,T) = \frac{\partial I}{\partial X}(L,T) = 0$ and $\frac{\partial P}{\partial X}(0,T) = \frac{\partial P}{\partial X}(L,T) = 0$ for all time T.

5.3 Non-spatial dynamics

Before we analyse the spatial dynamics, in particular the wavespeeds, we first have to get some basic understanding of the non-spatial dynamics. This is done by understanding the steady states and their stability.

- $(N^*,I^*,P^*) = (0,0,0)$. This always exists, and is stable if $g(0) < 0$, i.e. $b < m$.

- $(N^*,I^*,P^*) = (N^*,0,0)$, which satisfies $g(N^*) = 0$ $\left(\text{i.e. } N^* = \frac{b-m}{c}\right)$. This exists if $g(0) > 0$ (i.e. $b > m$), and is stable if $k(N^*,0) < 0$ $\left(\text{i.e. } R_0 = \frac{\beta N^*}{m+\mu+cN^*} < 1\right)$ and $f(N^*,0) < 1$ (i.e. $(b-m)(1-h_S) < c$)

- $(N^*,I^*,P^*) = (N^*,0,P^*)$, which satisfies $f(N^*,0) = 1$ $\left(\text{i.e. } N^* = \frac{1}{1-h_S}\right)$ and $P^* = N^* g(N^*) = \frac{(b-m)(1-h_S)-c}{(1-h_S)^2}$. This exists if $h_S < 1$ and $(b-m)(1-h_S) > c$. This is stable if the disease can not establish in the presence of predators $\left(k(N^*,0) < P^* f_I(N^*,0), \text{ i.e. } R_0^P = \frac{\beta N^*}{m+\mu+cN^*+P^* f_I(N^*,0)} < 1\right)$ as well as $g(N^*) - cN^* - P^* \frac{\partial f(N^*,0)}{\partial N} < 0$. The latter condition is the result of a Hopf bifurcation at $g(N^*) - cN^* - P^* \frac{\partial f(N^*,0)}{\partial N} = 0$, and thus stable limit cycles are likely to occur if this condition is broken.

- $(N^*,I^*,P^*) = (N^*,I^*,0)$, which satisfies $k(N^*,I^*) = 0$ $\left(\text{i.e. } I^* = N^*\left(1 - \frac{m+\mu+cN^*}{\beta N^*}\right)\right)$ and $N^* g(N^*) = \mu I^*$. This equation forms a quadratic in terms of N^*, which always has one positive and one negative solution. This exists if $0 < I^* < N^*$. It is stable when $f(N^*,I^*) < 1$.

- $(N^*,I^*,P^*) = (N^*,I^*,P^*)$, which satisfies $f(N^*,I^*) = 1$, $k(N^*,I^*) = f_I(N^*,I^*)P^*$ and $g(N^*) = \mu I^* + P^*$. This exists when $P^* > 0$ and $N^* > I^* > 0$. We have not

investigated its stability, but understand that this steady state can lose its stability via a Hopf bifurcation.

It is important to note that, at most, only one steady state is stable. There is no bistability between steady states, this does not say anything about possible bistability involving cyclic and chaotic attractors (like those in Chapter 3, i.e. Bate and Hilker, 2013a). If we assume that $a_R = 1$ and $h_S = h_I$, then the non-spatial model would be the same as Chapter 4 (i.e. Bate and Hilker, 2014) but with a Holling Type II functional response instead of a Holling Type IV functional response.

5.4   Travelling waves

From this point on, we will consider the various invasion scenarios. We assume that the native species are at their corresponding steady state everywhere (be it prey only, prey with endemic disease or disease-free predator–prey steady state), but we will introduce an invader, either the predator or the disease, at a low density in a small region of the spatial domain. In such invasion scenarios, the solutions converge over time to travelling waves.

Before going on to numerical solutions, we will find some analytical minimum wavespeeds. This is done by assuming there is a travelling wave solution with constant wavespeed. By doing so, we use the transformation $Z = X - \omega T$ (where ω is the constant wavespeed) to arrive at a system of ODEs. After linearising ahead of the wave (i.e. at the native steady state) we look at the eigenvalues to see if there is any complex eigenvalues that would lead to unrealistic travelling waves (negative populations). This is sufficient for finding the actual wavespeed on the assumption we have 'linear determinacy'(Lewis et al, 2002), i.e. linearising ahead of the travelling wave gives the wavespeed. In single species systems, it is sufficient for there to be no Allee effect (assuming a constant diffusion coefficient, Aronson and Weinberger, 1975, 1978; Shigesada and Kawasaki, 1997). Many systems have been shown to exhibit this, but the theory for this is lacking for multispecies system (Bell et al, 2009), with a notable exception of competitive/cooperative systems (Lewis et al, 2002). Despite the lack of theory, analogous arguments to scalar systems (like linearising in front of the wave) wave provided a great deal of success to calculation the wavespeed (Bell et al, 2009), i.e. linear determinacy has been shown to be true in many multispecies systems, usually numerically. However, this is not always true, there are cases where the actual wavespeed is substantially faster than the calculated minimum wavespeed (Hosono, 1998).

The derivation of the analytic minimal wavespeeds is in Appendix 5.A, and we find that numerical solutions agree with this wavespeed (at least in the absence of preytaxis). For simplicity we will assume that infecteds move in the same way as susceptibles, i.e. $D_R = 1$.

- Predator invasion in the absence of infected prey:
  $\omega_{crit} = 2\sqrt{D_P(f(N^*, 0) - 1)}$, where N^* is the density of prey at the disease-free prey-only steady state.

- Predator invasion in the presence of infected prey:
  $\omega_{crit} = 2\sqrt{D_P(f(N^*, I^*) - 1)}$, where N^* and I^* are the densities of the total prey and infected prey at the endemic prey-only steady state, respectively.

- Disease invasion in the absence of predators:
  $\omega_{crit} = 2\sqrt{K(N^*, 0)}$, where N^* is the density of prey at the disease-free prey-only steady state.

- Disease invasion in the presence of predators:
  $\omega_{crit} = 2\sqrt{K(N^*, 0) - P^* f_I(N^*, 0)}$, where N^* and P^* are the densities of the prey and predator at the disease-free prey–predator steady state, respectively.

These minimum wavespeeds are independent of preytaxis terms. This is because these wavespeeds are calculated ahead of the invasion (where the system is near the native steady state, with negligible gradients) which results in negligible preytaxis terms. In the absence of preytaxis, we expect that the travelling wave will form and will move at the minimum speed ω_{crit} (after some transient), since the initial condition has compact support (as the initial condition is finite). This is usually very hard to prove mathematically even for simpler models (Edelstein-Keshet, 1988; Murray, 2003), but we can verify numerically that these wavespeeds are attained (after some transient).

5.5   Results

For all results, we will use a spatial domain of $[0, 250]$. The initial conditions will be the relevant native steady state, distributed everywhere on the entire domain, with parameters chosen such that it is stable (at least in the non-spatial system) in the absence of the invader. We will add an invader, using a step function as an initial condition (unless stated otherwise). This step function has the invader at a density of 0.1 for $x \in [0, 20]$ and at a density of 0 elsewhere. A full discussion about the numerical

methods used is in Appendix 5.B. Also, we will assume that susceptible and infected prey only differ by the inclusion of disease-induced mortality and different preytaxis coefficients (i.e. $a_R = 1$, $D_R = 1$ and $h_S = h_I$).

5.5.1 Predator invasion in the absence of infected prey

Without preytaxis ($F_S = 0$)

In the absence of preytaxis, we have a reaction–diffusion predator–prey model. Similar models have been analysed elsewhere (for example Murray, 2003). During the initial stages of the invasion, the dynamics are dominated by the predator establishing and growing locally at the expense of prey (Figure 5-1(a)). By the time $t = 5$, a wave front is largely established, with a predator–prey steady state behind the wave front and a prey-only steady state ahead of the wave. Figure 5-1(b) demonstrates that the wave follows the 'moving line', which tells us that the predator invasion wave is moving at the same speed as the analytically derived minimum speed ω_{crit}. Behind the wavefront, there are some dampened spatiotemporal oscillations. This seems consistent with what would be expected since with the chosen parameter values, the predator–prey steady state is a stable focus.

With positive preytaxis ($F_S > 0$)

Now, incorporating preytaxis into the predator–prey dynamics gives us a reaction–diffusion–taxis predator–prey model. First, let's consider positive preytaxis, i.e. predators move from places of low prey density to places of high prey density, with a velocity proportional to the prey gradient.

At early stages, growth is similar to that of no taxis, with Figure 5-2(a) looking nearly identical to Figure 5-1(a). However, over time, results change substantially. Whereas in Figure 5-1(b), we have that the wave travels at the same speed as the 'moving line', Figure 5-2(b) shows the wave front overtakes the 'moving line', telling us that the travelling wave is moving at a speed significantly faster than the analytically derived minimum speed ω_{crit}. This means that positive preytaxis has increased the wave speed.

To demonstrate this effect further, we have set predator diffusion $D_P = 0$ in Figure 5-3 (and 5-14). By doing so, the analytic wave speed of the predator wave is zero, i.e. the predator can only grow in regions it is established. (Actually, since the initial condition in Figure 5-3 has predators everywhere, a wave should form from growth alone, given enough time. However, we get the same wavespeed from a step function

in 5-14, which tells us that the travelling wave depends on preytaxis, and not just the growth of the initial condition.) This is clearly not the case since there is a travelling wave of constant shape and speed in Figures 5-3 and 5-14. This wave has moved approximately 175 spatial units to the right by $t = 100$. Compare this with Figure 5-2(b), where the wave moved approximately 225 spatial units to the right by $t = 100$ (only about 25 spatial units ahead of the moving line). This suggests that increasing diffusion will reduce the effect of preytaxis. Presumably, this effect is largely due to the fact that diffusion flattens the wavefront, reducing prey gradients and thus the strength of preytaxis as a result.

With negative preytaxis ($F_S < 0$)

In this subsection, we will assume that predators find susceptible prey repulsive and thus move down prey gradients. This may not seem that realistic, although possible cases where it may occur are presented in the Discussion. However, the idea of repulsive infected prey seems more plausible, and the results in this subsection will help in understanding the results that include infected prey.

Figure 5-4(a) shows that by time $t = 5$, the predator distribution is far from uniform around the wavefront, especially as a spike in predator density (with a corresponding trough in prey density) is formed. The wavefront stabilises as time goes on (Figure 5-4(b)), and moves at the analytic wavespeed. Immediately behind the wave, some dampened oscillations take place, which is consistent with the fact that the predator–prey steady state is a stable focus in the absence of spatial effects. However, further behind the wavefront, some spatiotemporal oscillations and/or chaos start to appear. In this case, the predator–prey steady state is not actually stable once spatial effects are taken into account.

Why would negative preytaxis encourage oscillations? Well, since the steady state is a focus (in the absence of spatial effects), we would expect some (damped) oscillations. Given this, we can suppose there are regions with (relatively) high predator density and (relatively) low prey density. In such regions, we expect both prey and predator densities to decline further, prey because of the large numbers of predators, and predators because of the lack of prey to sustain them. However, if nearby there are regions with higher prey densities and lower predator densities, then the predators would migrate into the high-predator–low-prey region. If this movement is strong enough to replenish the predators lost from lack of prey and diffusion, then the peak in predator density is sustained. A similar argument applies to the persistence of troughs in predator density.

So why is the wavespeed the same as the analytically derived wavespeed for negative preytaxis? Well, the wave can not be any slower, as the analytic wavespeed was calculated as a minimum wavespeed. But negative preytaxis should slow the wave, by the same argument as positive preytaxis speeding up the wave. We suspect that instead, the negative preytaxis picks a travelling wave that would otherwise move faster than the minimum wavespeed and be unstable in the absence of negative preytaxis. In this case, the predator wavefront is much shallower, which has been associated with faster travelling waves before (page 446 of Murray, 2002, shows this for the Fisher model). A way of understanding why shallower waves are faster is that shallower waves have a larger spatial region where total population growth is large (regions both ahead and behind of the wavefront do not contribute much to the growth of the invading population), and thus should have a greater growth overall and thus a greater wavespeed. The negative preytaxis slows down this wave to the analytic minimum wavespeed.

5.5.2   Predator invasion in the presence of infected prey

In the absence of preytaxis ($F_S = F_I = 0$), we have that predators invade an infected prey steady state as expected, with the same wavespeed as the analytic wavespeed (Figure 5-5).

With positive preytaxis

Earlier, we demonstrated that positive preytaxis in the disease-free case increases the wavespeed substantially for a predator invasion. However, looking at Figure 5-6(a), if only susceptibles attract predators, then the wavespeed is only slightly increased, despite the fact that susceptibles are much more attractive here than earlier in Figure 5-2. However, if only infecteds are attractive, like in Figure 5-6(b), then the wavespeed of the predator invasion is substantially faster. Well, how can this be explained? We suspect that this phenomenon can be explained by the effect the predator has on each prey class. The effect of the predator on susceptible prey is that they are reduced by predation. However, infected prey take a much greater hit; not only do they experience the additional predation like susceptible prey, but also there are fewer susceptibles to infect. Consequently, an invasion of predators has a much greater effect on infected prey. This means that the gradient of infected prey is steep, whereas the susceptible prey gradient is much more shallow (the changes in total prey density is largely explained by the changes in infected prey density). Consequently, infected prey have steeper gradients and thus a greater preytaxis effect than the shallower gradients of

susceptible prey.

We do note that Figure 5-6(a) has a large proportion of infected prey. For cases where infected prey take up a smaller proportion of the total prey, the increase in wavespeed from attractive infected prey is smaller (and conversely, a larger increase from attractive susceptible prey). In particular, since infected prey always suffer (disproportionately) from a predator invasion, there will alway be an increase in wavespeed from attractive infected prey. The purpose of this example is to demonstrate that infected prey have a disproportionate effect.

With negative preytaxis

Figure 5-7(a) and (b) show that negative preytaxis does not slow the wave. However, the predator wave in Figure 5-7(b) is much shallower than the predator wave in Figure 5-5. This suggests a similar phenomenon to what happened without the disease, that negative preytaxis can lead to shallower wavefronts. However, since this effect is not obvious in Figure 5-7(a), we can conclude that infected prey can have a stronger negative preytaxis effect than susceptible prey. This is for the same reasons too, i.e. the wavefront has a much larger infected prey gradient since predators have a bigger impact on the infected prey class. Also, just as we had in the absence of the disease, negative preytaxis can lead to spatiotemporal oscillations and/or chaos.

5.5.3   Disease invasion in the absence of predators

Since there are no predators, there is no preytaxis to consider.

For a disease invasion in the absence of predators, we have a reaction–diffusion epidemic model. Similar models have been analysed before elsewhere (for example, the rabies models in Murray, 2003). As we had in the predator invasion, for earlier time steps, the dominating dynamics are local growth of the infected class, with a corresponding small reduction to total prey from the additional mortality. However, we also have that in this time scale, infected prey are drifting across. By time $t = 5$, a travelling wave has been formed, behind the wave the dynamics are nearly at the endemic steady state, whereas in front of the wave, we have the disease-free steady state. In between we have a wave front. Comparing the position of the wave front with the 'moving line' in Figure 5-8, we see that the wave front is moving at the same speed as the analytically derived minimum speed ω_{crit}.

5.5.4 Disease invasion in the presence of predators

If the predator does not exhibit preytaxis, then the disease spreads at the same speed as expected (see Figure 5-9). It is worth noting that because of the presence of predators, it is harder for a disease to become endemic due to both the additional deaths from predation and the reduced susceptible prey density from such predation (see Figure 5-8 where the susceptible prey density is 5, whereas in Figure 5-9 prey density is approximately 1.5). Consequently, a significant increase of transmissibility is needed for the disease to establish. On top of this, the invasion of the disease (once fully established locally) does not change the prey density and instead the predator density has been reduced. This reduction in predator density is consistent with the idea that the predator and disease are exploitative competitors (Hardin, 1960, discussed in more detail in Chapter 4, i.e. Bate and Hilker, 2014).

With positive preytaxis

Now we consider that predators are attracted to susceptible prey. Figure 5-10(a) demonstrates that the stabilising effect of positive preytaxis (discussed in the Introduction, Lee et al, 2009) does not have a substantial effect, with the wavespeed for disease invasion remaining the same as the analytic wavespeed. The wavefront is a little steeper than in Figure 5-9.

Now, suppose that infected prey attract predators. If this effect is relatively weak, the wavespeed seems, by eye, to be no different. However, if this attraction is sufficiently strong, a clear increase in wavespeed is found. For example, in Figure 5-10(b), the disease wave has overtaken the 'moving line'. The suspected reason for this is as follows. Once a wavefront is formed, predators would move up the wavefront resulting in a trough in predator density just ahead of the wave and a peak of predator density just behind the wavefront. Having a reduced predator density directly in front of the wave means that (susceptible) prey density is higher. Combining these two effects (their relative importance is not known), the infected prey can spread a little faster since there are more susceptibles to infect as well as a reduced death rate from the reduction in predator density just ahead of the wavefront.

With negative preytaxis

Figure 5-11 demonstrates some interesting results that occur when susceptible prey repel predators. In Figure 5-11(a), the wave is moving faster than expected, with oscillations in the tail.

Why is this wave faster than expected? As we have seen in the predator invasion with negative prey taxis (Figure 5-4(b)), the system can be oscillatory/chaotic. Given this, the presence of an infection seems to perturb the predator–prey steady state, resulting in such oscillations and chaos. We will call these oscillations and chaos within the predator–susceptible-prey system 'turbulence'. This 'turbulence' spreads over time at its own speed. In this turbulence, we have that predator density is on average smaller than at the steady state, and total prey density is on average higher than at the steady state (akin to $\overline{N} > N^*$ and $\overline{P} < P^*$ described in Chapter 2, i.e. Bate and Hilker (2013b) and Armstrong and McGehee (1980)). If this turbulence is moving fast enough to 'escape' the disease (as is the case in Figure 5-11(a)) the assumption of a predator–prey steady state ahead of the infection wave for the analytic wavespeed is no longer valid, and instead the infection wavespeed should be based on the (probably average) densities of the turbulence ahead of the wave.

Now suppose that the disease has frequency dependent transmission and compare Figure 5-11(b) with Figure 5-11(a). Figure 5-11(b) shows the same turbulence as Figure 5-11(a). However, the disease wave moves only at the analytic wavespeed and no faster. This means that the turbulence does not speed up the wave. This supports the idea that the increase in wavespeed in Figure 5-11(a) is due to the change in the average predator and prey densities in the turbulence, since $\overline{R_0}$ does not change with density for frequency dependent transmission, but does for density dependent transmission (much like Chapter 2, i.e. Bate and Hilker, 2013b, in fact, this also suggests the wavespeed is independent of predator density for both frequency dependent and density dependent transmission, just as we had for R_0^* and $\overline{R_0}$ in Chapter 2).

Back to density dependent transmission, if we increase transmissibility from $\beta = 1$ (Figure 5-11(a)) to $\beta = 1.2$ (Figure 5-12), then there are no oscillations in the tail and the wavespeed is not faster than the infected prey. Instead, there is a pulse in prey density around invasion wavefront, but prey density behind the wavefront is the same as ahead of the wavefront. Firstly, the disappearance of oscillations is probably the result of the increase in the infected class from the increase in transmissibility, which increases the total mortality of the total prey class. This additional mortality is known to stabilise Rosenzweig–MacArthur predator–prey oscillations (Hilker and Schmitz, 2008, and references therein, also see Chapter 2). It also restricts the susceptible population, probably flattening susceptible prey gradients, and thus reducing the strength of preytaxis. Likewise, increasing transmissibility from $\beta = 1$ to $\beta = 1.2$ increases the analytical wavespeed. This means that the infection wave is now fast enough to keep up with the turbulence, and stabilises it. In such a case, there is no turbulent 'pull' and

the wavespeed is the same as the analytic wavespeed.

Figure 5-13 considers the case where infected prey repel predators. In Figure 5-13, the wavespeed is the same as the analytic wavespeed, i.e. the negative preytaxis does not speed up or slow down the travelling wave. In the tail behind the wave, there is a short window where the system is near the coexistent steady state before there is a shift to a regime of spatiotemporal oscillations/chaos in the wake of the travelling wave, a phenomena already seen for negative preytaxis for predator invasions.

5.6 Discussion

In this chapter, we analysed the wavespeed of various invasion scenarios in a susceptible-prey–infected-prey–predator system and investigated the effect preytaxis has on the wavespeed of these invasions. In the absence of preytaxis, the wavespeed of the travelling wave is the same as the analytical minimum wavespeed. Adding preytaxis does not necessarily change the travelling wave's wavespeed. However, there are many cases where preytaxis has increased the wavespeed for predator and disease invasion waves.

A positive preytaxis increases the wavespeed for a predator invasion, a phenomenon found in Ainseba et al (2008). In particular, there can be a preytaxis-induced wave where there would be no wave due to no predator diffusion in the absence of preytaxis. On the other hand, negative preytaxis does not seem to slow down the wavespeed. The suspected reason for this is that the analytically derived wavespeed is a minimum speed for a travelling wave to exist (although some transient waves can be slower; Hastings, 1996). This is counter-intuitive as we expect negative preytaxis to slow down travelling waves. We suspect that this difference can be resolved if we consider that the shape of the wave would be that of a faster, shallower wave that is unstable when there is no preytaxis, but the preytaxis slows down this wave and makes it the stable wave. (Murray, 2002, Chapter 13 (in particular page 446 and Figure 13.3) suggests that faster waves are shallower, at least for the Fisher model.)

On top of the wavespeed, we found that negative preytaxis has a destabilising effect, creating and exacerbating predator–prey oscillations which do not exist in the absence of preytaxis. For example, we found many scenarios where, in the absence of spatial effects, the predator–prey steady state is stable, but with spatial effects, the predator–prey steady state is unstable and instead spatiotemporal oscillations and/or chaos are the dominant dynamics. The oscillations seem to have the hallmarks of convective instability (Sherratt et al, 2014; Dagbovie and Sherratt, 2014, and refer-

ences therein). In particular, there are windows of dynamical stabilisation (Petrovskii and Malchow, 2000), where there is some region behind the travelling wave where the (convectively) unstable predator–prey steady state appears to be stable. Dynamical stabilisation usually occurs with convective instability where the instability moves more slowly than the travelling wave. As far as the author knows, if convective instability can be confirmed, this would be the first case of convective instability where the steady state is stable when only considering the underlying kinetic ODEs.

The effect preytaxis has on an invasion of predators on an endemic prey population is largely predictable. In the absence of preytaxis and if there is only negative preytaxis for either susceptible or infected prey (or both), the travelling wave moves at the analytic wavespeed. If preytaxis is positive, then the travelling wave is usually faster than the analytic wavespeed. However, this increase can be very different in magnitude when comparing attractive infected prey and attractive susceptible prey, and depends on several factors. For example, with higher disease transmissibility, there are more infecteds at the endemic steady state and thus the relative strength of infected preytaxis increases. However, on top of this, we have that the invasion of predators has a greater impact on the size of infected prey than on susceptible prey (at least for density dependent transmission). This means that the gradient of infected prey at the wavefront is proportionally greater then that of susceptible prey and thus would cause a greater preytactic 'pull' (at least proportionally). This suggests that infected prey can have a particularly large effect on the wavespeed of the invading predator. In particular, if a non-attractive/repulsive infection ($F_I = 0$) in the host population where susceptible host is attractive to predators ($F_S > 0$), the predator invasion is slowed down greatly, from a wavespeed much faster than expected (Figure 5-2), but in the presence of unattractive infected prey, the predators essentially follow a significantly slower wavespeed (Figure 5-6(a)).

In the absence of preytaxis, the disease wave behaves as expected, moving at the analytic wavespeed. However, the inclusion of preytaxis can increase the wavespeed, indirectly. In particular, we found two cases where preytaxis can increase the wavespeed. The first case was when infected prey attract predators. This seems counter-intuitive since attracting predators should increase the death rate of infected prey and thus slow the disease down. However, what preytaxis does here is to draw predators away from the infection wavefront and into regions where the disease is already established. This means that the tip of the disease wavefront has a considerably smaller predator density and thus a reduced death rate from predation for infecteds ahead. Also, because of the reduction of predators locally, the susceptible prey density is also higher, and thus

disease transmission is increased. Putting these two effects together, we would have a faster wavespeed.

The second case is in some parameter regimes where susceptible prey repel predators and where transmissibility is small enough for the disease wave to be relatively slow. In this case, the perturbation of the infection wave leads to a turbulent wave which spreads ahead of the infection wave due to the destabilising effect of negative preytaxis. This results in predator–susceptible-prey oscillations ahead of the wave. With such oscillations, the average prey density is higher than at equilibrium and the average predator density is lower than at equilibrium. This leads to a faster growth of infections and thus an increased infection wavespeed. This is reminiscent of Chapter 2 (i.e. Bate and Hilker, 2013b), where the criteria for a density dependent disease (but not for a frequency dependent disease) to invade predator–prey oscillations is dependent on the time-averaged density of the host species. In particular, if the disease has frequency dependent transmission, there is no such increase in wavespeed in these spatiotemporal predator–prey oscillations.

Given this result and those in Chapter 2 (i.e. Bate and Hilker, 2013b), we suspect that the disease invading a predator–prey system with spatiotemporal oscillations and chaos would have a wavespeed which will, on average, move at a wavespeed based on the average prey density.

5.6.1   Preytaxis and model assumptions

Here, we have assumed that the preytaxis coefficients are constant. This is the simplest assumption to make, and has been used elsewhere (Grünbaum, 1998; Lee et al, 2009), but other choices of taxis can be made. For example, Lee et al (2009) also consider $F_S \to \frac{F_S}{S}$, the same form as that in the chemotactic model (Keller and Segel, 1971). Lee et al (2008) adapted this by using $\frac{F_S}{S+\tau}$ and $\frac{F_S}{(S+\tau)^2}$ (which was also suggested for chemotaxis by Tyson et al, 1999), to avoid the singularity around $S = 0$. Ainseba et al (2008) did not give an explicit form for the preytaxis, but assumed that there is no preytaxis once prey density is above some threshold. However, others have modelled preytaxis by having a separate equation for velocity (Arditi et al, 2001; Sapoukhina et al, 2003; Chakraborty et al, 2007), which incorporates both preytaxis and velocity 'diffusion' to harmonise the movement of predators. This choice of preytaxis would increase the complexity of the system.

The choice of preytaxis terms focuses on the gradient of prey density. But surely the predator would benefit most from moving towards areas that maximise growth.

This means preytaxis would be based on the gradient of the functional response and not of prey density. In fact, there are many cases discussed in Chapter 4, i.e. Bate and Hilker (2014), where moving towards regions of high prey density would be a bad strategy for predators.

We have only considered preytaxis, the movement of predators towards or away from prey. However, prey could also find predators repulsive or attractive. In fact, Murray (2003, Chapter 1) describes such spatial systems as 'pursuit and evasion', suggesting prey movement is equally important to predator movement in predator–prey interactions. But preytaxis only considers whether predators actively pursue prey. It is very reasonable to consider prey evading predators or 'predataxis' (Berleman et al, 2008). It is usually in the prey's interest to avoid predators. For example, white-tailed deer tend to gather in between wolf pack territories (Murray, 2003, Chapter 14). Likewise, there are many predators that attract prey using chemical, light or other effects. Angler fish attract prey with light and pitcher plants attract flies using their distinctive smell. Including predataxis could lead to other interesting (and possibly counterintuitive) results. For example, given that attractive infected prey in an infection wave increase the infection's wavespeed, then a repulsive predator wave (i.e. negative predataxis) should lead to a gathering of prey just ahead of the predator wave, leading to an increased predator wavespeed. However, such predataxis should also be dependent on the predation pressure itself and not just on the number of predators. This means that prey have safety in numbers as they saturate the predator's functional response, at least until predator density increases from movement and growth.

There are some cases in this chapter that may not seem realistic. For example, many of the most interesting dynamics occur when there exists negative preytaxis, but negative preytaxis seems counter-intuitive.

Repulsive infected prey are easier to give examples. Predators may wish to avoid infected prey for the unpleasant taste, sight or smell. Predators may also fear of getting sick from eating prey. This does require infected prey to be distinguishable from susceptibles from a distance, or at least for predators to gain a sense of the density of infected prey from a distance. If susceptible and infected prey are indistinguishable for predators, the experience of meeting infected prey may put predators off prey in general, and thus susceptible prey may also become repulsive.

It may seem difficult to understand a predator finding susceptible prey repulsive (in the absence of disease). However, the repulsiveness of susceptible prey could be a variety of defence mechanisms. For example, negative preytaxis could occur for defence mechanisms that do not require direct encounters. For example, susceptible prey may

expel repellent chemicals or sounds. Susceptible prey could also alter the environment to something uncomfortable for predators; perhaps predators prefer environments with a particular density of foliage which is altered by a herbivore prey. It is also plausible that high prey densities attract enemies of the predator, enemies the predator would actively avoid. Such mechanisms could be forms of group defence discussed in Chapter 4 (Bate and Hilker, 2014), but these mechanisms do not necessarily influence the functional response. It is also worth noting that for predator invasion, the predator (and prey) may be naive to each other, although this argument does fall down if the time for the travelling wave to form and spread is at a comparable or slower time-scale than the time needed for the naivety to disappear.

In the presence of infection, predators may prefer moving towards regions of high infected prey densities as infected prey are often weaker and more vulnerable. Likewise, infected prey may attract predators if the infection is trophically transmitted. In such cases, repulsive susceptible prey can be understandable as predators find them difficult to overcome.

In conclusion, we have found that by including preytaxis in an eco-epidemiological model, we can find many cases where preytaxis increases the wavespeed of predator and disease invasions. Preytaxis can also change the shape of the travelling wave and cause some spatiotemporal oscillations and/or chaos, but preytaxis can not slow down predator and disease invasions.

5.A   Analytic wavespeeds

For travelling waves, we will seek solutions of the form $(N(X,T),I(X,T),P(X,T)) = (N(Z),I(Z),P(Z))$, where $Z = X - \omega T$ and ω is the wavespeed. We will also assume, for theoretical purposes, that the spatial domain is infinite. This is not a big assumption since the spatial domain is much larger than the wave itself. Likewise, we have assumed that $D_R = 1$. With this, the PDEs in equations (5.10)-(5.12) become:

$$-\omega \frac{dN}{dZ} = \frac{d^2N}{dZ^2} + Ng(N) - \mu I - f(N,I)P, \tag{5.13}$$

$$-\omega \frac{dI}{dZ} = \frac{d^2I}{dZ^2} + I(k(N,I) - f_I(N,I)P), \tag{5.14}$$

$$-\omega \frac{dP}{dZ} = D_P \frac{d^2P}{dZ^2} - \frac{d}{dZ}\left(PF_S\frac{dN}{dZ} + P(F_I - F_S)\frac{dI}{dZ}\right) + P(f(N,I) - 1). \tag{5.15}$$

Equations (5.13)-(5.15) can be rewritten as a system of six first order ODEs,

$$\frac{dN}{dZ} = \dot{N}, \tag{5.16}$$

$$\frac{d\dot{N}}{dZ} = -\omega\dot{N} - (Ng(N) - \mu I - Pf(N,I)), \tag{5.17}$$

$$\frac{dI}{dZ} = \dot{I}, \tag{5.18}$$

$$\frac{d\dot{I}}{dZ} = -\omega\dot{I} - I(K(N,I) - Pf_I(N,I)), \tag{5.19}$$

$$\frac{dP}{dZ} = \dot{P}, \tag{5.20}$$

$$\begin{aligned}
\frac{d\dot{P}}{dZ} &= \frac{-1}{D_P}\left(\omega\dot{P} + P(f(N,I) - 1) - P\left(F_S\left(\dot{P}\dot{N} + P\frac{d\dot{N}}{dZ}\right) + (F_I - F_S)\left(\dot{P}\dot{I} + P\frac{d\dot{I}}{dZ}\right)\right)\right) \\
&= \frac{-1}{D_P}[\dot{P}(\omega - F_S\dot{N} - (F_I - F_S)\dot{I}) + P(f(N,I) - 1)... \\
&\quad ... - P[F_S[-\omega\dot{N} - (Ng(N) - \mu I - Pf(N,I))]... \\
&\quad ... + (F_I - F_S)[-\omega\dot{I} - I(K(N,I) - Pf_I(N,I))]]].
\end{aligned} \tag{5.21}$$

Without any preytaxis ($F_S = F_I = 0$), then equation (5.21) becomes:

$$\frac{d\dot{P}}{dZ} = \frac{-1}{D_P}(\omega\dot{P} + P(f(N,I) - 1)).$$

The Jacobian for equations (5.16)-(5.21) (including preytaxis) is:

$$\begin{bmatrix}
0 & 1 & 0 & \cdots \\
-g(N) - N\frac{\partial g(N)}{\partial N} + P\frac{\partial f(N,I)}{\partial N} & -\omega & \mu & \cdots \\
0 & 0 & 0 & \cdots \\
-I\left(\frac{\partial K(N,I)}{\partial N} - P\frac{\partial f_I(N,I)}{\partial N}\right) & 0 & -(K(N,I) - Pf_I(N,I)) - I\left(\frac{\partial K(N,I)}{\partial I} - P\frac{\partial f_I(N,I)}{\partial I}\right) & \cdots \\
0 & 0 & 0 & \cdots \\
\frac{-P}{D_P}\left(\frac{\partial f}{\partial N}(N,I) + F_S(g(N) + N\frac{\partial g(N)}{\partial N} - P\frac{\partial f(N,I)}{\partial N}) + (F_I - F_S)I\left(\frac{\partial K(N,I)}{\partial N} - P\frac{\partial f_I(N,I)}{\partial N}\right)\right) & \frac{-F_S}{D_P}(\omega P - \dot{P}) & \frac{-P}{D_P}\left(\frac{\partial f}{\partial I}(N,I) + F_S\left(\mu + \frac{\partial f}{\partial I}(N,I)\right) + (F_I - F_S)((K(N,I) - Pf_I(N,I)) + I\left(\frac{\partial K(N,I)}{\partial I} - P\frac{\partial f_I(N,I)}{\partial I}\right))\right) & \cdots
\end{bmatrix}$$

$$\begin{bmatrix}
\cdots & 0 & 0 & 0 \\
\cdots & 0 & f(N,I) & 0 \\
\cdots & 1 & 0 & 0 \\
\cdots & -\omega & If_I(N,I) & 0 \\
\cdots & 0 & 0 & 1 \\
\cdots & \frac{-(F_I - F_S)}{D_P}(\omega P - \dot{P}) & \frac{-1}{D_P}(f(N,I) - 1 + F_S[\omega\dot{N} + (Ng(N) - \mu I - 2Pf(N,I))] + (F_I - F_S)[\omega\dot{I} + I(K(N,I) - 2Pf_I(N,I))]) & \frac{-1}{D_P}(\omega - F_S\dot{N} - (F_I - F_S)\dot{I})
\end{bmatrix}$$

5.A.1 Predator invasion in the absence of infected prey

Consider that there is a prey-only steady state in front of a travelling wave of predators (thus we will ignore all infected prey equations/terms). We can linearise around this

steady state, $(N, \dot{N}, P, \dot{P}) = (N^*, 0, 0, 0)$, where $g(N^*) = 0$, and ignore the disease, to get the Jacobian:

$$\begin{pmatrix} 0 & 1 & 0 & 0 \\ cN^* & -\omega & \mu & 0 \\ 0 & 0 & 0 & 1 \\ 0 & 0 & -\frac{f(N^*,0)-1}{D_P} & -\frac{\omega}{D_P} \end{pmatrix}$$

Fortunately, this Jacobian is block upper triangular, so the eigenvalues are the eigenvalues of $\begin{pmatrix} 0 & 1 \\ cN^* & -\omega \end{pmatrix}$ and $\begin{pmatrix} 0 & 1 \\ -\frac{f(N^*,0)-1}{D_P} & -\frac{\omega}{D_P} \end{pmatrix}$. The former has eigenvalues $\frac{-\omega \pm \sqrt{\omega^2 + 4cN^*}}{2}$, which are always real, whereas the latter has eigenvalues $\frac{-\omega \pm \sqrt{\omega^2 - 4D_P(f(N^*,0)-1)}}{2D_P}$, which are real as long as $\omega \geq 2\sqrt{D_P(f(N^*,0)-1)}$. This means that a travelling wave with invade at a minimum speed of $\omega_{crit} = 2\sqrt{D_P(f(N^*,0)-1)}$. It is worth noting that this is independent of the preytaxis coefficient. The reason for this is that at the leading edge of the predator invasion, prey density is nearly constant and thus there is no prey gradient for the predator to move along. However, this does not mean that preytaxis will have no effect on the wave away from the front edge.

5.A.2   Predator invasion in the presence of infected prey

Starting with the steady state $(N, \dot{N}, I, \dot{I}, P, \dot{P}) = (N^*, 0, I^*, 0, 0, 0)$, where $N^* g(N^*) = \mu I^*$ and $K(N^*, I^*) = 0$, the Jacobian becomes:

$$\begin{pmatrix} 0 & 1 & 0 & 0 & 0 & 0 \\ -g(N^*) + cN^* & -\omega & \mu & 0 & f(N^*,I^*) & 0 \\ 0 & 0 & 0 & 1 & 0 & 0 \\ -I^* \frac{\partial K(N^*,I^*)}{\partial N} & 0 & -I^* \frac{\partial K(N^*,I^*)}{\partial I} & -\omega & I^* f_I(N^*,I^*) & 0 \\ 0 & 0 & 0 & 0 & 0 & 1 \\ 0 & 0 & 0 & 0 & \frac{-1}{D_P}(f(N^*,I^*)-1) & \frac{-\omega}{D_P} \end{pmatrix}$$

Again, this is block upper-triangular, and thus we get the subsystem $\begin{pmatrix} 0 & 1 \\ -\frac{f(N^*,I^*)-1}{D_P} & -\frac{\omega}{D_P} \end{pmatrix}$. This has eigenvalues $\frac{-\omega \pm \sqrt{\omega^2 - 4D_P(f(N^*,I^*)-1)}}{2D_P}$. This means that the travelling wave has a minimal wavespeed of $\omega_{crit} = 2\sqrt{D_P(f(N^*,I^*)-1)}$.

The rest of the system is:

$$\begin{pmatrix} 0 & 1 & 0 & 0 \\ -g(N^*) + cN^* & -\omega & \mu & 0 \\ 0 & 0 & 0 & 1 \\ -(\beta - c)I^* & 0 & \beta I^* & -\omega \end{pmatrix}$$

This subsystem has eigenvalues $\lambda = \frac{-\omega \pm \sqrt{\omega^2 - 2(A \pm \sqrt{A^2 - 4B})}}{2}$, where $A = g(N^*) - cN^* - \beta I^* < 0$ and $B = I(\beta(\mu + cN^* - g(N^*)) - c\mu) > 0$ (these are the trace and deter-

minant of the Jacobian of the susceptible-infected prey subsystem around the endemic steady state, and $A^2 - 4B < 0$ is the condition for the steady state to be a stable focus). These eigenvalues, however, can have complex parts since $N^*, I^* > 0$, and thus a focus around (N^*, I^*) can be realistic (i.e. no issue about negative populations) and consequently this subsystem should not pose a restriction of the wave speed.

5.A.3   Disease invasion in the absence of predators

Consider that there is a prey-only steady state in front of a travelling wave of infection (thus we will ignore all predator equations/terms). We can linearise around this steady state, $(N, \dot{N}, I, \dot{I}) = (N^*, 0, 0, 0)$, where $g(N^*) = 0$, and ignore the predator, to get the Jacobian:

$$\begin{pmatrix} 0 & 1 & 0 & 0 \\ cN & -\omega & \mu & 0 \\ 0 & 0 & 0 & 1 \\ 0 & 0 & -K(N,0) & -\omega \end{pmatrix}$$

Fortunately, this Jacobian is block upper triangular, of which the top block has already been considered, with eigenvalues that are always real. The bottom block is $\begin{pmatrix} 0 & 1 \\ -K(N^*,0) & -\omega \end{pmatrix}$, and has eigenvalues $\frac{-\omega \pm \sqrt{\omega^2 - 4K(N^*,0)}}{2}$, which are real if $\omega \geq 2\sqrt{K(N^*,0)}$. This means that the disease will invade at a minimum speed $\omega_{crit} = 2\sqrt{K(N^*,0)}$.

5.A.4   Disease invasion in the presence of predators

Here, we start with the steady state $(N, \dot{N}, I, \dot{I}, P, \dot{P}) = (N^*, 0, 0, 0, P^*, 0)$, where $f(N^*, 0) = 1$ and $P^* = N^* g(N^*)$ (and $g(N^*) - cN^* - P^* \frac{\partial f(N^*, 0)}{\partial N} < 0$ for the steady state to be stable). Then the Jacobian becomes:

$$\begin{pmatrix} 0 & 1 & 0 & 0 & 0 & 0 \\ -g(N^*) + cN^* + P^* \frac{\partial f(N^*,0)}{\partial N} & -\omega & \mu & 0 & 1 & 0 \\ 0 & 0 & 0 & 1 & 0 & 0 \\ 0 & 0 & -(K(N^*,0) - P^* f_I(N^*,0)) & -\omega & 0 & 0 \\ 0 & 0 & 0 & 0 & 0 & 1 \\ \frac{-P^*}{D_P}\left(\frac{\partial f}{\partial N}(N^*,0) + F_S(g(N^*) - cN^* - P^* \frac{\partial f(N^*,0)}{\partial N})\right) & \frac{-F_S \omega P^*}{D_P} & \frac{-P^*}{D_P}\left(\frac{\partial f}{\partial I}(N^*,0) + F_S(\mu + \frac{\partial f}{\partial I}(N^*,0)) + (F_I - F_S)(K(N^*,0) - P^* f_I(N^*,0))\right) & \frac{(F_S - F_I)\omega P^*}{D_P} & \frac{F_S P^*}{D_P} & \frac{-\omega}{D_P} \end{pmatrix}$$

The middle two rows (for I and $\dot{I}$) can be separated as all other terms in these rows are zero. Thus we have the matrix $\begin{pmatrix} 0 & 1 \\ -(K(N^*,0) - P^* f_I(N^*,0)) & -\omega \end{pmatrix}$, which has the eigenvalues $\frac{-\omega \pm \sqrt{\omega^2 - 4(K(N^*,0) - P^* f_I(N^*,0))}}{2}$. These are real if $\omega^2 \geq 4(K(N^*,0) - P^* f_I(N^*,0))$ and thus the suspected minimum wavespeed is $\omega_{crit} = 2\sqrt{K(N^*,0) - P^* f_I(N^*,0)}$.

However, we need to check the other eigenvalues, namely of,

$$\begin{pmatrix} 0 & 1 & 0 & 0 \\ -\pi & -\omega & 1 & 0 \\ 0 & 0 & 0 & 1 \\ \frac{-P^*}{D_P}\left(\frac{\partial f}{\partial N}(N^*,0)+F_S\pi\right) & \frac{-F_S\omega P^*}{D_P} & \frac{F_S P^*}{D_P} & \frac{-\omega}{D_P} \end{pmatrix} \qquad (5.22)$$

where $\pi = g(N^*) - cN^* - P^*\frac{\partial f}{\partial N}(N^*,0)$. The eigenvalues of this system are complex and difficult to find. However, they do not need to be real as they represent the predator–prey subsystem and spiraling around the predator–prey steady state poses no threat of negative populations. Thus we do not have any more restrictions on the values for ω.

However, if we assume that $F_S = 0$ and $D_P = 1$, then we can reduce the system from a quartic equation to a quadratic equation: $\tau^2 + \pi\tau + P^*\frac{\partial f}{\partial N}(N^*,0)$, where $\tau = \lambda(\lambda+\omega)$ and $\pi = g(N^*) - cN^* - P^*\frac{\partial f}{\partial N}(N^*,0) < 0$. From this, we have $\tau = \frac{-\pi \pm \sqrt{\pi^2 - 4P\frac{\partial f}{\partial N}(N^*,0)}}{2}$. Thus we have $\lambda = \frac{-\omega \pm \sqrt{\omega^2+4\tau}}{2}$. Since $\pi < 0$ and $\frac{\partial f}{\partial N}(N^*,0) > 0$, then all λ's are real if and only if τ is real, i.e. $\pi^2 > 4P^*\frac{\partial f}{\partial N}(N^*,0)$. This condition is the same as the condition for the predator–prey steady state to be stable. The eigenvalues for other values of F_S and D_P have not been found.

5.B   Numerical methods

The initial condition consists of two parts. First, there are the native specie(s), which we assume will be at the relevant (stable, at least in a non-spatial sense) coexistent steady state. For both the predator–prey and endemic prey steady state initial condition are derived by running MATLAB's 'ode45' and taking their densities at the final time ($t = 1000$). The invading initial condition will generally be a step function of 0.1 for $x \leq 20$ and zero otherwise. However, for some scenarios, in particularly when predator diffusion is very small (or zero), it is preferable for a smooth initial condition to be used. In these cases, a smooth approximation of the step function, $0.05(1 - tanh(x - 20))$, is used.

The numerical scheme can be written as follows:

$$N(x,t+t_{step}) = N(x,t) + N_{growth}(x,(t,t+t_{step})) + N_{diffusion}(x,(t,t+t_{step})), \quad (5.23)$$

$$I(x,t+t_{step}) = I(x,t) + I_{growth}(x,(t,t+t_{step})) + I_{diffusion}(x,(t,t+t_{step})), \quad (5.24)$$

$$P(x,t+t_{step}) = P(x,t) + P_{growth}(x,(t,t+t_{step})) + P_{diffusion}(x,(t,t+t_{step}))...$$

$$... + P_{taxis}(x,(t,t+t_{step})). \quad (5.25)$$

where, for example $N_{growth}(x,(t,t+t_{step}))$, is the growth of N at point x over the time interval $(t,t+t_{step})$.

However, each of these terms have different properties. In particular, using one numerical scheme to deal with all these simultaneously would be highly problematic. In particular, the diffusion terms suggest using a scheme appropriate for parabolic PDEs, but such schemes would have real difficulty handling the taxis terms. Instead of trying to use one scheme to solve the whole system simultaneously, we will split the system into a sequence of smaller problems using a Strang splitting scheme (Chapter 18 of LeVeque, 1992; Tyson et al, 2000). This scheme is implemented as follows.

First, solve the diffusion only problem numerically for half a time step and take this as the new solution at time t, i.e. for predators we have:

$$P^*(x,t) := P(x,t+0.5*t_{step}) = P(x,t) + P_{diffusion}(x,(t,t+0.5t_{step})) \quad (5.26)$$

Do the same for susceptible and infected prey to derive $N^*(x,t)$ and $I^*(x,t)$, respectively. Following this, we then perform a taxis half step using an appropriate numerical scheme to again get a new solution at time t (note, this step only changes the predators since there is no taxis in the other classes).

$$P'(x,t) := P^*(x,t+0.5t_{step}) = P^*(x,t) + P_{taxis}(x,(t,t+0.5t_{step})) \quad (5.27)$$

The next step is to take a full time step with only the growth dynamics, using an appropriate solver. This will form a new solution, which will be centered at time $t+0.5t_{step}$.

$$\hat{P}(x,t+0.5t_{step}) := P'(x,t+t_{step}) = P'(x,t) + P_{growth}(x,(t,t+t_{step})) \quad (5.28)$$

Likewise, you get $\hat{N}(x,t+0.5t_{step})$ and $\hat{I}(x,t+0.5t_{step})$ by the same method, using $N'(x,t)$ and $I'(x,t)$ instead, respectively. Next, another taxis half step is taken (which

only affects the predator equation). This gives a new solution at time $t + 0.5t_{step}$.

$$\bar{P}(x, t + 0.5t_{step}) := \hat{P}(x, t + t_{step}) = \hat{P}(x, t) + P_{taxis}(x, (t + 0.5t_{step}, t + t_{step})) \quad (5.29)$$

Finally, we take this solution and incorporate a half step of diffusion to get a final solution for time $t + t_{step}$.

$$P(x, t + t_{step}) := \bar{P}(x, t + 0.5t_{step}) + P_{diffusion}(x, (t + 0.5t_{step}, t + t_{step})) \quad (5.30)$$

Do the same with $\hat{N}(x, t + 0.5t_{step})$ and $\hat{I}(x, t + 0.5t_{step})$ to get $N(x, t + t_{step})$ and $I(x, t + t_{step})$, respectively.

This scheme splits the problem into several smaller, more manageable steps, as well as allowing us to choose appropriate numerical methods for each subproblem instead of trying to use one scheme that would have difficulty handling the whole. One key advantage of this scheme is that it is of order 2 as long as each subproblem is order 2 or better.

For the growth step, the dynamics are local and thus a simple explicit ODEs solver can be used. We used the midpoint method (2nd order Runge–Kutta). This is a reliable scheme for ODE, and because of this, it was chosen for the full step. For diffusion, both a forward-time–centered-space (FTCS) scheme and a Crank–Nicolson scheme were used and compared. The former is of order 1 with respect to time (order 2 with respect to space). This scheme is conditionally stable; it is stable if $\frac{t_{step}}{(x_{step})^2} < 0.5$. The latter scheme is implicit and of order two with respect to time and space. It is unconditionally stable, although there are still numerical issues about artificial oscillations during the first few steps if $\frac{t_{step}}{(x_{step})^2}$ is too large and initial condition is too spiky. Consequently, the same step sizes will be used for both FTCS and Crank–Nicolson. Results between the two schemes have been compared and agree very well, the only visible difference being around $x = 0$ in some cases of spatiotemporal chaos. There are no noticeable differences with respect to the wavespeed and the wavefront.

For the taxis term, we have used a two-step Lax–Wendroff scheme. It is an explicit second order (with respect to both time and space) scheme for hyperbolic PDEs (Chapter 11 of LeVeque, 1992; Morton and Mayers, 2002). It is very good at following suitably smooth solutions, but has issues around very large gradients and discontinuities, where solutions will overshoot and oscillate around sharp (i.e. non-smooth) points, particularly behind the discontinuity. These oscillations dampen away from the discontinuity. This can lead to issues in a few cases, especially if this results in negative populations. However, this scheme does follow the magnitude of peaks and

their wavespeed very well. Note that this issue only really matters if negative prey-taxis is too strong compared to diffusion in predators. In particular, if $D_P = 0$, then the numerical scheme breaks down for any negative preytaxis as negative populations arise. Other numerical schemes were considered. For example, an upwind scheme was considered, but it is only of order 1 in time and space. It does not have these oscillations around sharp points, but instead these points are smeared over as if there was some strong diffusive force. Another second order scheme is Beam–Warming, which is like the Lax–Wendroff scheme except the oscillations are ahead of the wave (LeVeque, 1992, Chapter 11), potentially altering the dynamics ahead of the wave, and may lead to negative populations in cases of positive preytaxis. Likewise, the leapfrog scheme is order two, but it has oscillations behind the wave that do not die out (Morton and Mayers, 2002). These oscillations are generic for second order schemes (LeVeque, 1992, Chapter 11).

It is well worth noting that the inclusion of predator diffusion increases the smoothness of the numerical solutions, which improves the reliability of the Lax–Wendroff scheme. This is why the step function is used for every figure where $D_P > 0$. However, in the absence of predator diffusion, Figure 5-14(a) shows that the step function initial condition does not smooth out but instead brings in fuzziness in the back edge of the wavefront. This contrasts with Figure 5-3(a), where a smooth wave forms. However, even by $t = 5$, the solution in Figure 5-14(a) is largely smooth for the predator. In fact, both Figure 5-3(b) and 5-14(b) show that the wave move at the same speed (actually, in Figure 5-14(a) the travelling wave stays about 0.25 spatial units behind Figure 5-3(b) over times $t = 5, 10, 20, 50$ and 100, this difference can be explained by the time taken to converge to the wavefront). However, without diffusion, even the slightest negative preytaxis results in negative predator populations and the eventual breakdown of the numerical solution.

Boundary conditions are incorporated by setting the first and last spatial point to be equal to their immediate neighbour (and thus there is zero flux). This is done after each substep.

All figures have step sizes of $t_{step} = 0.0005$ and $x_{step} = 0.05$ for time and space, respectively (unless stated otherwise). This means that the diffusion step is fine for both FTCS and Crank-Nicolson because $\frac{t_{step}}{(x_{step})^2} = 0.2 < 0.5$ (in fact, it probably is 0.1 due to the half steps). Other time and space step sizes have been considered and results do not look different as long as they are sufficiently small and the condition $\frac{t_{step}}{(x_{step})^2} < 0.5$ is satisfied.
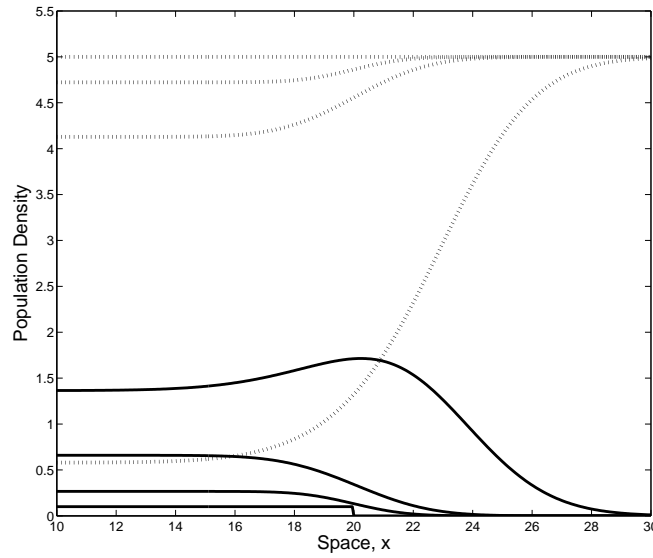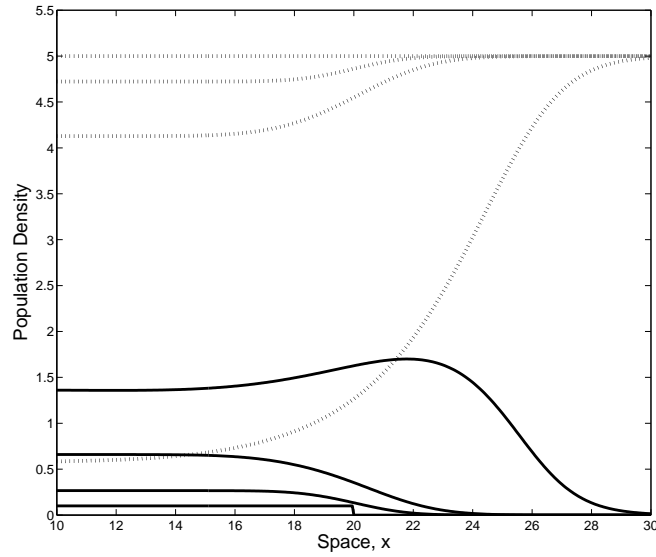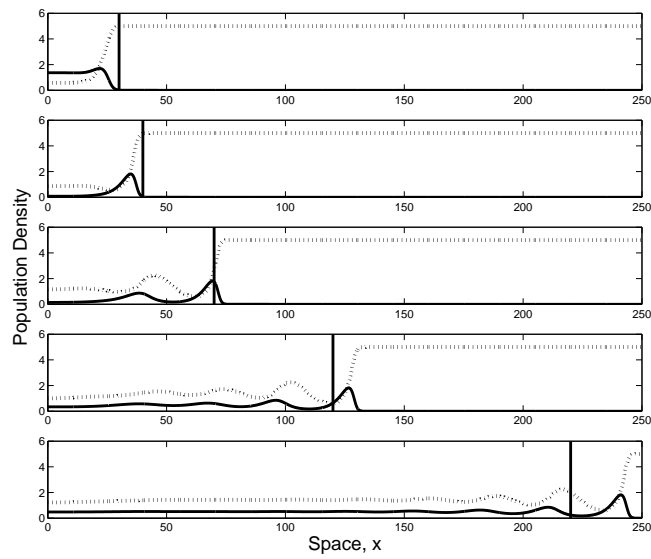
(a)
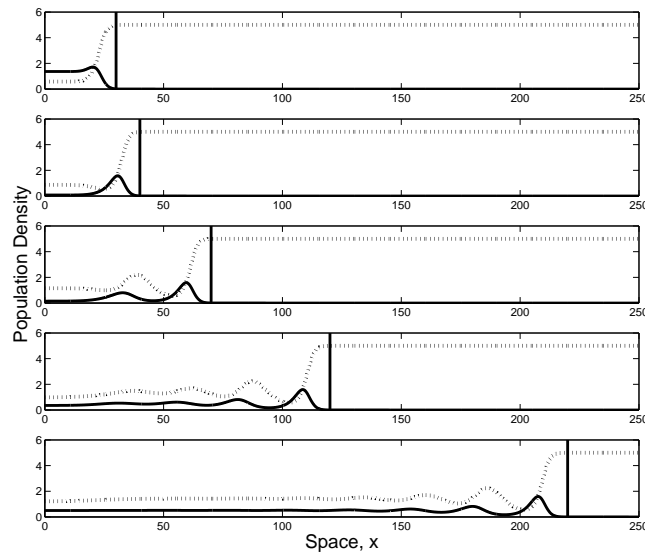
(b)

Figure 5-1: *Predator invasion in the absence of disease. No preytaxis. (a) shows the initial stages of predator invasion, where the predators grow locally up to steady state and spread to converge to the shape of the travelling wave. (b) shows that after this convergence, the wave travels with a speed that agrees with the analytic speed. For (a) the times are $T = 0, 1, 2, 5$ whereas for (b) the times are $T = 5, 10, 25, 50, 100$. The dotted lines (top) represent total prey density, whereas the bold lines (bottom) represent predator density. The vertical lines in (b) represent the expected position of the wavefront $20 + \omega_{crit} * T$, where ω_{crit} is the analytical wavespeed. Parameter values: $b = 1$, $m = 0.5$, $c = 0.1$, $h_S = 0.3$, $D_P = 1$ and $F_S = 0$.*
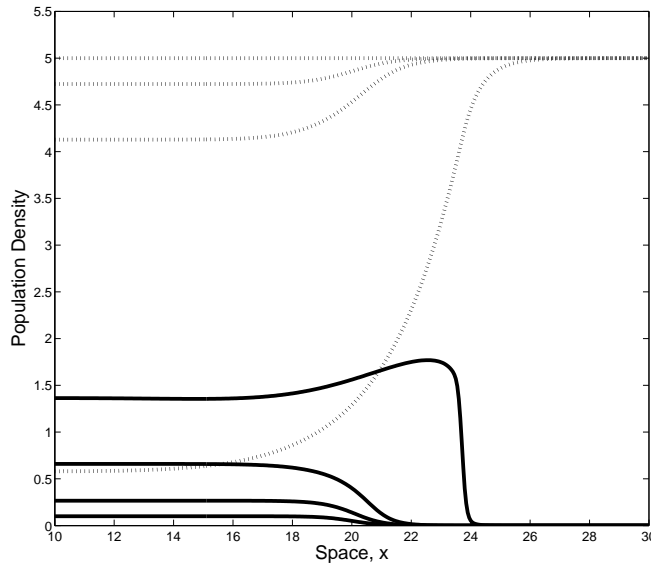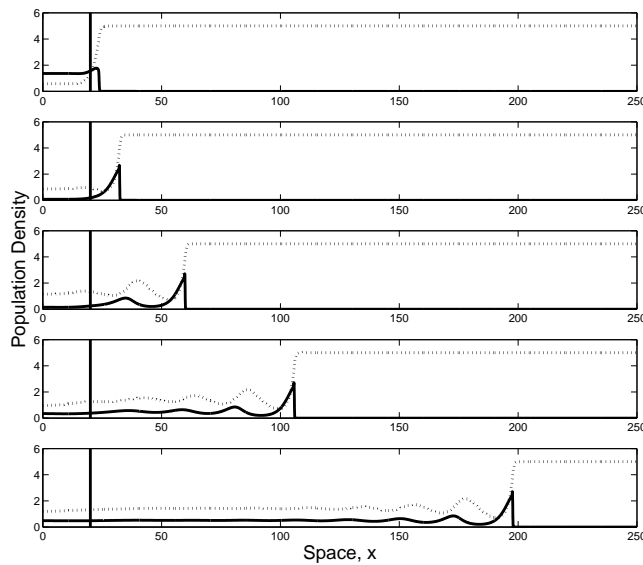
(a)

(b)

Figure 5-2: *Predator invasion in the absence of disease. Positive preytaxis. (a) shows the initial stages of predator invasion, where the predators grow locally up to steady state and spread to converge to the shape of the travelling wave. (b) shows that after this convergence, the wave travels faster than the analytic speed. The times and lines used are the same as Figure 5-1. Parameter values: $b = 1$, $m = 0.5$, $c = 0.1$, $h_S = 0.3$, $D_P = 1$ and $F_S = 1$.*
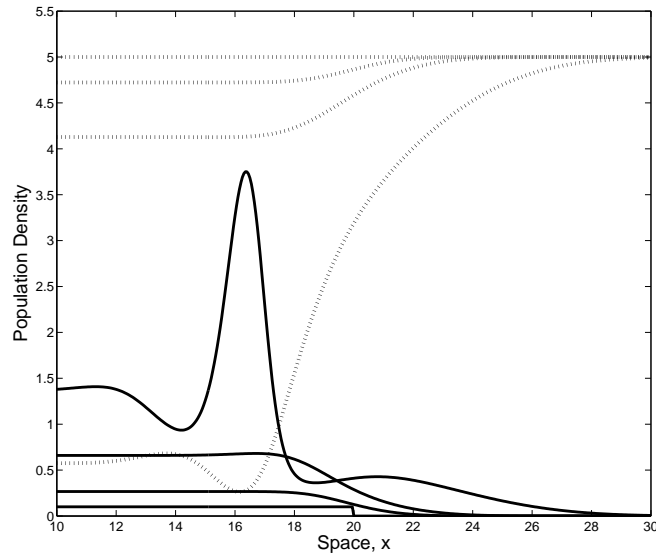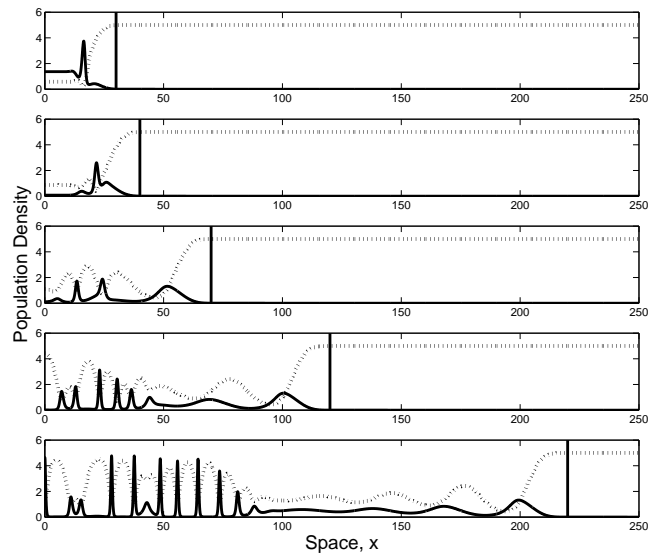
(a)

(b)

Figure 5-3: *Predator invasion in the absence of disease. Positive preytaxis, no predator diffusion. (a) shows the initial stages of predator invasion, where the predators grow locally up to steady state and spread to converge to the shape of the travelling wave. (b) shows that after this convergence, the wave moves (at some wavespeed) where it should not in the absence of preytaxis. Parameter values: $b = 1$, $m = 0.5$, $c = 0.1$, $h_S = 0.3$, $D_P = 0$ and $F_S = 1$. The initial condition is a smoothed approximation of the step function $(0.05(1 - tanh(x - 20)))$. Results for the normal step function initial conditions are in Figure 5-14. The times and lines used are the same as Figure 5-1.*

(a)

(b)

Figure 5-4: *Predator invasion in the absence of disease. Negative preytaxis. (a) shows the initial stages of predator invasion, where the predators grows locally up to steady state and spreads to converge to the shape of the travelling wave. (b) shows that after this convergence, the wave travels with a speed that agrees with the analytic speed. Parameter values: $b = 1$, $m = 0.5$, $c = 0.1$, $h_S = 0.3$, $D_P = 1$ and $F_S = -3$. The times and lines used are the same as Figure 5-1.*
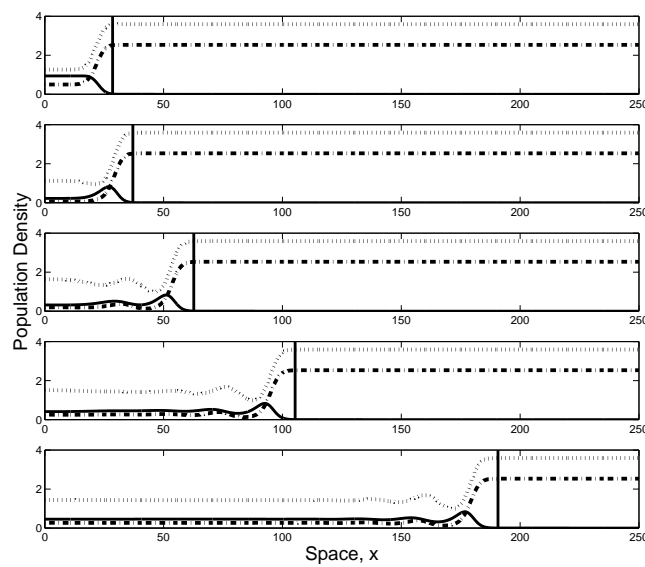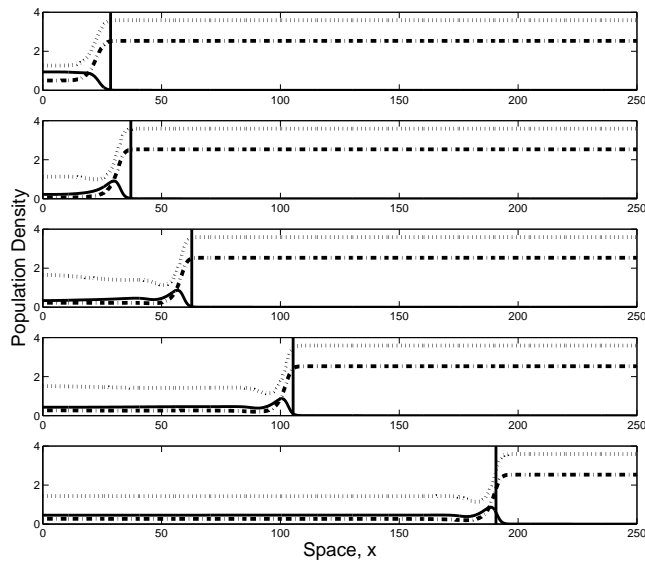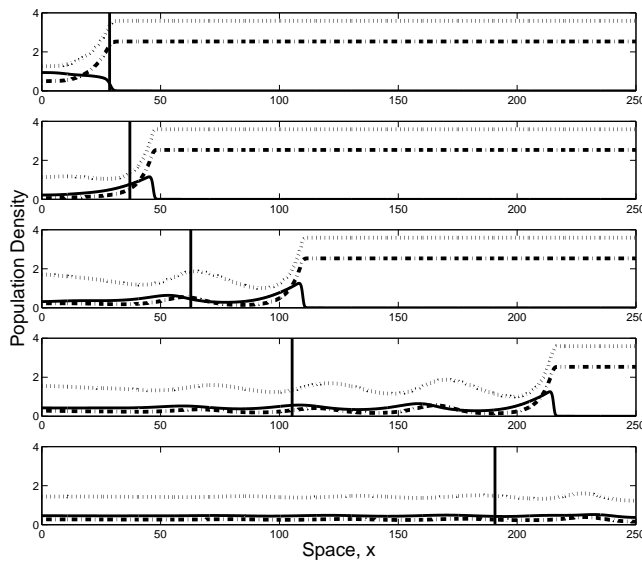
Figure 5-5: *Predator wave invading an endemic prey-only steady state. No preytaxis. The predators spread at the same speed as the analytic wavespeed. The dotted lines represent total prey density, the bold lines represent predator density and the dash-dotted line represent infected prey. The times are (from top to bottom) $T = 5, 10, 25, 50, 100$. The vertical lines represent the expected position of the wavefront $20 + \omega_{crit} * T$, where ω_{crit} is the analytical wavespeed. Parameter values: $F_S = 0$, $F_I = 0$, $\beta = 1$, $b = 1$, $m = 0.5$, $\mu = 0.2$, $c = 0.1$, $h_S = 0.3$, $h_I = 0.3$, $a_R = 1$, $D_R = 1$ and $D_P = 1$.*
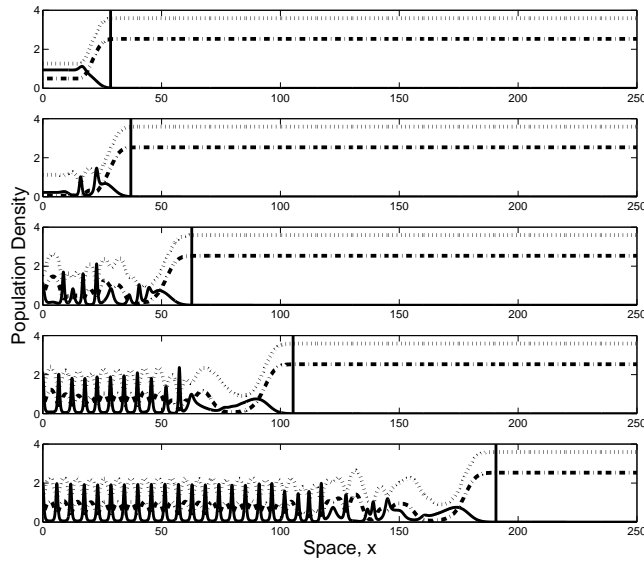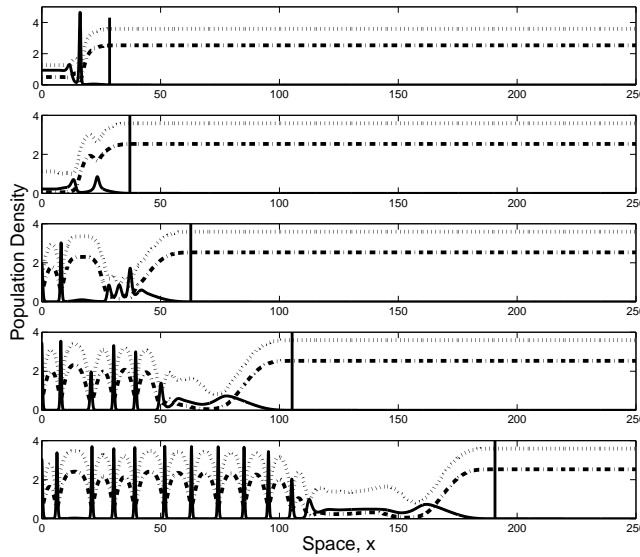
(a)

(b)

Figure 5-6: *Predator wave invading an endemic prey-only steady state. Predators are attracted to (a) susceptible prey ($F_S = 10$, $F_I = 0$) and (b) infected prey ($F_S = 0$, $F_I = 10$). In (a) the predator wave is marginally faster than the analytic wavespeed, whereas in (b) the predator wave is much faster than the analytic wavespeed. Other parameters: $\beta = 1$, $b = 1$, $m = 0.5$, $\mu = 0.2$, $c = 0.1$, $h_S = 0.3$, $h_I = 0.3$, $a_R = 1$, $D_R = 1$ and $D_P = 1$. The times and lines used are the same as Figure 5-5.*

(a)

(b)

Figure 5-7: *Predator wave invading an endemic prey-only steady state. Predators are repelled by (a) susceptible prey ($F_S = -10$, $F_I = 0$) and (b) infected prey ($F_S = 0$, $F_I = -10$). Both (a) and (b) demonstrate that the predator wave spreads at the analytic wavespeed, and that spatiotemporal chaos or oscillations occur far behind the wavefront. Other parameters: $F_S = 0$, $\beta = 1$, $b = 1$, $m = 0.5$, $\mu = 0.2$, $c = 0.1$, $h_S = 0.3$, $h_I = 0.3$, $a_R = 1$, $D_R = 1$ and $D_P = 1$. The times and lines used are the same as Figure 5-5.*
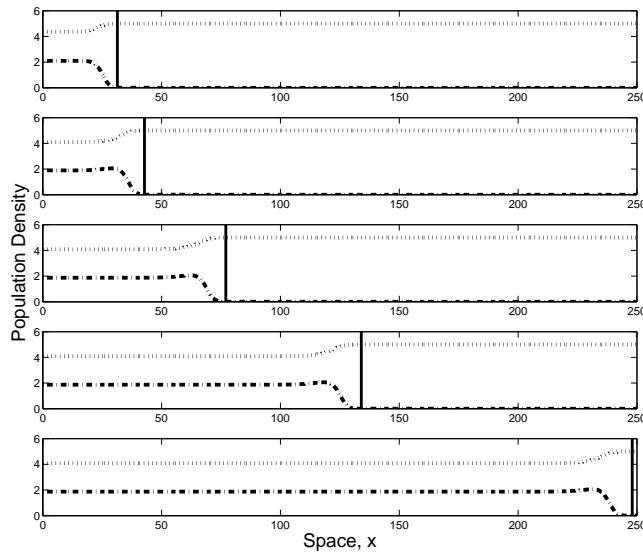
130

Figure 5-8: *Infection wave invading a prey-only steady state. The travelling wave moves at the analytic wavespeed. Parameter values: $b = 1$, $m = 0.5$, $c = 0.1$, $\beta = 0.5$, $D_R = 1$ and $\mu = 0.2$. The times are (from top to bottom) $T = 5, 10, 25, 50, 100$. The dotted lines (top) represent total prey density, whereas the dash-dotted line (bottom) represent infected prey density. The vertical lines represent the expected position of the wavefront $20 + \omega_{crit} * T$, where ω_{crit} is the analytical wavespeed.*
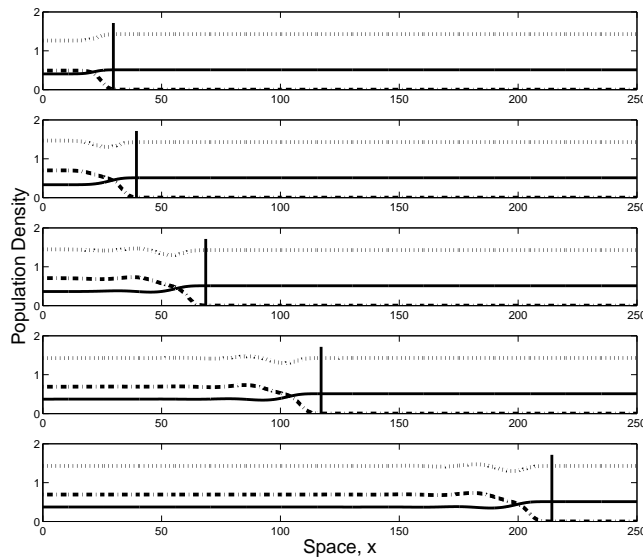
Figure 5-9: *Infection wave invading predator–prey steady state. No preytaxis. The disease spreads at the analytic wavespeed, which is represented by the vertical line, as before. Bold line is total prey density, dashed line is predator density and dotted line is infected prey density. Times are $T = 5, 10, 25, 50, 100$. Parameter values $F_S = F_I = 0$, $b = 1$, $m = 0.5$, $\mu = 0.2$, $c = 0.1$, $h_S = 0.3$, $h_I = 0.3$, $\beta = 1.5$, $a_R = 1$, $D_R = 1$ and $D_P = 1$.*
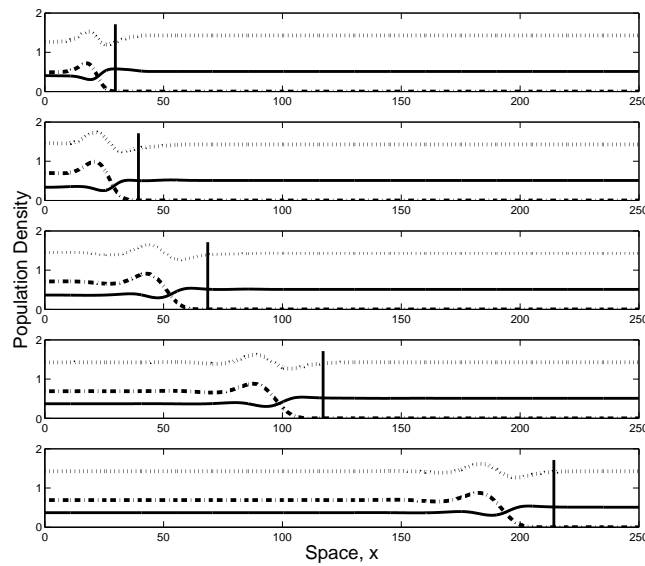
(a)
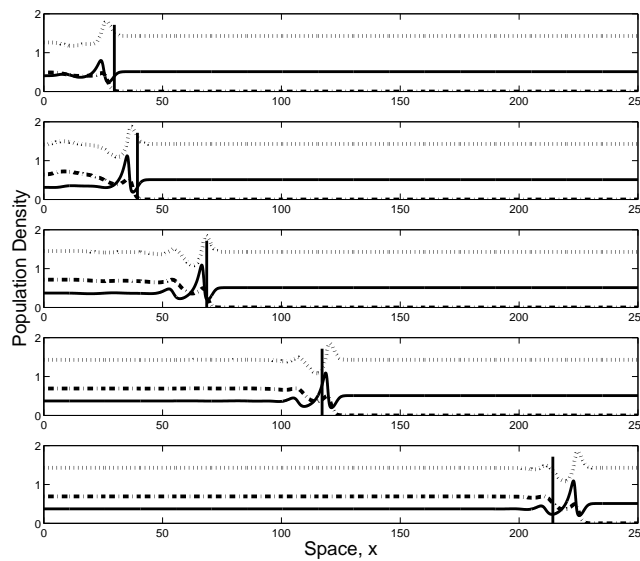
(b)

Figure 5-10: *Infection wave invading predator–prey steady state. (a) susceptible prey attract predators ($F_S > 0$), and (b) infected prey attract predators ($F_I > 0$). In (a), the infection wave moves at the analytic wavespeed, whereas in (b), the wavespeed is faster than the analytic wavespeed. Parameter values (a) $F_S = 20$ and $F_I = 0$ and (b) $F_S = 0$ and $F_I = 20$. Other parameters: $\beta = 1.5$, $b = 1$, $m = 0.5$, $\mu = 0.2$, $c = 0.1$, $h_S = 0.3$, $h_I = 0.3$, $a_R = 1$, $D_R = 1$ and $D_P = 1$. The times and lines used are the same as Figure 5-5.*

(a)

(b)

Figure 5-11: *Infection wave invading predator–prey steady state. Susceptible prey repel preda-tors. Comparison of (a) density dependent and (b) frequency dependent transmission. In (a), the wave moves faster than the analytic wavespeed, whereas in (b) the wave moves at the same speed as the analytic wavespeed. The arrows and grey lines in (b) represent the expected po-sition of the wavefront $20 + \omega_{crit} * T$, where ω_{crit} is the analytic wavespeed. Parameter values (a) $\beta = 1$ and (b) $\beta_{FD} = 1.5$. Other parameters: $F_S = -5$, $F_I = 0$, $b = 1$, $m = 0.5$, $\mu = 0.2$, $c = 0.1$, $h_S = 0.3$, $h_I = 0.3$, $a_R = 1$, $D_R = 1$ and $D_P = 1$. The times and lines used are the same as Figure 5-5.*
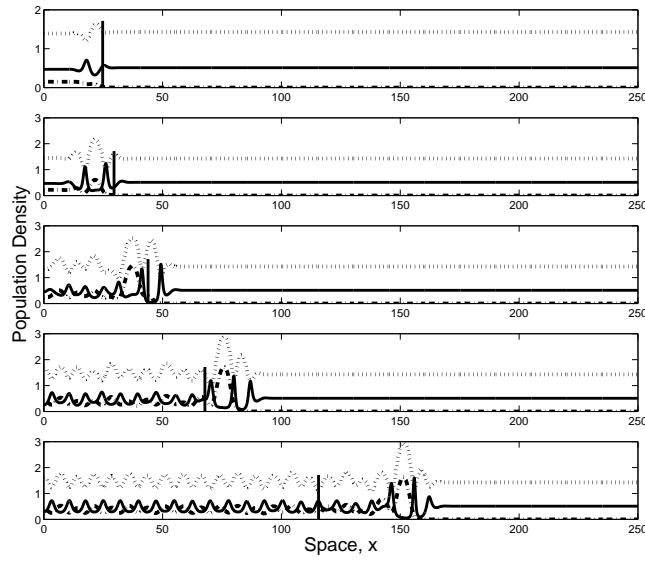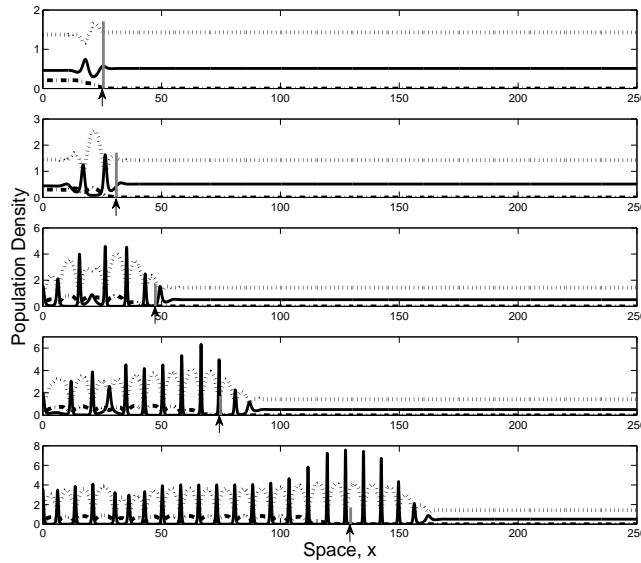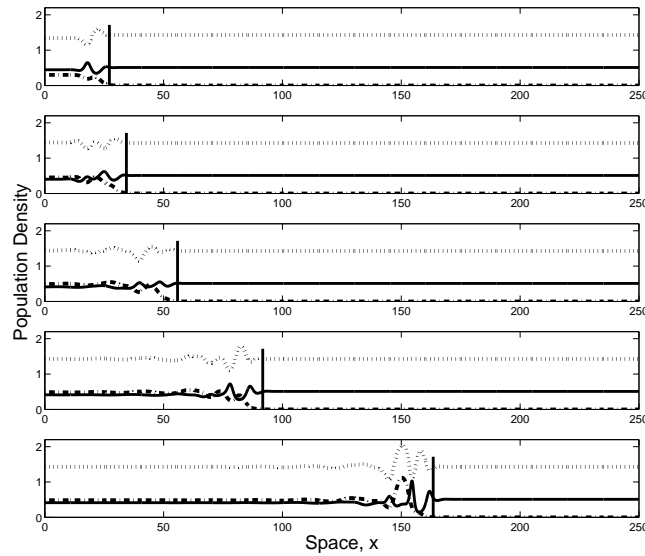
Figure 5-12: *Infection wave invading predator–prey steady state. Susceptible prey repel predators. Higher transmissibility than Figure 5-11(a). The disease spreads at the same speed as the analytic wavespeed. Parameter values: $\beta = 1.2$, $F_S = -5$, $F_I = 0$, $b = 1$, $m = 0.5$, $\mu = 0.2$, $c = 0.1$, $h_S = 0.3$, $h_I = 0.3$, $a_R = 1$, $D_R = 1$ and $D_P = 1$. The times and other lines used are the same as Figure 5-5.*

Figure 5-13: *Infection wave invading predator–prey steady state. Infected prey repel predators. The infection wave spreads at the same speed as the analytic wavespeed. Behind the wavefront the dynamics are oscillatory or chaotic. Parameter values: $\beta = 1.5$, $F_S = 0$, $F_I = -10$, $b = 1$, $m = 0.5$, $\mu = 0.2$, $c = 0.1$, $h_S = 0.3$, $h_I = 0.3$, $a_R = 1$, $D_R = 1$ and $D_P = 1$. The times and other lines used are the same as Figure 5-5.*
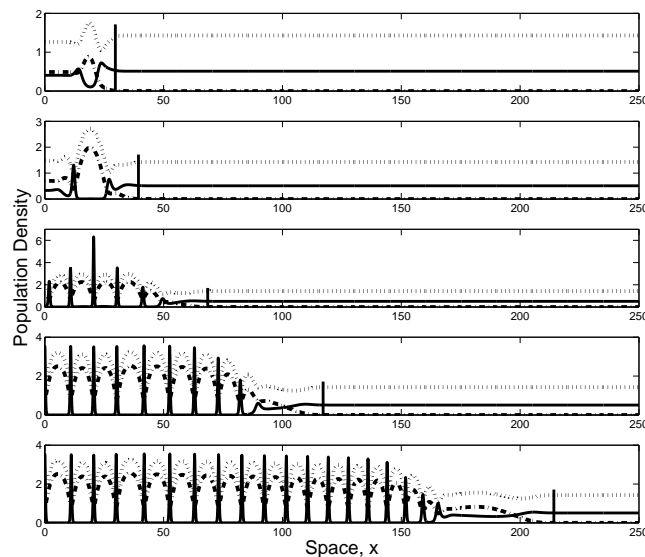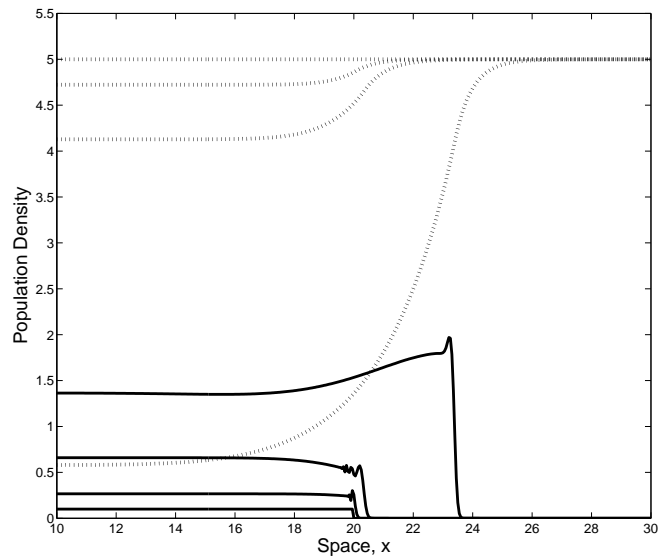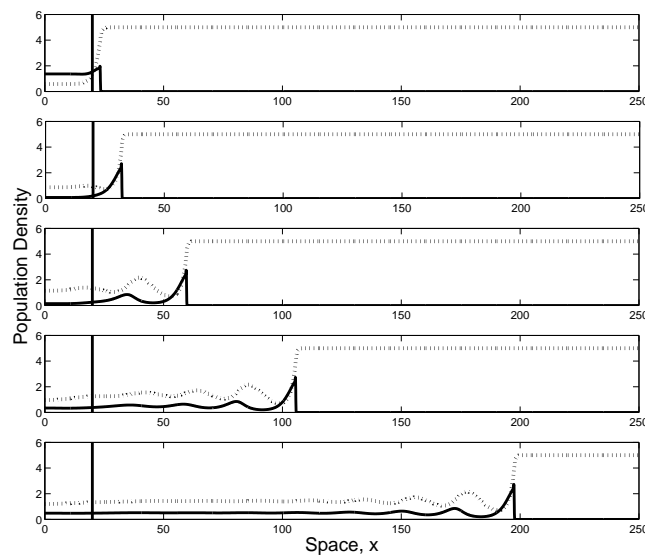
(a)

(b)

Figure 5-14: *Predator model. Positive preytaxis, no predator diffusion. These figures are same as Figure 5-3 but with the usual step function as an initial condition.*

Chapter 6

Overall conclusion

Each chapter has its own discussion, where each chapter's results are put into context. Here, we synthesise these results.

In this thesis, we have found many results that are novel not only in the field of eco-epidemiology, but also in the much larger fields of theoretical ecology and epidemiology. In particular, one common consideration within this thesis is looking at cases where predator–prey oscillations occur, with each chapter having some key result around (endogenous) predator–prey oscillations.

The results from Chapters 2 and 3 are inextricably linked. This is no surprise as they have a common origin. Both chapters were developed from an investigation into whether density dependent transmission alters the main finding in Hilker and Schmitz (2008), that diseases can stabilise predator–prey oscillations. In verifying this, we discovered (a) that the disease became endemic at a different threshold in transmissibility to what was expected from steady state calculations, contrary to the results in Hilker and Schmitz (2008), and (b) various bistabilities involving endemic oscillations.

Chapter 2 (i.e. Bate and Hilker, 2013b) attempts to generalise phenomenon '(a)' by considering various models involving (endogenous) predator–prey oscillations. We establish that this difference in endemic threshold is based on the difference between the steady-state host density and time-averaged host density of the predator–prey oscillations. In Rosenzweig–MacArthur-based models, prey have a higher time-averaged density when oscillating than the corresponding (unstable) steady state (Armstrong and McGehee, 1980). For frequency dependent transmissibility, the endemic threshold is independent of host density and thus there is no difference between the endemic threshold of the predator–prey oscillations and steady state, akin to Hilker and Schmitz (2008).

Further investigation into phenomenon '(b)' shed light onto more complex dynam-

ics, not only in the density dependent model, but also in the model in Hilker and Schmitz (2008). When investigating cases where predators and prey oscillate in the absence of the disease, we found more and more complex dynamics in these models, including various bistabilities, in particular bistability between endemic and disease free states (which requires prior knowledge of Chapter 2 to understand), period doubling cascades into chaos and tristability between disease-free oscillations, endemic equilibria and an endemic torus. The comparison of the dynamics found in these two models is in Chapter 3, i.e. Bate and Hilker (2013a).

One aspect overlooked in the diseased-prey model in Chapter 2 is that both the predator and disease can coexist at equilibrium. Such coexistence is common in many eco-epidemiological models (including some models in Anderson and May, 1986; Chattopadhyay and Bairagi, 2001; Xiao and Chen, 2001b,a; Chattopadhyay and Pal, 2002; Hethcote et al, 2004; Singh et al, 2004; Haque and Venturino, 2006; Hilker and Malchow, 2006; Greenhalgh and Haque, 2007; Upadhyay et al, 2008; Haque et al, 2009; Chatterjee et al, 2012, among others), but that is because infected prey are assumed to be more (or less) vulnerable to predation. However, in Chapter 2 (i.e. Bate and Hilker, 2013b), infection does not alter vulnerability to predators. This means that the eco-epidemiological system is in fact an exploitative competition system, using the rescaling in Figure 1-1(a). In such systems, the established rule is that the predator and disease can not coexist (the principle of competitive exclusion Hardin, 1960), or if they do, only in oscillatory dynamics (either temporally or spatially McGehee and Armstrong, 1977; Chesson, 2000). Consequently, we have found an apparent contradiction. This contradiction is resolved by the fact that prevalence exhibits some kind of density dependence, an often overlooked counterexample found Gurney and Nisbet (1998). If in addition, we consider group defence, predators may not only coexist with a disease in the prey, but the predators may actually benefit from the disease, as the disease may restrict prey densities to more manageable levels for the predator. The resulting investigation into these phenomena is Bate and Hilker (Chapter 4, i.e. 2014).

In Chapter 4, we find that the disease in the prey can benefit a predator in several ways. In particular, we have that the disease can allow for coexistence in cases where it could not without the disease. For example, the introduction of a disease can allow predators and prey to coexist by reversing a homoclinic bifurcation that destroys the predator–prey limit cycle. Likewise, the disease can restrict prey populations to levels where the prey's group defence is easier for the predator to overcome.

Chapters 3 and 4 (i.e. Bate and Hilker, 2013b,a, respectively) have several aspects in common; bistability, homoclinic bifurcations and period-doubling cascades

into chaos. This means that we have established that such complex dynamics can occur in both diseased-predator and diseased-prey models, and it seems plausible that complex dynamics like chaos could occur in many eco-epidemiology models. In particular, although this was not investigated, we suspect that some of these phenomena (particularly chaos) would occur in Chapter 4's model when we take out group defence, considering that in Scenarios 2B and 3B of Chapter 4, chaos occurs in regions where group defence is not particularly strong and thus the Rosenzweig-MacArthur dynamics dominate.

For Chapter 5, we go beyond the homogeneous, mean-field world of ODEs, which assumes that the world is a perfect mixture of water, clay and Marmite (among many other things). This was done by using PDEs, meaning that we incorporate a spatial dimension, which allows for spatial heterogeneity as well as movement through space. This movement incorporates both diffusion and preytaxis terms. Preytaxis is the movement of predators along prey gradients. With such preytaxis, we find many new phenomena. For example, preytaxis can change the wavespeed and the wavefront's shape of an invading travelling wave. On top of this, we have found that negative preytaxis can give rise to spatiotemporal oscillations, even when, in the absence of spatial effects, there is a stable equilibrium.

One interesting phenomenon found in Chapter 5 was the case where an infection wave was invading in spatiotemporal oscillation. In such a case, the wavespeed increased much like $\overline{R_0} > R_0^*$ was in the diseased-prey model in Chapter 2, i.e. Bate and Hilker (2013b).

6.1   Future work and extensions

First and foremost, we need to explore the predator–prey spatiotemporal oscillations/ chaos that occur when considering negative preytaxis in Chapter 5. At the moment, we suspect the oscillations are due to some destabilisation effect that preytaxis has on the predator–prey steady state. On first inspection, the dispersion relation (using methods in Sherratt et al, 2014; Dagbovie and Sherratt, 2014) contains preytaxis terms, just like the determinant of (5.22), suggesting that the preytaxis terms can change the spatiotemporal eigenvalues. If it is that the destabilisation is the result of a change in the spatiotemporal eigenvalues, then we will have a case of absolute or convective instability. The next steps would be to analyse the dispersion relation further to see if there are any interesting bifurcations that could explain the spatiotemporal oscillations.

One missing aspect in this thesis is that we did not investigate the disease in both

predator and prey. We did briefly consider a disease that infects both predator and prey in Chapter 2 (i.e. Bate and Hilker, 2013b), using it to demonstrate that predator–prey oscillations can increase or decrease the endemic criteria, but we have not investigated this effect thoroughly.

Likewise, we suspect the model in Hadeler and Freedman (1989) (where there is a disease in both predator and prey) to have complex dynamics and that this could be investigated. In fact, given that we have found complex dynamics in Chapters 3, 4 and 5, we suspect many eco-epidemiological models exhibit chaos, bistabilities and possibly other complex dynamics, although the parameter values for these to occur might be unrealistic.

Recently, Roberts and Heesterbeek (2013) have suggested the use of next-generation matrices (Diekmann et al, 2010, 1990) for finding basic reproductive numbers in eco-epidemiological systems. It is a tool commonly used in epidemiology but has not yet been applied in eco-epidemiology. This should be a powerful tool for finding when a disease becomes endemic in eco-epidemiological models with multiple infected classes. In particular, this should be very useful for analysing models where a disease infects both predator and prey.

In Chapter 4, we used a nice 2D argument for the model with frequency dependent transmission, allowing us to gain insight into the 3D model with density dependent transmission. However, we feel that 3D model could be explored further.

One issue, raised in Bairagi and Chattopadhyay (2008), is that there has been a lack of work analysing evolution within an eco-epidemiology context. Recently, Andrew Morozov and co-authors (Morozov and Adamson, 2011; Morozov and Best, 2012) have tried to address this by using adaptive dynamics on a trade off between disease virulence and disease-induced mortality or disease-related mortality from predation, respectively. However, there are still many other evolutionary questions that can be addressed. For example, if the disease infects both predator and prey and is trophically transmitted, the evolutionary aspects of a trade off between trophic transmission and disease-induced mortality would be particularly interesting.

Another area that has been overlooked is age structure. Age structure is important in both ecology and epidemiology. Many predators target life stages of their prey, for example, predators may only target the eggs, larvae or adults of a prey population. Likewise, predators may target different prey during different life stages; the diet of a tadpole is different to the diet of a frog. With respect to epidemiology, the age of the host can greatly affect many aspects like the transmission rate and the disease-induced mortality.

6.2   Final summary

The following bulletpoints summarise the key results in this thesis:

- Diseases with density dependent transmission have different endemic thresholds when the host(s) are in predator–prey oscillations than at the (unstable) predator–prey equilibrium (Chapter 2, used in Chapters 3 and 5).

- Considering predator–prey oscillations as the disease-free state, a disease can induce many different complex dynamics, including bistabilty/tristability between disease-free and endemic attractors (Chapter 3).

- Diseases can induce chaos via period doubling cascades (Chapters 3 and 4).

- Diseases in prey and predators can coexist at a stable steady state, even under indiscriminate predation (Chapters 2, 4 and 5).

- A disease in a group-defending prey can benefit predators, either by reversing a homoclinic bifurcation of the predator–prey limit cycle or by reducing prey densities to more manageable levels for the predator (Chapter 4).

- The travelling waves from disease and predator invasions have a wavespeed that depends on the strength of preytaxis (Chapter 5).

- Negative preytaxis does not slow down wavespeed, but it seems to have a destabilising effect (Chapter 5).

Bibliography

Abrams PA (2009) When does greater mortality increase population size? The long history and diverse mechanisms underlying the hydra effect. Ecology Letters 12:462–474

Ainseba BE, Bendahmane M, Noussair A (2008) A reaction–diffusion system modeling predator–prey with prey-taxis. Nonlinear Analysis: Real World Applications 9:2086–2105

Ajraldi V, Pittavino M, Venturino E (2011) Modelling herd behaviour in population systems. Nonlinear Analysis: Real World Applications 12:2319–2338

Allen WE (1920) Behavior of loon and sardines. Ecology 1:309–310

Altizer S, Dobson A, Hosseini P, Hudson P, Pascual M, Rohani P (2006) Seasonality and the dynamics of infectious diseases. Ecology Letters 9:467–484

Anderson RM, May RM (1986) The invasion, persistence and spread of infectious disease within animal and plant communities. Philosophical Transactions of the Royal Society of London Series B, Biological Sciences 314:533–570

Andrews JF (1968) A mathematical model for the continuous culture of microorganisms utilizing inhibitory substrates. Biotechnology and Bioengineering 10:707–723

Arditi R, Tyutyunov Y, Morgulis A, Govorukhin V, Senina I (2001) Directed movement of predators and the emergence of density-dependence in predator–prey models. Theoretical Population Biology 59:207–221

Armstrong RA, McGehee R (1980) Competitive exclusion. American Naturalist 115:151–170

Aronson DG, Weinberger HF (1975) Multidimensional nonlinear diffusion arising in population genetics. In: Goldstein EA (ed) Partial differential equations and related topics, Lecture Notes in Mathematics, vol 446, Springer-Verlag, Berlin, pp 5–49

Aronson DG, Weinberger HF (1978) Multidimensional nonlinear diffusion arising in population genetics. Advances in Mathematics 30:38–76

Bacaër N (2007) Approximation of the basic reproduction number R_0 for vector-borne diseases with a periodic vector population. Bulletin of Mathematical Biology 69:1067–1091

Bacaër N, Abdurahman X (2008) Resonance of the epidemic threshold in a periodic environment. Journal of Mathematical Biology 57:649–673

Bacaër N, Ait Dads EH (2012) On the biological interpretation of a definition for the parameter R_0 in periodic population model. Journal of Mathematical Biology 65:601–621

Bacaër N, Guernaoui S (2006) The epidemic threshold of vector-borne diseases with seasonality. Journal of Mathematical Biology 53:421–436

Bairagi N, Chattopadhyay N (2008) The evolution on eco-epidemiological systems theory and evidence. In: Simos TE (ed) Journal of Physics: Conference Series, vol 96, p 012205

Bairagi N, Roy PK, Chattopadhyay J (2007) Role of infection on the stability of a predator–prey system with several response functions — A comparative study. Journal of Theoretical Biology 248:10–25

Bate AM, Hilker FM (2013a) Complex dynamics in an eco-epidemiological model. Bulletin of Mathematical Biology 75:2059–2078

Bate AM, Hilker FM (2013b) Predator–prey oscillations can shift when dieases become endemic. Journal of Theoretical Biology 316:1–8

Bate AM, Hilker FM (2014) Disease in group-defending prey can benefit predators. Theoretical Ecology 7:87–100

Beardmore I, White KAJ (2001) Spreading disease through social groupings in competition. Journal of Theoretical Biology 212:253–269

Beeton N, McCallum H (2011) Models predict that culling is not a feasible strategy to prevent extinction of Tasmanian devils from facial tumour disease. Journal of Applied Ecology 48:1315–1323

Begon M, Bennett M, Bowers RG, French SM N P Hazel, Turner J (2002a) A classi-fication of transmission terns in host-microparasite models: numbers, densities and areas. Epidemiology and Infection 129:147–153

Begon M, Townsend CR, Harper JL (2002b) Ecology, 4th edn. Blackwell Publishing, Oxford

Bell SS, White A, Sherratt JA, Boots M (2009) Invading with biological weapons: the role of shared disease in ecological invasion. Theoretical Ecology 2:53–66

Beltrami E, Carroll TO (1994) Modeling the role of viral disease in recurrent phyto-plankton blooms. Journal of Mathematical Biology 32:857–863

Berezovskaya FS, Song B, Castillo-Chavez C (2010) Role of prey dispersal and refuges on predator-prey dynamics. SIAM Journal on Applied Mathematics 70:1821–1839

Berleman JE, Scott J, Chumley T, Kirby JR (2008) Predataxis behavior in Myxococcus xanthus. Proceedings of the National Academy of Sciences 105:17,127–17,132

Berryman AA, Millstein JA (1989) Are ecological systems chaotic - and if not, why not? Trends in Ecology & Evolution 4:26–28

Biggs R, Carpenter SR, Brock WA (2009) Turning back from the brink: Detecting an impending regime shift in time to avert it. Proceeding of the National Academy of Sciences of the United States of America 106:826–831

Britton NF (2003) Essential Mathematical Biology. Springer, London

Chakraborty A, Singh M, Lucy D, Ridland P (2007) Predator–prey model with prey-taxis and diffusion. Mathematical and Computer Modelling 46:482–498

Chatterjee S, Kesh D, Bairagi N (2012) How population dynamics change in presence of migratory prey and predator's preference. Ecological Complexity 11:53–66

Chattopadhyay J, Arino O (1999) A predator–prey model with disease in the prey. Nonlinear Analysis 36:747–766

Chattopadhyay J, Bairagi N (2001) Pelicans at risk in Salton Sea — an eco-epidemiological model. Ecological Modelling 136:103–112

Chattopadhyay J, Pal S (2002) Viral infection on phytoplankton–zooplankton system — a mathematical model. Ecological Modelling 151:15–28

Chattopadhyay J, Srinivasu PDN, Bairagi N (2003) Pelicans at risk in Salton Sea - an eco-epidemiological model-II. Ecological Modelling 167:199–211

Chesson P (2000) General theory of competitive coexistence in spatially-varying environments. Theoretical Population Biology 58:211–237

Collings JB (1997) The effects of the functional response on the bifurcation behavior of a mite predator-prey interaction model. Journal of Mathematical Biology 36:149–168

Dagbovie AS, Sherratt JS (2014) Absolute stability and dynamical stabilisation in predator–prey systems. Journal of Mathematical Biology 68:1403–1421

Das KP, Chattopadhyay J (2012) Role of environmental disturbance in an eco-epidemiological model with disease from external source. Mathematical Methods in the Applied Sciences 35:659–675

Das KP, Roy S, Chattopadhyay J (2009) Effect of disease-selective predation on prey infected by contact and external sources. BioSystems 95:188–199

Das KP, Kundu K, Chattopadhyay J (2011) A predator–prey mathematical model with both the populations affected by diseases. Ecological Complexity 8:68–80

Dickman CR (1996) Impact of exotic generalist predators on the native fauna of Australia. Wildlife Biology 2:185–195

Diekmann O, Heesterbeek JAP, Metz JAJ (1990) On the definition and computation of the basic reproduction ratio R_0 in models for infectious diseases in heterogeneous populations. Journal of Mathematical Biology 28:365–382

Diekmann O, Heesterbeek JAP, Roberts MG (2010) The construction of next-generation matrices for compartmental epidemic models. Journal of the Royal Society Interface 7:873–885

van den Driessche P, Watmough J (2002) Reproductive numbers and sub-threshold endemic equilibria for compartmental models of disease transmission. Mathematical Biosciences 180:29–48

Edelstein-Keshet L (1988) Mathematical Models in Biology. Random House, New York

Fenton A, Rands SA (2006) The impact of parasite manipulation and predator foraging behavior on predator-prey communities. Ecology 87:2832–2841

Ferrari MJ, Perkins SE, Pomeroy LW, Bjørnstad ON (2011) Pathogens, social networks, and the paradox of transmission scaling. Interdisciplinary Perspectives on Infectious Disease 2011:267,049

Ferreri L, Venturino E (2013) Cellular automata for contact ecoepidemic processes in predator–prey systems. Ecological Complexity 13:8–20

Freedman HI, Wolkowicz GSK (1986) Predator–prey systems with groups defence: the paradox of enrichment revisited. Bulletin of Mathematical Biology 48:493–508

Gause G (1934) The Struggle for Existence. Williams and Wilkins, Baltimore

Geritz SAH, Gyllenberg M (2013) Group defence and the predator's functional response. Journal of Mathematical Biology 66:705–717

Gilpin ME (1979) Spiral chaos in a predator–prey model. American Naturalist 113:306–308

González-Olivares E, Rojas-Palma A (2011) Multiple limit cycles in a Gause type predator–prey model with Holling type III functional response and Allee effect on prey. Bulletin of Mathematical Biology 73:1378–1397

Grassly NC, Fraser C (2006) Seasonal infectious disease epidemiology. Proceedings of the Royal Society B 273:2541–2550

Greenhalgh D, Haque M (2007) A predator–prey model with disease in the prey species only. Mathematical Methods in the Applied Sciences 30:911–929

Greenman JV, Norman RA (2007) Environmental forcing, invasion and control of ecological and epidemiological systems. Journal of Theoretical Biology 247:492–506

Grünbaum D (1998) Using spatially explicit models to characterize foraging performance in heterogeneous landscapes. American Naturalist 151:97–115

Gurney WSC, Nisbet RM (1998) Ecological Dynamics. Oxford University Press

Hadeler KP, Freedman HI (1989) Predator–prey populations with parasitic infection. Journal of Mathematical Biology 27:609–631

Hall SR, Duffy MA, Cáceres CE (2005) Selective predation and productivity jointly drive complex behavior in host–parasite systems. American Naturalist 165:70–81

Han L, Ma Z, Hethcote HW (2001) Four predator prey models with infectious diseases. Mathematical and Computer Modelling 34:849–858

Haque M (2010) A predator-prey model with disease in the predator species only. Nonlinear Analysis: Real World Applications 11:2224–2236

Haque M, Chattopadhyay J (2007) Role of transmissible disease in an infected prey-dependent predator–prey system. Mathematical and Computer Modelling of Dynamical Systems 13:163–178

Haque M, Venturino E (2006) The role of transmissible disease in the Holling-Tanner predator-prey model. Theoretical Population Biology 70:273–288

Haque M, Venturino E (2007) An eco-epidemiological model with disease in predator: the ratio-dependent case. Mathematical Methods in the Applied Sciences 30:1791–1809

Haque M, Zhen J, Venturino E (2009) An ecoepidemiological predator–prey model with standard disease incidence. Mathematical Methods in the Applied Sciences 32:875–898

Haque M, Sarwardi S, Preston S, Venturino E (2011) Effect of delay in a Lotka–Volterra type predator–prey model with transmissible disease in the predator species. Mathematical Biosciences 234:47–57

Hardin G (1960) The competitive exclusion principle. Science 131:1292–1297

Hastings A (1996) Models of spatial spread: A synthesis. Biological Conservation 78:143–148

Hastings A, Powell T (1991) Chaos in a three-species food chain. Ecology 72:896–903

Hatcher MJ, Dunn AM (2011) Parasites in Ecological Communities: From interactions to ecosystems. Cambridge University Press, Cambridge

Hethcote HW, Wang W, Han L, Ma Z (2004) A predator-prey model with infected prey. Theoretical Population Biology 66:259–268

Hilker FM (2010) Population collapse to extinction: the catastrophic combination of parasitism and Allee effect. Journal of Biological Dynamics 4:86–101

Hilker FM, Malchow H (2006) Strange periodic attractors in a prey–predator system with infected prey. Mathematical Population Studies 13:119–134

Hilker FM, Schmitz K (2008) Disease-induced stabilization of predator–prey oscillations. Journal of Theoretical Biology 255:299–306

Hilker FM, Malchow H, Langlais M, Petrovskii SV (2006) Oscillations and waves in a virally infected plankton system. Part II: Transition from lysogeny to lysis. Ecological Complexity 3:200–208

Hilker FM, Langlais M, Malchow H (2009) The Allee effect and infectious diseases: extinction, multistability, and the (dis-)appearance of oscillations. American Naturalist 173:72–88

Hochberg ME (1991) Population dynamic consequences of the interplay between parasitism and intraspecific competition for host–parasite systems. OIKOS 61:297–306

Holling CS (1959) Some characteristics of simple types of predation and parasitism. The Canadian Entomologist 91:385–398

Holt RD, Roy M (2007) Predation can increase the prevalence of infectious disease. American Naturalist 169:690–699

Hosono HG (1998) The minimal speed of traveling fronts for a diffusive Lotka–Volterra competition model. Bulletin of Mathematical Biology 60:435–448

Hudson PT, Dobson AP, Newborn D (1992) Do parasites make prey vulnerable to predation? Red grouse and parasites. Journal of Animal Ecology 61:681–692

Hurtado PJ, Hall SR, Ellner SP (2014) Infectious disease in consumer populations: dynamic consequences of resource-mediated transmission and infectiousness. Theoretical Ecology 7:163–179

Inaba H (2012) On a new perspective of the basic reproductive number in heterogeneous environments. Journal of Mathematical Biology 65:309–348

Johnson CG (1967) International dispersal of insects and insect-borne viruses. Netherlands Journal of Plant Pathology 1:21–43

Kareiva P, Odell G (1987) Swarms of predators exhibit "preytaxis" if individual predators use area-restricted search. American Naturalist 130:233–270

Keller EF, Segel LA (1971) Traveling band of chemotactic bacteria: A theoretical analysis. Journal of Theoretical Biology 130:235–248

Kermack WO, McKendrick AG (1927) A contribution to the mathematical theory of epidemics. Proceedings of the Royal Society of London A 115:700–721

Koen-Alonso M (2007) A process-oriented approach to the multispecies functional response. In: From energetics to ecosystems: the dynamics and structure of ecological systems, Springer, pp 1–36

Kooi BW, van Voorn GAK, Das KP (2011) Stabilization and complex dynamics in a predator–prey model with predator suffering from an infectious disease. Ecological Complexity 8:113–122

Kot M (2001) Global bifurcations in predator–prey models. In: Elements of Mathematical Ecology, Cambridge, pp 140–160

Krause J, Ruxton GD (2002) Living in Groups. Oxford University Press

Kuznetsov YA (1995) Elements of Applied Bifurcation Theory. Springer–Verlag, New York

Lafferty KD (1999) The evolution of trophic transmission. Parasitology Today 15:111–115

Langer WL (1964) The black death. Scientific American February:114–121

Lee JM, Hillen T, Lewis MA (2008) Continuous traveling waves for prey-taxis. Bulletin of Mathematical Biology 70:654–676

Lee JM, Hillen T, Lewis MA (2009) Pattern formation in prey-taxis systems. Journal of Biological Dynamics 3:551–573

LeVeque RJ (1992) Numerical Methods for Conservation Laws. Birkhäuser, Basel

Lewis MA, Li B, Weinberger HF (2002) Spreading speed and linear determinacy for two-species competition models. Journal of Mathematical Biology 45:219–233

Lloyd HG (1983) Past and present distribution of red and grey squirrels. Mammal Review 13:69–80

Malchow H, Hilker FM, Petrovskii SV, Brauer K (2004) Oscillations and waves in a virally infected plankton system. Part I: The lysogenic stage. Ecological Complexity 1:211–223

Malchow H, Hilker FM, Sarkar RR, Brauer K (2005) Spatiotemporal patterns in an excitable plankton system with lysogenic viral infection. Mathematical and Computer Modelling 42:1035–1048

May R (1974) Biological populations with nonoverlapping generations: stable points, stable cycles, and chaos. Science 186:645–647

McCallum H, Barlow N, Hone J (2001) How should pathogen transmission be modelled? Trends in Ecology and Evolution 16:295–300

McGehee R, Armstrong RA (1977) Some mathematical problems concerning the ecological principle of competitive exclusion. Journal of Differential Equations 23:30–52

Middleton AD (1930) Ecology of the american gray squirrel in the british isles. Proceedings of the Zoological Society London 2:809–843

Miller RC (1922) The significance of gregarious habit. Ecology 3:122–126

Morozov A, Best A (2012) Predation on infected host promotes evolutionary branching of virulence and pathogens' biodiversity. Journal of Theoretical Biology 307:29–36

Morozov AY (2012) Revealing the role of predator-dependent disease transmission in the epidemiology of a wildlife infection: a model study. Theoretical Ecology 5:517–532

Morozov AY, Adamson MW (2011) Evolution of virulence driven by predator–prey interaction: Possible consequences of population dynamics. Journal of Theoretical Biology 276:181–191

Morton KW, Mayers DF (2002) Numerical Solution of Partial Differential Equations. Cambridge University Press, Cambridge

Murdoch WW (1972) The functional response of predators. Biological Control 15:237–40

Murray JD (2002) Mathematical Biology I: An Introduction. Third Edition, 3rd edn. Springer, New York

Murray JD (2003) Mathematical Biology II: Spatial Models and Biomedical Applications, 3rd edn. Springer, New York

Nakata Y, Kuniya T (2010) Global dynamics of a class of SEIRS epidemic models in a periodic environment. Journal of Mathematical Analysis and Applications 363:230–237

Oksanen L, Fretwell SD, Arruda J, Niemelä P (1981) Exploitation ecosystems in gradients of primary productivity. American Naturalist 118:240–261

Oliveira NM, Hilker FM (2010) Modelling disease introduction as biological control of invasive predators to preserve endangered prey. Bulletin of Mathematical Biology 72:444–468

Ono M, Igarashi T, Ohno E, Sasaki M (1995) Unusual thermal defence by a honeybee against mass attack by hornets. Nature 377:334–336

Packer C, Holy RD, Hudson PJ, Lafferty KD, Dobson AP (2003) Keeping the herds healthy and alert: implications of predator control for infectious disease. Ecology Letters 6:797–802

Petrovskii SV, Li BL (2006) Exactly Solvable Models of Biological Invasion. Chapman and Hall/CRC, Boca Raton, Florida

Petrovskii SV, Malchow H (2000) Critical phenomena in plankton communities: KISS model revisited. Nonlinear Analysis: Real World Applications 1:37–51

Roberts MG, Heesterbeek JAP (2013) Characterizing the next-generation matrix and basic reproduction number in ecological epidemiology. Journal of Mathematical Biology 66:1045–1064

Rosenzweig ML, MacArthur RH (1963) Graphical representation and stability conditions of predator–prey interactions. The American Naturalist 97:209–223

Ruan S, Xiao D (2001) Global analysis in a predator–prey system with nonmonotonic functional response. SIAM Journal on Applied Mathematics 61:1445–1472

Sapoukhina N, Tyutyunov Y, Arditi R (2003) The role of prey taxis in biological control: A spatial theoretical model. American Naturalist 162:61–76

Sarwardi S, Haque M, Venturino E (2011) Global stability and persistence in LG–Holling type II diseased predator ecosystems. Journal of Biological Physics 37:91–106

Scheffer M (2009) Critical Transitions in Nature and Society. Princeton University Press, Princeton

Seppälä O, Karvonen A, Valtonen ET (2008) Shoaling behaviour of fish under parasitism and predation risk. Animal Behaviour 75:145–150

Seydel R (1988) From Equilibrium to Chaos- Practical Bifurcation and Stability Analysis. Elsevier, New York

Sherratt JS, Dagbovie AS, Hilker FM (2014) A mathematical biologist's guide to absolute and convective instability. Bulletin of Mathematical Biology 76:1–26

Shigesada N, Kawasaki K (1997) Biological Invasions: Theory and Practice. Oxford University Press, Oxford

Sieber M, Hilker FM (2011) Prey, predators, parasites: intraguild predation or simpler community models in disguise? Journal of Animal Ecology 80:414–421

Sieber M, Hilker FM (2012) The hydra effect in predator–prey models. Journal of Mathematical Biology 64:341–360

Sieber M, Malchow H, Schimansky-Geier L (2007) Constructive effects of environmental noise in an excitable prey–predator plankton system with infected prey. Ecological Complexity 4:223–233

Sieber M, Malchow H, Hilker FM (2013) Disease-induced modifications of prey competition in eco-epidemiological models. Ecological Complexity DOI: 10.1016/j.ecocom.2013.06.002

Siekmann I (2013) On competition in ecology, epidemiology and eco-epidemiology. Ecological Complexity 14:166–179

Siekmann I, Malchow H, Venturino E (2008) Predation may defeat spatial spread of infection. Journal of Biological Dynamics 2:40–54

Siekmann I, Malchow H, Venturino E (2010) On competition of predators and prey infection. Ecological Complexity 7:446–457

Singh BK, Chattopadhyay J, Sinha S (2004) The role of virus infection in a simple phytoplankton zooplankton system. Journal of Theoretical Biology 231:153–166

Skellam JG (1951) Random dispersal in theoretical populations. Biometrika 38:196–218

Stiefs D, Venturino E, Feudel U (2009) Evidence of chaos in eco-epidemic model. Mathematical Biosciences and Engineering 6:855–871

Su M, Hui C (2011) The effect of predation on the prevalence and aggregation of pathogens in prey. BioSystems 105:300–306

Su M, Hui C, Zhang YY, Li Z (2008) Spatiotemporal dynamics of the epidemic transmission in a predator–prey system. Bulletin of Mathematical Biology 70:2195–2210

Su M, Hui C, Zhang Y, Li Z (2009) How does the spatial structure of habitat loss affect the eco-epidemic dynamics? Ecological Modelling 220:51–59

Susser M, Susser E (1996) Choosing a future for epidemiology: II. From black box to Chinese boxes and eco-epidemiology. American Journal of Public Health 86:674–677

Thomas WR, Pomerantz MJ, Gilpin ME (1980) Chaos, asymmetric growth and group selection for dynamical stability. Ecology 61:1312–1320

Tompkins DM, White AR, Boots M (2003) Ecological replacement of native red squirrels by invasive greys driven by disease. Ecology Letters 6:189–196

Turchin P (2003) Complex Population Dynamics: a Theoretical/Empirical Synthesis. Princeton University Press

Tyson R, Lubkin SR, Murray JD (1999) Model and analysis of chemotactic bacterial patterns in a liquid medium. Journal of Mathematical Biology 38:359–375

Tyson R, Stern LG, LeVeque RJ (2000) Fractional step methods applied to a chemotaxis model. Journal of Mathematical Biology 41:455–475

Upadhyay RK, Bairagi N, Kundu K, Chattopadhyay J (2008) Chaos in eco-epidemiological problem of the Salton Sea and its possible control. Applied Mathematics and Computation 196:392–401

Venturino E (1994) The influence of disease on Lotka–Volterra systems. Rocky Mountain Journal of Mathematics 24:381–402

Venturino E (2002) Epidemics in predator–prey models: disease in predators. IMA Journal of Mathematics Applied in Medicine and Biology 19:185–205

Venturino E (2010) Eco-epidemic models with disease incubation and selective hunting. Journal of Computational and Applied Mathematics 234:2883–2901

Venturino E (2011a) A minimal model for ecoepidemics with group defense. Journal of Biological Systems 19:763–785

Venturino E (2011b) Simple metaecoepidemic models. Bulletin of Mathematical Biology 73:917–950

Wang W, Zhao XQ (2008) Threshold dynamics for compartmental epidemic models in periodic environments. Journal of Dynamics and Differential Equations 20:699–717

Wesley CL, Allen LJS (2009) The basic reproduction number in epidemic models with periodic demographics. Journal of Biological Dynamics 3:116–129

Williams ES, Miller NM, Kreeger TJ, Kahn RH, Thorne ET (2002) Chronic wasting disease of deer and elk: a review with recommendations for management. The Journal of Wildlife Management 66:551–563

Woodroffe R, Donnelly CA, Jenkins HE, Johnston WT, Cox DR, Bourne FJ, Cheeseman CL, Delahay RJ, Clifton-Hadley RS, Gettinby G, Gilks P, Hewinson RG, McInerney JP, Morrison WI (2002) Culling and cattle controls influence tuberculosis risk for badgers. The Journal of Wildlife Management 66:551–563

Xiao Y, Chen L (2001a) Analysis of a three species eco-epidemiological model. Journal of Mathematical Analysis and Application 258:733–754

Xiao Y, Chen L (2001b) Modeling and analysis of a predator-prey model with disease in the prey. Mathematical Biosciences 171:59–82

Xiao Y, Van Den Bosch F (2003) The dynamics of an eco-epidemic model with biological control. Ecological Modelling 168:203–214